Publication No. 02-002-004

EVALUATION OF PHOSPHATIC CLAY DISPOSAL AND RECLAMATION METHODS

Volume 2: Mineralogy of Phosphatic Clays

Prepared by Ardaman & Associates, Inc.
under a grant sponsored by the
Florida Institute of Phosphate Research
Bartow, Florida

December, 1982

FIPR-02-002-004

FLORIDA INSTITUTE OF PHOSPHATE RESEARCH

EVALUATION OF PHOSPHATIC CLAY DISPOSAL AND RECLAMATION METHODS

Volume 2: Mineralogy of Phosphatic Clays

Research Project FIPR 80-02-002
Final Report, December 1982

Prepared by

Ardaman & Associates, Inc.
8008 South Orange Avenue
Orlando, Florida 32809

Principal Investigators

Anwar E. Z. Wissa
Nadim F. Fuleihan
Thomas S. Ingra

Prepared for

Florida Institute of Phosphate Research
1855 West Main Street
Post Office Box 877
Bartow, Florida 33830

FIPR Program Managers

David P. Borris
Henry L. Barwood

DISCLAIMER

The contents of this report are reproduced herein as received from the contractor.

The opinions, findings, and conclusions expressed herein are not necessarily those of the Florida Institute of Phosphate Research, nor does mention of company names or products constitute endorsement by the Florida Institute of Phosphate Research.

EVALUATION OF PHOSPHATIC CLAY DISPOSAL AND RECLAMATION METHODS

Research Project FIPR 80-02-002

PREFACE

As part of a Florida Institute of Phosphate Research project titled “Evaluation of Phosphatic Clay Disposal and Reclamation Methods”, Ardaman & Associates, Inc. performed a comprehensive study to evaluate the engineering properties of a wide range of phosphatic clays and sand-clay mixes, and developed a methodology for forecasting the performance of phosphatic clay settling areas during disposal and reclamation. The findings of this study are presented in a series of six complementary volumes.

Laboratory evaluations of the engineering properties of phosphatic clays and sand-clay mixes were performed on phosphatic clays from twelve different mine sites. Volumes 1, 2 and 3 titled “Index Properties of Phosphatic Clays", “Mineralogy of Phosphatic Clays”, and "Sedimentation Behavior of Phosphatic Clays”, respectively, present extensive data on the twelve clay sources selected in the study. The findings were used to screen the samples and select six clays covering the full range of anticipated behavioral characteristics. The selected clays were subjected to a comprehensive testing program for determining engineering parameters pertaining to consolidation and strength. Extensive sophisticated strength testing of three of the six phosphatic clays and corresponding sand-clay mixes was then subsequently undertaken. The results are presented in Volumes 4 and 5 titled “Consolidation Behavior of Phosphatic Clays” and “Shear Strength Characteristics of Phosphatic Clays”, respectively.

Concurrent with the laboratory evaluation of phosphatic clay engineering properties, a theoretical model to evaluate disposal systems was developed. The finite difference program SLURRY can also be used in reclamation planning. In an attempt to verify and refine the prediction modeling technique, a preliminary field investigation program at six phosphatic clay settling areas ranging from retired to active sites was undertaken. Volume 6 discusses the theoretical model and presents a comparison of predictions based on laboratory data with actual field measurements.

A more extensive second phase field testing program is proposed to further refine and improve predictive capability based on actual field conditions. Conventional phosphatic clay disposal and the sand-clay mix disposal methods can then be critically evaluated for phosphatic clays with differing characteristics to quantify advantages/disadvantages of disposal/reclamation methods and outline their relative merits. The results should allow mine planners to select an optimum disposal method based on the clay characteristics at a particular mine.

EVALUATION OF PHOSPHATIC CLAY DISPOSAL AND RECLAMATION METHODS

Volume 2: Mineralogy of Phosphatic Clays

Research Project FIPR 80-02-002
Final Report, December 1982

ABSTRACT

Twelve phosphatic clays and three sand tailings from Florida phosphate mining areas were examined by X-Ray Diffraction (XRD), Scanning Electron Microscopy (SEM) and chemical analysis. Two hundred XRD traces on specimens after various pretreatments were obtained. Quantitative estimates of mineral species were made using sample XRD data and XRD data obtained on reference minerals, and sample mass attenuation coefficients calculated from X-ray fluorescence total chemical data.

The non-clay mineral species detected in XRD data from twelve clay samples were apatite, quartz, dolomite, wavellite, crandallite and feldspar. The non-clay minerals constituted 35 to 60% by weight of phosphatic clays, with an average of about 50%. Apatite content ranged from 7 to 40%, with five samples having an apatite content greater than 30%. Apatite is the dominant non-clay mineral typically constituting about 53% of the mean summation of all non-clay minerals. Chemically determined P_20_5 correlated well with the apatite content found by XRD. The mean P_2O_5 content equalled about 10%. Quartz, dolomite and wavellite are relatively small constituents each typically comprising 6 to 8% by weight of phosphatic clay. The dolomite content from XRD data was highly variable but correlated well with the MgO content found chemically. Wavellite was found in six clays and comprised 10 to 20% of these samples. Quartz was present in all clay samples. Crandallite and feldspar are minor constituents typically comprising less than 1% of phosphatic clays.

Clay mineral species detected by XRD were smectite, illite, palygorskite, kaolinite and interstratified clay material. Quantitative mineralogic analyses indicated that clay minerals account for 40 to more than 65% of phosphatic clays. Smectite was the most abundant clay specie in eight samples and palygorskite was the most abundant clay specie in the remaining four samples. The smectite content ranged from 6 to 51% with an average of 22%. Palygorskite content ranged from 0 to 35%. Illite content ranged from 5 to 18% and correlated well with chemically determined K_2O content. Kaolinite, while present in eleven of twelve samples, was a minor component, the maximum content being less than 4%. The clay mineral phase is often strongly aggregated.

The total clay content calculated from XRD random powder data on the clay prism peak (4.45 Å) was generally greater than the total clay content calculated from the summation of individual clay minerals. The discrepancy between total clay and sum of clay species is attributed to interstratified and amorphous clay material, which did not contribute to specific clay basal spacings that were used to calculate mineral percent, but had sufficient crystallinity to contribute to the 4.45 Å clay peak.

Quartz and apatite were the significant crystalline phases found in the three sand tailing samples analyzed. The apatite content ranged from 7 to 38%, and the quartz content ranged from 60 to 93%.

Attempts to correlate engineering properties with mineralogic composition were not very successful. A correlation between palygorskite content and sedimentation behavior was found valid for ten of twelve phosphatic clays.

ACKNOWLEDGEMENTS

The support and sponsorship provided by the Florida Institute of Phosphate Research to conduct this research is gratefully acknowledged. The cooperation and assistance provided by the various mining companies named in this report and their representatives during collection of clay samples is greatly appreciated, namely:

- Agrico Chemical Company
- AMAX Phosphate, Inc.
- Beker Phosphates
- Brewster Phosphates
- CF Mining Corporation
- Estech, Inc.
- Hopewell Land Corporation
- International Minerals and Chemicals Corporation
- Mobil Chemical Company
- Occidental Chemical Company
- United States Steel Corporation Agrichemicals Division
- W R Grace and Company

The authors would like to acknowledge the assistance and technical expertise of Dr. R. T. Martin, clay mineralogist and Senior Research Associate in the Constructed Facilities Division of the Department of Civil Engineering, Massachusetts Institute of Technology, Cambridge, Massachusetts. Dr. Martin and his staff performed the mineralogic analyses and formulated many of the conclusions presented in this volume.

TABLE OF CONTENTS

TABLE OF CONTENTS (cont'd)

TABLE OF CONTENTS (cont'd)

LIST OF TABLES

LIST OF TABLES (cont'd)

LIST OF FIGURES

LIST OF FIGURES (cont'd)

SYMBOLS

A	Activity of a Clay
A	XRD Net Peak Amplitude
Å	Angstroms
A_{001}	First Order Peak Amplitude
a	The Mineral Apatite When Used as a Subscript
C_u	Uniformity Coefficient
C.V.	Coefficient of Variation
c	Mineral Crandallite When Used as a Subscript
d	Basal or Atomic Plane Spacing
d	The Mineral Dolomite When Used as a Subscript
$\bar{d}$	Mean Basal Plane Spacing
d_{001}	First Order Basal Spacing
LL	Liquid Limit
PI	Plasticity Index
p	The Mineral Palygorskite When Used as a Subscript
Q	Settling Velocity
Q_1	Maximum Laboratory Settling Velocity
q	The Mineral Quartz When Used as a Subscript
R_i	Relative Peak Amplitude Ratio
$\bar{R}_i$	Mean Relative Peak Amplitude Ratio
r	Correlation Coefficient
S	Solids Content
S_i	Initial Solids Content
S_F	Final Settled Solids Content
W_i	Weight Fraction of Chemical Constituent
w	Mineral Wavellite When Used as a Subscript
X_i	Weight Fraction of Mineral Constituent
λ	Wave Length of Incident X-ray
η_a	Apparent Viscosity
μ	Mass Attenuation Coefficient
μ_i	Mineral Mass Attenuation Coefficient
μ_s	Sample Mass Attenuation Coefficient
ρ	Specific Gravity
θ	Angle of X-ray Diffraction
σ	Standard Deviation

Section 1

RESEARCH BACKGROUND AND OBJECTIVES

1.1 **Introduction**

An adequate description of the mineralogic composition of phosphatic clays and variations in composition from one source to another are essential to reliably understand and predict clay behavior in current and future mining, disposal and reclamation operations. Typically, Florida phosphatic clays contain: kaolinite, illite, smectite and palygorskite clay minerals; quartz, apatite, dolomite and wavellite non-clay minerals; and occasionally the clay mineral sepiolite and non-clay mineral crandallite. Existing mineralogic data on phosphatic clays indicates that the clay mineral often causing disposal problems is palygorskite (attapulgite). Some research has suggested that the relative quantity of the clay mineral palygorskite present within a clay may control the settling rate, viscosity and final settled solids content (Lamont et al., 1975).

1.2 **Previous Research**

Lamont et al. (1975, Bromwell and Oxford (1977), Bromwell and Raden (1979) and Carrier et al. (1981) indicate a correlation between palygorskite content and final settled solids content. This correlation was largely developed from settling tests and mineralogic analyses performed by Lamont et al. (1975) on 15 phosphatic clays. The clays were collected from 15 of the 16 beneficiation plants in operation in Florida at the time the study was performed. The clays, therefore, represent a broad range of geographic location and, hence, a potentially broad range in mineralogic composition. The correlation, shown in Figure l-l, clearly illustrates that the higher the palygorskite content, as indicated by the palygorskite net peak amplitude, A_p, the lower the final settled solids content, S_F, after 30 days.

The settling tests were reportedly performed from an initial solids content, S_i, of 3.7% in 1,000 cm^3 glass graduated cyclinders. The results from the settling tests are illustrated in Figure l-2. As shown, the clays exhibit a wide range of settling characteristics with final solids contents of 5.7 to 15.9%. The clay minerals present in each. sample were determined with X-ray diffraction analyses on the -44 µm size fraction. The net peak amplitude, A, in counts/second for the clay minerals smectite, illite, kaolinite and palygorskite are shown in Table l-l. The data indicate that smectite is the dominant clay mineral and occurs in all samples. Palygorskite is generally the second most abundant clay mineral. Illite and kaolinite appear to be relatively minor constituents in most samples. The net peak amplitudes were reportedly determined on oriented aggregate glycerol solvated prepared films for basal spacings of: 18 Å for smectite; 7 Å for kaolinite; 10.6 Å for palygorskite; and 10 Å for illite. Since the peak amplitudes for reference minerals and sample mass attenuation coefficients were not obtained, the net peak amplitudes cannot be converted into quantitative estimates of the weight fraction of each mineral.

As shown in Figure 1-1, we found from the Lamont et al.(1975) data that the palygorskite net peak amplitude correlates very well with the final settled solids content according to an exponential relation. The exponential relation has a correlation coefficient, r, of -0.908, indicating that 82% of the variation in the final settled solids content is explained by the variation in the palygorskite net peak amplitude*. Using multivariate curve fitting techniques could suggest that the greater the amount of smectite within a clay for a given palygorskite content, the greater the final settled solids content (Figure 1-3). The improvement in the correlation coefficient, however, is minor, and the simpler correlation is equally satisfactory.

A correlation between palygorskite relative peak amplitude ratio, R_p**, and settled solids content, S, was also shown by Bromwell (1974) for phosphatic clay from the Occidental White Springs phosphate mine. The linear R versus S correlation shown in Figure 1-4 recommended by Bromwell (1974) is reportedly the best fit to the settled solids content from laboratory settling tests on samples of plant slurry after 25 days of settling. Note that the in situ pond samples consistently yield higher solids contents than the laboratory settling tests at the same palygorskite relative peak amplitude ratio, probably due to consolidation and/or desiccation.

A weak correlation between laboratory settling rate, Q, and palygorskite net peak amplitude was reported by Lamont et al. (1975). The correlation shown in Figure 1-5 suggests that the laboratory settling rate increases as the palygorskite content decreases. This correlation is expected since settling tests have generally shown correlations indicating that the lower the settled solids content, the slower the laboratory settling rate. The exponential relation shown in Figure 1-5 was developed from our evaluation of the published data and provided the best fit from numerous relations (i.e., linear, polynomial and logarithmic). The correlation coefficient of -0.766 implies that only 59% of the variation in settling rate can be accounted for by the palygorskite content.

Lamont et al. (1975) also suggest that a correlation exists between viscosity and palygorskite content. Viscosity measurements from their study on 15 phosphatic clays at a solids content of 3.7% are illustrated in Figure 1-6. As shown, the data indicates that as the palygorskite content increases, the apparent viscosity, n_a, increases. The apparent viscosity was determined with a Brookfield viscometer. The shear strain rate, spindle type and time of shear strain at which the apparent

---

*This correlation cannot be specifically applied to other mineralogic studies of phosphatic clays to determine A_p from a given value of S_F, since: the X-ray diffraction instrument calibration; type of radiation; degree of clay film orientation; concentration of clay slurry used to prepare the films; type of cation saturation; method of glycerol solvation; and other testing factors will influence the measured value of A_p.

**The relative peak amplitude ratio, R_p is the unknown sample palygorskite net peak amplitude, A_p, divided by the net peak amplitude determined for a palygorskite reference mineral. For pure palygorskite, therefore, R_p = 100%.

viscosity was measured, however, were not reported. Our evaluations indicate that the logarithmic relation shown in Figure l-6 is the best fit correlation to the data, yielding a correlation coefficient of 0.873.

In summary, available studies of the mineralogy of phosphatic clays indicate that although smectite is typically the dominant clay mineral, the less dominant clay mineral palygorskite influences the final settled solids content. Other behavior characteristics, including viscosity and settling rate, also correlate with palygorskite content.

1.3 Purpose of investigation.

Although mineralogic analyses of phosphatic clays have been routinely performed in the past for characterization studies and comparison with limited engineering properties, there is an obvious lack of quantitative mineralogic analyses and correlations to a wide range of detailed index, consolidation and shear strength properties. Accordingly, as part of research project FIPR 80-02-002 “Evaluation of Phosphatic Clay Disposal and Reclamation Methods” performed for the Florida Institute of Phosphate Research, twelve phosphatic clays, sampled from various mine sites, were subjected to quantitative mineralogic analyses. The sites were selected to provide a range of geographic locations and mining concerns. The locations of the mine sites are illustrated in Figure l-7 and the specific settling areas and sampling dates are summarized in Table l-2. The results from these quantitative mineralogic analyses are presented in this report.

The purpose of the mineralogic analyses was to: (i) quantitatively characterize the clay and non-clay minerals present within phosphatic clays; (ii) develop a set of investigation procedures and a data base of reference minerals for future use in characterizing phosphatic clays; and (iii) develop correlations between mineralogic composition and index, settling, consolidation and shear strength properties. Detailed descriptions of the engineering properties used in our attempt to establish correlations can be found in Volumes 1, 3, 4 and 5.*

1.4 Scope of Investigation

The scope of the mineralogic analyses included determining the mineralogic composition of twelve phosphatic clays and three sand tailings from Central and North Florida phosphate mines. Sand tailings were investigated since the engineering properties of sand-clay mixes were also determined for evaluating sand-clay mix reclamation methods.

To quantitatively determine the weight fraction of specific minerals in phosphatic clays, X-ray diffraction analyses were used extensively. A total of over 200 X-ray diffraction traces were obtained on twelve phosphatic clay samples. First, a set of reference minerals were established. For each reference mineral the charac-

---

*The index properties, settling behavior, consolidation behavior and shear strength characteristics are presented in Volumes 1, 3, 4 and 5, respectively.

teristic peak amplitude and basal spacing were determined for a fixed set of preparation techniques. The mass attenuation coefficient and specific gravity of each reference mineral were determined from ideal chemical composition. The X-ray diffraction preparation techniques are described in Section 2. The reference mineral data are presented in Section 3.

Based on X-ray diffraction analyses of the phosphatic clay samples and reference minerals, the quantitative composition of each clay was determined. Sample mass attenuation coefficients, needed to determine quantitative mineralogic composition, were evaluated from total chemical composition obtained from X-ray fluorescence chemical analyses. The results from quantitative mineralogic analyses are presented in Section 4 for phosphatic clays and in Section 5 for sand tailings. Finally, in Section 6, correlations between mineralogic composition and engineering properties are presented.

Table 1-1

NET PEAK AMPLITUDE FOR CLAY MINERALS IN THE -44 μm SIZE FRACTION

	Net Peak Amplitude, A (counts/second)				S_F for S_i=3.7%
Sample	Smectite	Illite	Kaolinite	Palygorskite	(%)
Agrico-Payne Creek	640	110*	130	100*	9.3
Agrico-Saddle Creek	120	115	680	n	15.9
Agrico-Palmetto	370	80*	125	60*	11.5
AMAX-Teneroc	1850	n	310	130*	8.5
Brewster-Haynsworth	900	90*	120	25**	10.9
Estech-Watson	250	n	n	510	6.1
Estech-Silver City	1280	80*	210	35**	13.8
Gardinier-Fort Meade	3200	210	60	n	15.2
IMC-Noralyn	2330	n	n	1270*	5.7
IMC-Kingsford	1750	110	25**	n	15.5
IMC-Clear Springs	480	n	145	290*	7.9
Mobil-Fort Meade	1320	35**	280	150*	12.6
Occidental-White Springs	270	n	n	860	5.7
USSAC-Rockland	2250	70*	50	45**	13.1
WR Grace-Bonny Lake	660	25**	90	90	10.5
Statistics					
Mean, $\bar{A}$ (c/s)	1198	162	148	238	10.8
C.V. (%)	76.1	99.0	118.7	155.6	32.8

Source: Adapted from Lamont, et al. "Characterization Studies of Florida Phosphate Slimes." U.S. Bureau of Mines, Report of Investigation 8089, 1975.

*The diffraction line for this peak was either not completely resolved from nearby peaks, or was in a 2θ angular region where numerous peaks from other minerals occurred, resulting in some uncertainty in the net peak amplitude.

**Net peak amplitudes are the probable maximum intensity for these minerals present in low concentrations.

Table 1-2

MINE SITES AND SETTLING AREAS SELECTED FOR PHOSPHATIC CLAY LABORATORY INVESTIGATIONS

Mine	Settling Area	Sampling Date
Agrico-Saddle Creek	Settling Area-2	1-28-81
AMAX-Big Four	Settling Area BF-1	6-05-81
Beker-Wingate Creek	Pilot Plant Samples	6-05-81
Brewster-Haynsworth	Settling Area-L	1-27-81
CF Mining-Hardee	Settling Area N-1	1-28-81
Estech-Watson	Settling Area 13	4-10-81
Hopewell-Hillsborough	Pilot Plant Samples	3-04-81
IMC-Noralyn	Settling Area N-14	2-23-81
Mobil-Nichols	Settling Area N-3	1-28-81
Occidental-Suwannee River	Settling Area-8	2-02-81
USSAC-Rockland	Settling Area-6	1-28-81
WR Grace-Four Corners	Pilot Plant Samples	9-11-81

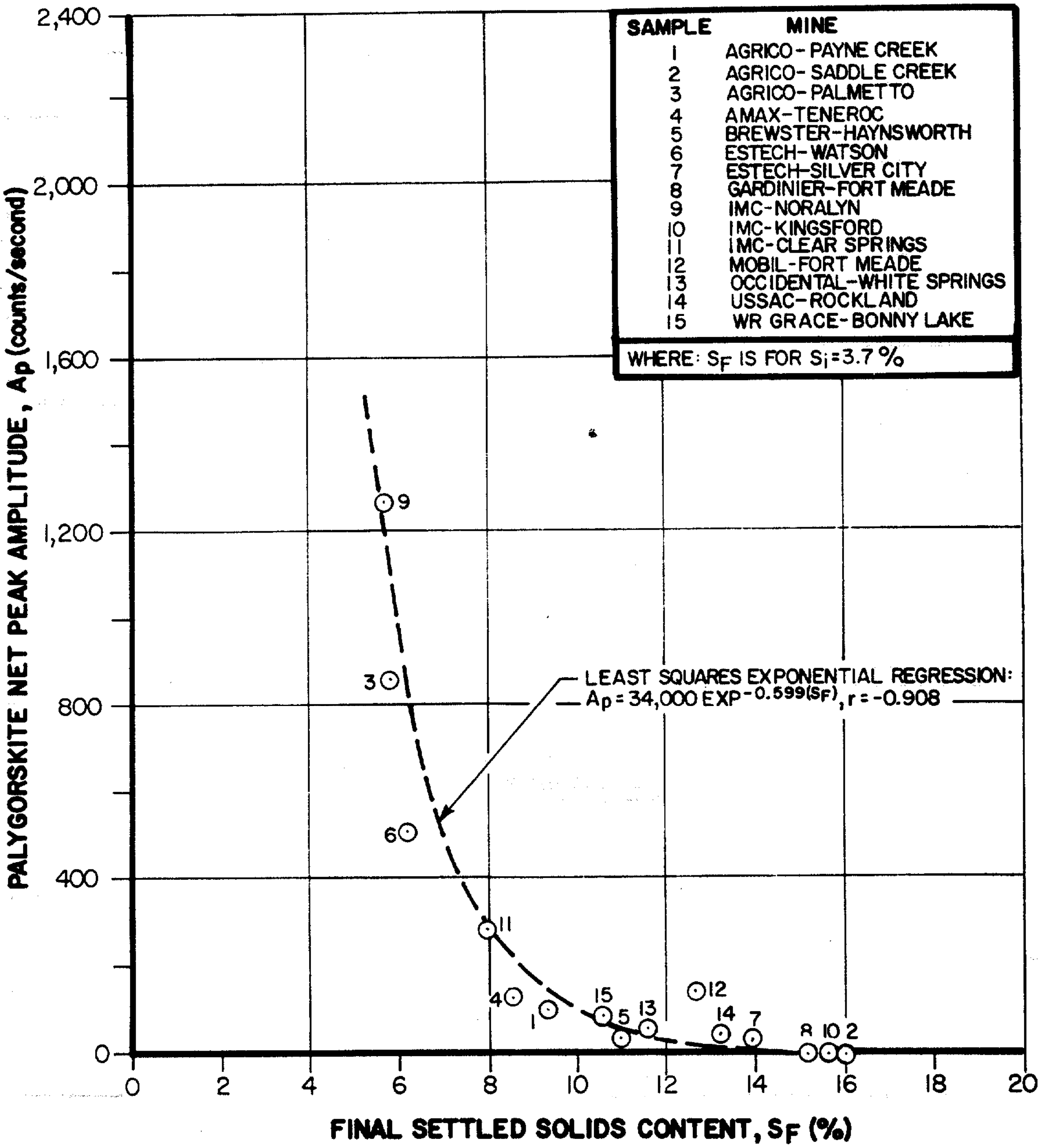

SOURCE: ADAPTED FROM LAMONT, ET AL. "CHARACTERIZATION STUDIES OF FLORIDA PHOSPHATE SLIMES." U.S. BUREAU OF MINES, REPORT OF INVESTIGATIONS 8089, 1975.

FINAL SETTLED SOLIDS CONTENT VS. PALYGORSKITE NET PEAK AMPLITUDE

FIGURE 1-1

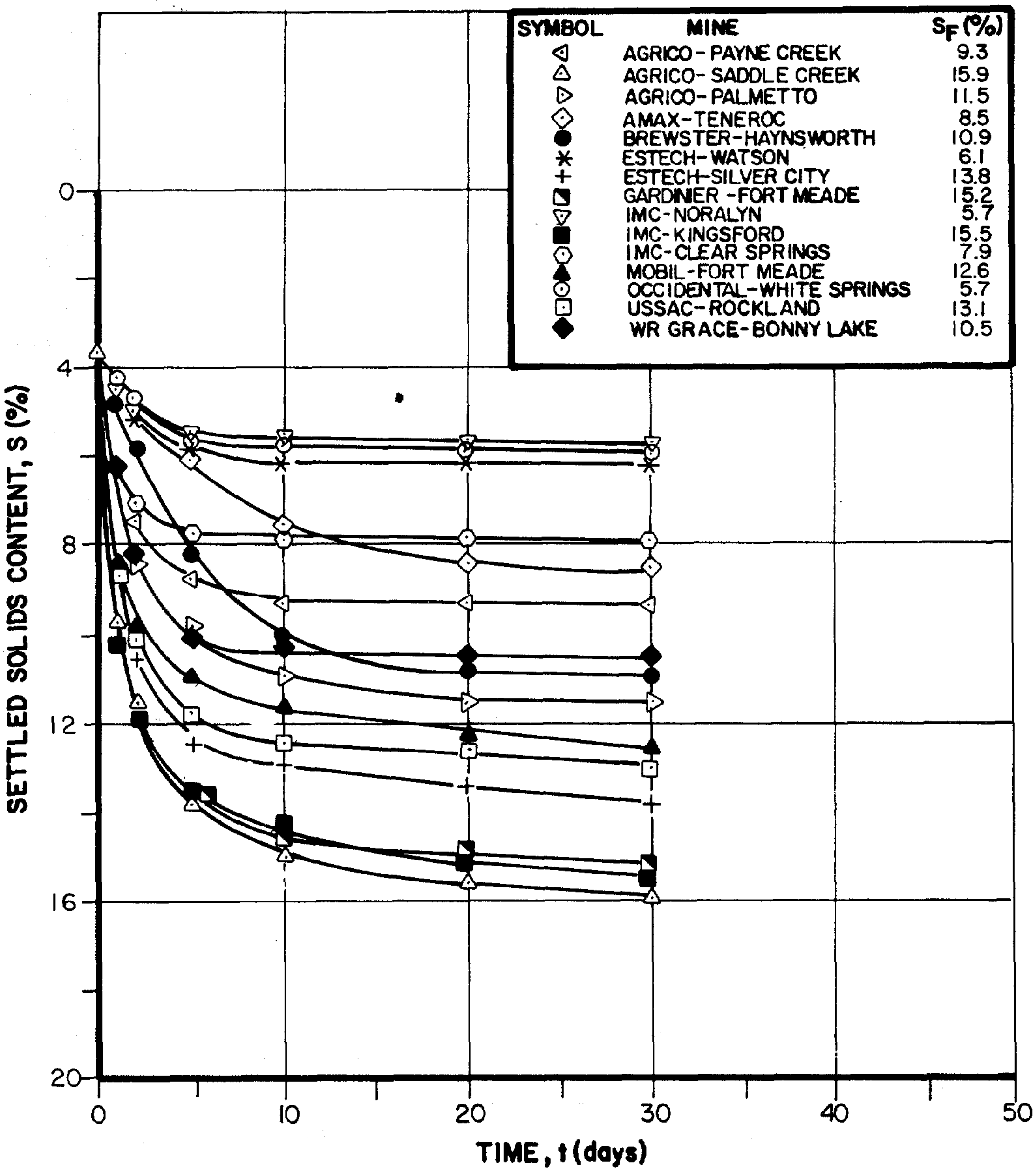

SOURCE: ADAPTED FROM LAMONT, ET AL. "CHARACTERIZATION STUDIES OF FLORIDA PHOSPHATE SLIMES." U.S. BUREAU OF MINES, REPORT OF INVESTIGATIONS 8089, 1975.

SETTLED SOLIDS CONTENT VS. TIME FOR PHOSPHATIC CLAY AT INITIAL SOLIDS CONTENT OF 3.7%

FIGURE 1-2

FIGURE 1-3

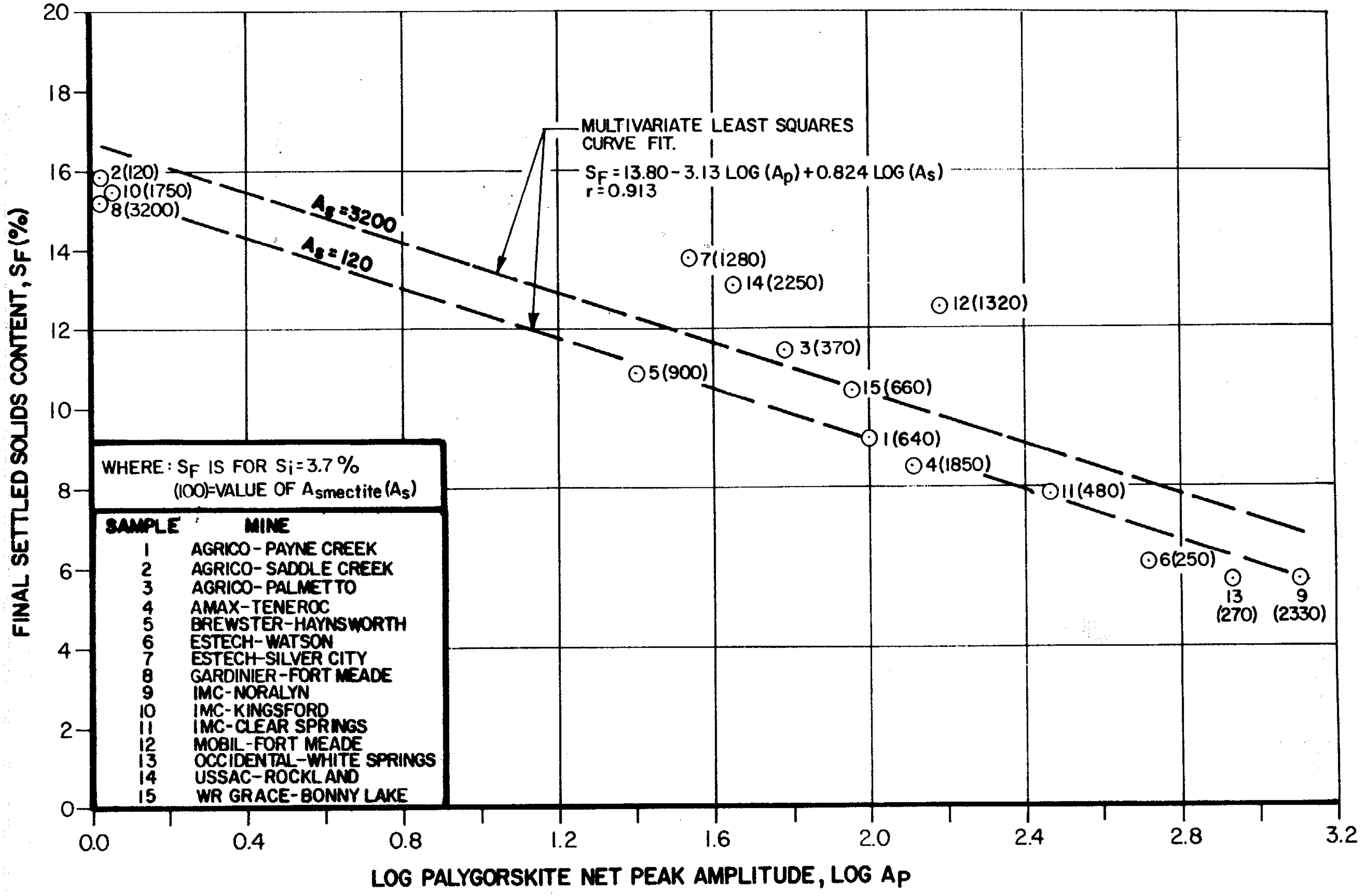

SOURCE: ADAPTED FROM LAMONT, ET AL. "CHARACTERIZATION STUDIES OF FLORIDA PHOSPHATE SLIMES." U.S. BUREAU OF MINES, REPORT OF INVESTIGATIONS 8089, 1975.

FINAL SETTLED SOLIDS CONTENT VS.
PALYGORSKITE AND SMECTITE NET PEAK AMPLITUDE

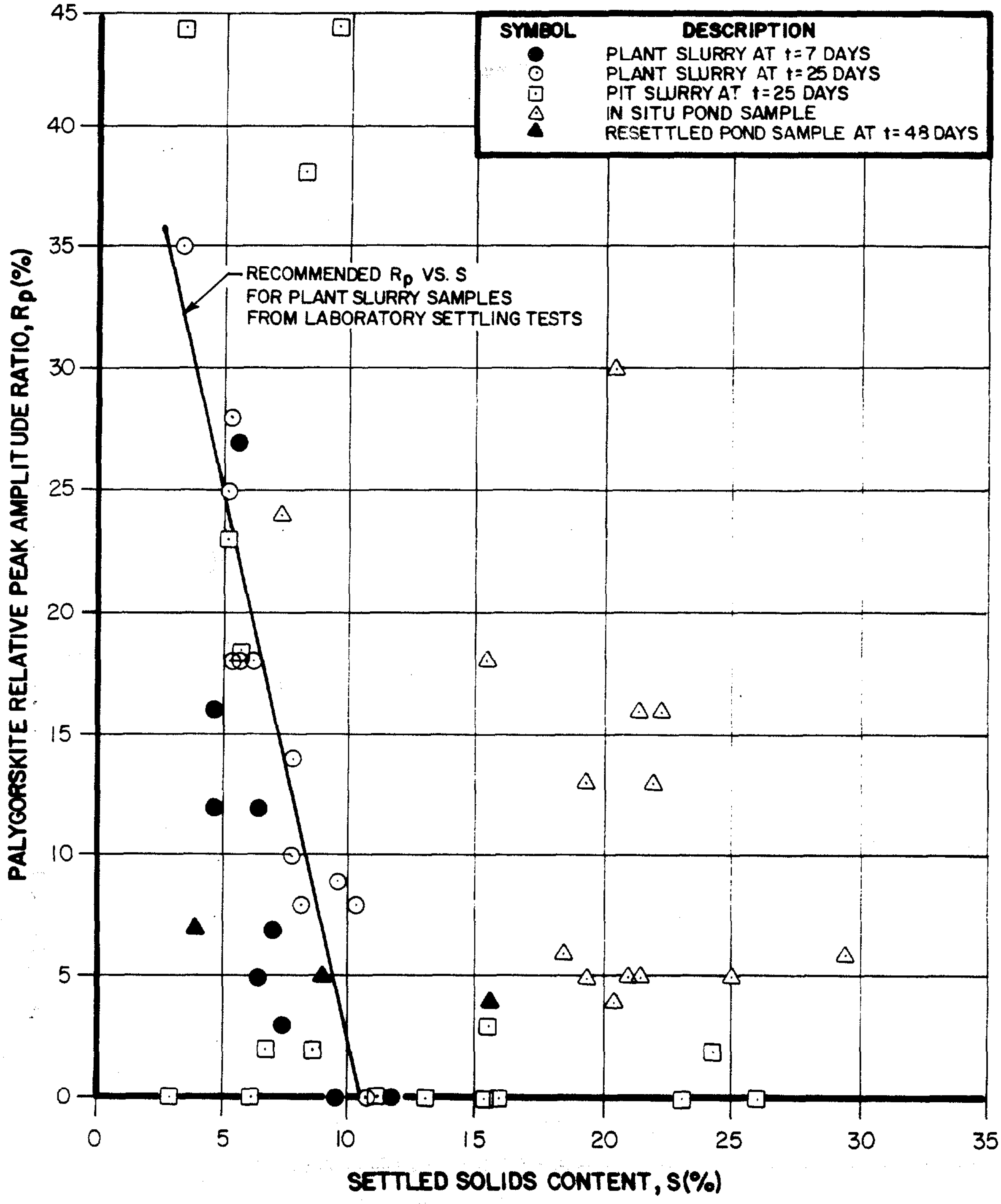

SOURCE: BROMWELL, L.G. "PROGRESS REPORT." FLORIDA PHOSPHATIC CLAY RESEARCH PROJECT, JANUARY-MARCH 1974.

SETTLED SOLIDS CONTENT VS. PALYGORSKITE RELATIVE PEAK AMPLITUDE FOR OCCIDENTAL PHOSPHATIC CLAY

FIGURE 1-4

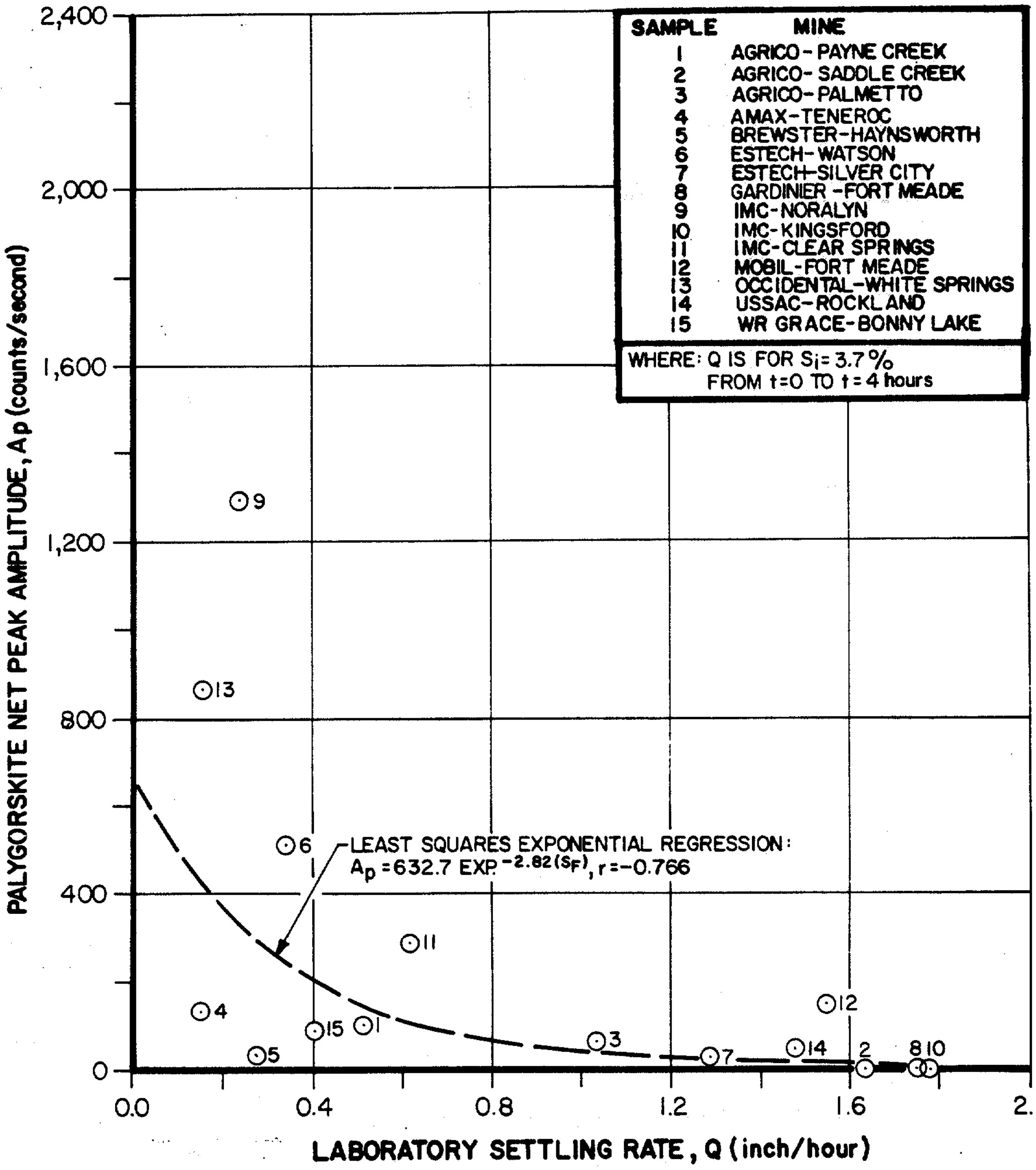

SOURCE: ADAPTED FROM LAMONT, ET AL. "CHARACTERIZATION STUDIES OF FLORIDA PHOSPHATE SLIMES." U.S. BUREAU OF MINES, REPORT OF INVESTIGATIONS 8089, 1975.

LABORATORY SETTLING RATE VS. PALYGORSKITE NET PEAK AMPLITUDE

FIGURE 1-5

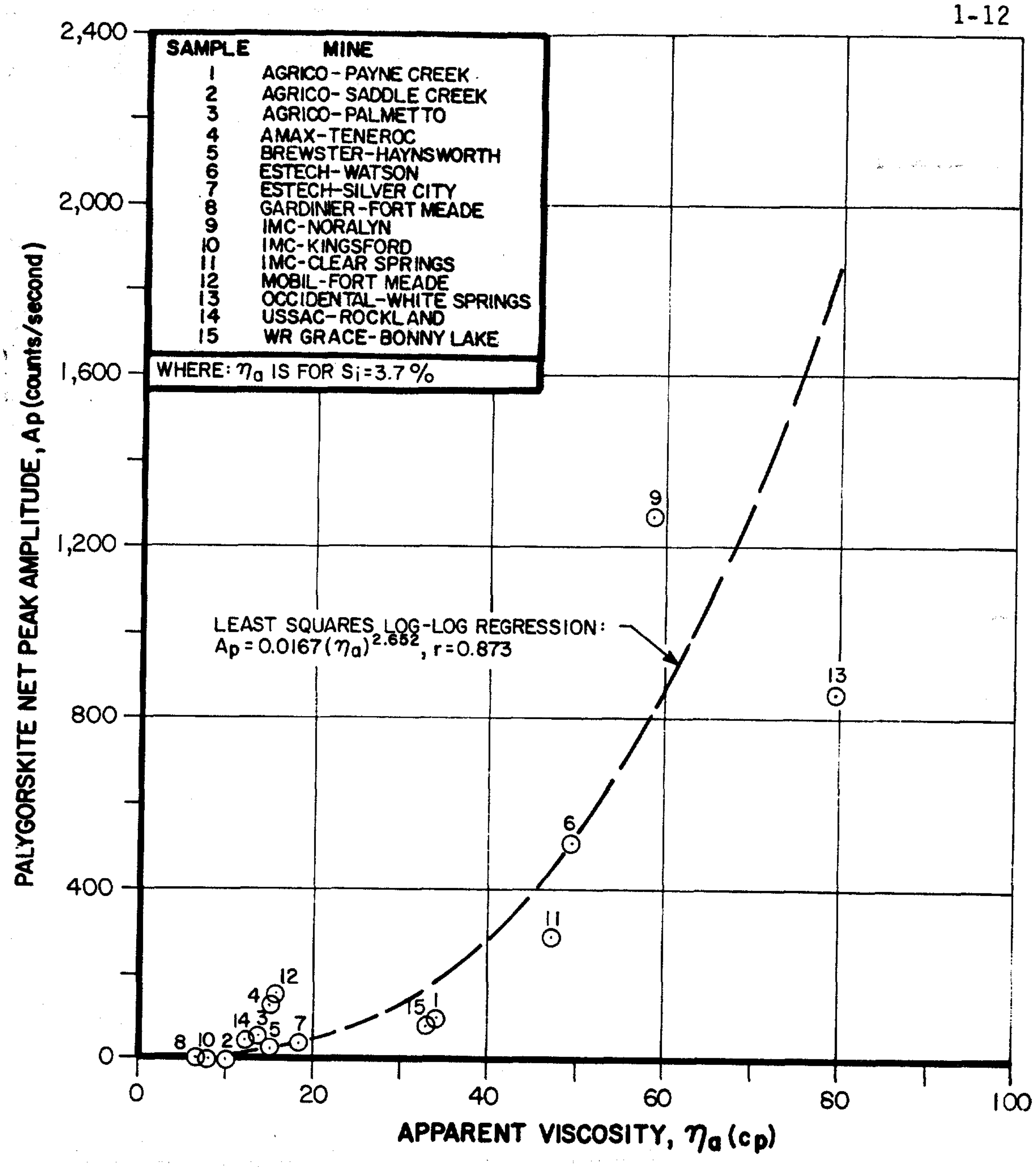

SOURCE: ADAPTED FROM LAMONT, ET AL. "CHARACTERIZATION STUDIES OF FLORIDA PHOSPHATE SLIMES." U.S. BUREAU OF MINES, REPORT OF INVESTIGATIONS 8089, 1975

VISCOSITY VS. PALYGORSKITE NET PEAK AMPLITUDE

FIGURE 1-6

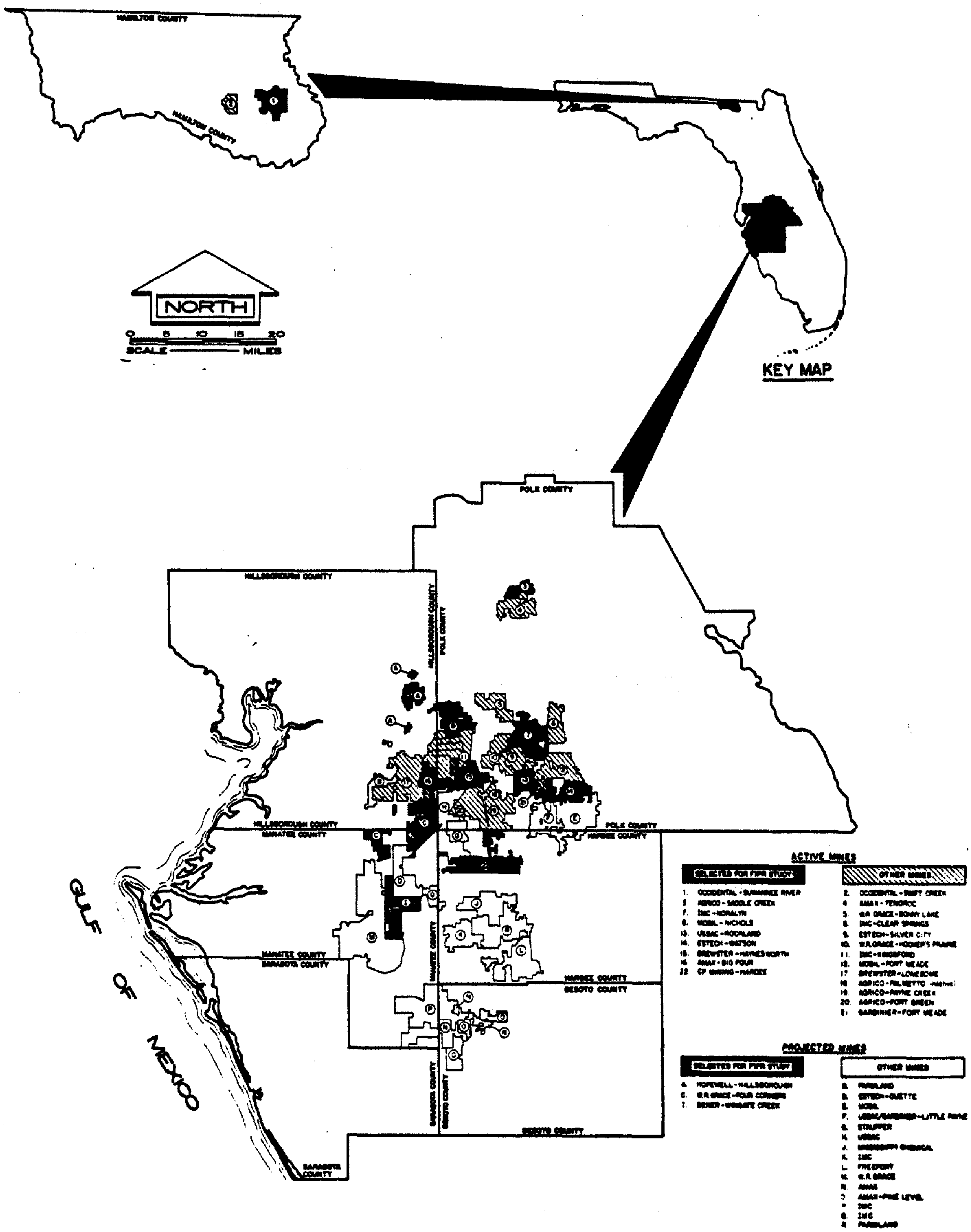

MINE SITES SELECTED FOR INVESTIGATION

FIGURE 1-7

Section 2

EXPERIMENTAL SCHEME, TESTING METHODS AND QUANTITATIVE EVALUATION CRITERIA

2.1 Introduction

The mineralogy determined for clay materials is sensitive to the specific procedures used to determine that mineralogy because clay crystals are generally rather poorly developed crystals. The objective for which the mineralogical data are to be employed also influences the methodology for determining mineralogy. At one ‘extreme is the examination of the mineralogical character of the indestructable silicate residue. At the other extreme is the examination of clay in its natural state. Although it is extremely difficult to prepare clay material for analysis in a truly natural state, the identification of and conclusions about mineralogy are generally restricted to laboratory analyses performed solely on clays in their natural state. Since this research has as one objective an attempt to relate mineralogy to dewatering and engineering properties, the emphasis in sample preparation was biased toward the natural state of the clays.

Twelve phosphatic clays and three sand tailings were examined by X-ray diffraction (XRD), scanning electron microscopy (SEM), energy dispersive analysis by X-ray (EDAX) and X-ray fluorescence chemical analyses. Over two hundred X-ray diffraction traces on specimens after various chemical and heat pretreatments were obtained. Scanning electron microscopy observations were obtained on seven phosphatic clays and on the palygorskite reference mineral, Chemical analyses by X-ray fluorescence were performed on each clay for calculating sample mass attenuation coefficients. The procedures used to perform these investigations and criteria used to quantitatively evaluate the test results are presented in this section.

2.2 XRD Sample Preparation and Testing Methods

2.2.1 Random Powder Mount Preparation

A flow chart of the experimental scheme used in mineralogic analysis of phosphatic clays by X-ray diffraction is shown in Figure 2-l. After field sampling, the clays were initially fractionated by wet-sieving into the sand size fraction (+105 µm* particle size) and the silt and clay size fraction (-105 µm particle size). The -105 µm size fraction was additionally fractionated by wet sieving into the -105 to 44 µm and -44 µm** size fractions. Subsamples from all four size fractions were air dried and ground to -44 µm for random powder mount X-ray diffraction analysis. The air dry powders were used to determine the total clay

---

*The U.S. Standard No. 140 sieve has a mesh size of 105 µm.
**The U.S. Standard No. 325 sieve has a mesh size of 44 µm.

content and relative amount of non-clay minerals (quartz, apatite, feldspar dolomite, crandallite and wavellite) in different size fractions, and organic matter content of the entire sample.

2.2.2 Oriented Aggregate Preparation

The -105 µm size fraction clay slurry was mixed for two minutes in a Waring blender at 4% solids content before -44 µm wet sieve fractioning. Pretreatment prior to Stoke's law settling for -1 µm size fractioning consisted of one to four distilled water washes which reduced the electrolyte concentration low enough to provide good dispersion of the clay species.

Homoionic clay was prepared from subsamples of the -44 µm and -1 µm size fractions for oriented aggregate mounts in X-ray diffraction analyses. The samples were made homoionic to remove all exchangable cations (such as sodium (Na); calcium (Ca) or iron (Fe)) prior to analysis. The homoionic slurries were used to identify specific clay minerals present within the -44 µm and -1 µm size fractions.

Clay subsamples were made homoionic to magnesium (Mg), potassium (K) and lithium (Li) by three washes of the clay with the appropriate cation in a 1.0 molar chloride salt solution followed by distilled water washes until the electrolyte concentration was about 10^{-3} molar as indicated by conductivity measurements on the supernatant. Oriented aggregates were prepared from the homoionic clays using 3.0 cm^3 of clay slurry at 3% solids content so that a uniform clay film was achieved for all specimens.

Glycerol solvation was by the slurry method (Novich and Martin, 1981), which was found to provide the best reproducibility of results. Prior to the introduction of the homoionic clay slurry to the glass slide, a known amount of liquid glycerol was added to the suspension. After thorough mixing, the treated slurry was pipetted onto the glass slide and air dried at room temperature (22^0C).

The Mg homoionic slurry was glycerol solvated prior to air drying and X-ray diffraction. Since clay minerals have different specific surface areas*, the amount of glycerol adsorbed on the clay minerals can be used to aid in the quantitative evaluation of the clay minerals. Kaolinite, for example, adsorbs relatively little glycerol, whereas smectite minerals adsorb relatively large amounts of glycerol.

---

*Where specific surface area, SSA, is defined as the ratio of the surface area of the individual clay particle to the weight of the particle in m^2/gram. Kaolinite has a relatively low SSA of 10-20 m^2 /gram, whereas the smectite mineral, sodium montmorillonite, has a relatively high SSA of 700-800 m^2 /gram. Results from Lamont et al. (1975) indicate phosphatic clay specific surface areas of 27.4 to 88.4 m^2 /gram with an average of 46.5 m /gram and a coefficient of variation of 37.1%.

All three homoionic slurries were used in conjunction with various heat treatments. Each clay mineral behaves differently after heat treatment. The heat treatments, therefore, are also used for quantitative evaluation of the specific clay minerals present in a sample. Kaolinite minerals, for example, are typically destroyed by heating to 500°C, whereas other clay minerals are not.

Seven of twelve oriented aggregates for the -44 µm size fraction homoionic potassium saturated specimens peeled from the slide during air drying. Scanning electron microscopy on the peeled film from an IMC clay indicated the problem was partially due to size segregation. As shown in Figure 2-2, there is a significant difference in particle size between the top and bottom surface of the X-ray diffraction oriented aggregate film.

While grain size was a contributing factor, additional unknown factors must also exist because magnesium saturated -44 µm size fraction slurry from the IMC clay sample did not peel. Further, the potassium saturated -1 µm size fraction slurry from an Estech clay sample peeled severely, while the Mg saturated -44 µm specimen did not peel even after heating to 400^0C. Size fractionation at about -10 µm yielded potassium saturated clay films that did not peel for the Agrico, Brewster, CF and Occidental clay samples. Potassium saturated clay films from the AMAX, Grace, Mobil and USSAC clay samples showed no tendency for peeling. It should be noted that rapid filtration onto a sintered steel plate or mixing glass fibers with the slurry before filtration failed to prevent peeling.*

2.2.3. XRD Testing Equipment

X-ray, diffraction was performed using Norelco equipment. Radiation was CuKa at 40KV and 20ma. Detection of diffracted radiation was with a scintillation counter behind a graphite crystal monochrometer. Goniometer speed was 1 or $1/4^0$ 2θ per minute. Recorder speed was either 2 or 4^0 2θ per inch of chart travel. Proper alignment of the equipment was verified using chloresterol (d_{001} = 33.6Å) and n-tetradecanal d_{001} = 39.63 Å) where the mean d_{001} for eight orders was 39.59 Å with a coefficient variation of 0.11%.

During X-ray examination all heated specimens were kept dry by a small silica gel desiccator having a mylar window for passage of the X-ray beam.

Random powder mounts were prepared by chopping with a razor blade. X-ray diffraction data using a pole figure device consistently indicated nearly ideal random orientation for random powder mounts carefully prepared,

---

*No consistent pattern in mineralogical factors was found to explain peeling during air drying. Further investigation of this phenomenon is needed.

2.2.4 Presentation of XRD Results

To indicate relative changes in a given mineral between samples or between size fractions, the X-ray diffraction data are reported as relative peak amplitude ratio, R. The relative peak amplitude ratio is the amplitude of a specific X-ray diffraction peak in the sample divided by the peak amplitude for that same X-ray diffraction peak taken from appropriate reference mineral data. The sample and the reference mineral data were collected on specimens uniformly prepared so that the R values reflect relative changes of a given mineral phase within the sample suite. To facilitate evaluation of the data, the values are tabulated in percent as 100R.

2.3 **Scanning Electron Microscopy Sample Preparation and Testing Methods**

Samples of phosphatic clay for scanning electron microscope examination were prepared from the -44 μm size fraction. Samples of the reference mineral palygorskite were prepared from the -1 μm size fraction. The types of preparation techniques used for examination included: (i) clay slurry; (ii) fractured clay lumps; and (iii) X-ray diffraction oriented aggregate mounts.

Clay slurry preparation consisted of 0.25 cm^3 of a 4% clay slurry diluted to 2 cm^3, thoroughly mixed, and one drop (0.5 cm^3) dried onto a microscope cover slip which yielded a total specimen for examination of 0.25 mg. Fractured clay lumps consisted of a well worked thick paste allowed to air dry and an approximate 1 cm^3 lump fractured to yield a surface for examination. The X-ray diffraction oriented aggregate mount was a specimen film that peeled from the glass slide during drying. The photomicrographs presented herein represent a small fraction of the total area visually examined for any particular sample.

2.4 **Organic Matter Content Testing Method**

The organic matter contents of the phosphatic clays were determined with the Walkley-Black method (Peech et al., 1947) on a composite sample from all size fractions. The organic matter contents were determined on air-dried samples from each size fraction (Figure 2-l) ground to -44 μm. This method determines the amount of readily oxidizable organic carbon, which is assumed to be the same as the organic matter content. Sucrose was used as the reference, which yields an organic matter content of 100% with the Walkley-Black method.

2.5 **X-Ray Fluorescence Chemical Analyses**

The total chemical composition of the phosphatic clays were determined with X-ray fluorescence on samples of phosphatic clay fused into glass pellets. Extensive standards and computer programs for matrix corrections were used to minimize the errors in the chemical analyses.

2.6 **Quantitative Evaluation Criteria**

The quantitative evaluation of the mineralogic composition of clay samples with X-ray diffraction is largely based on the first order peak position, d_{001}, the first order peak amplitude, A_{001}, and the coefficient of variation of the higher order series of basal reflections Additional information required includes individual mineral mass attenuation coefficients for minerals within the unknown sample and the entire unknown sample mass attenuation coefficient. Figure 2-3 presents a flow chart illustrating the experimental scheme for quantitative mineralogic analyses.

2.6.1 First Order Peak Position

Much of the mineralogic information obtained from X-ray diffraction analyses is derived from the position of the principal basal spacing, d_{001}. Studies performed concurrent with this research, however, indicate that clay mineral d_{001} peak positions and symmetry are influenced greatly by the degree of solvation (Novich and Martin, 1981). Since so much mineralogic qualitative inference is based upon the d_{001}, careful consideration of the effect of the solvation technique is required.

2.6.2 First Order Peak Amplitude

The peak amplitude of the first order peak, A_{001} , is commonly used for quantitative mineralogic analysis, because it is usually the strongest and sometimes only basal reflection detected. It is important that this peak intensity be accurately determined and represent the amount of component phase present within the unknown sample, relative to some reference mineral.

2.6.3 Coefficient of Variation

The principal criterion for distinguishing regularly interstratified clay from randomly ordered structures is the presence or lack of an integral series of basal reflections. This can be quantified with the determination of the coefficient of variation, C.V., for the series. The coefficient of variation is a statistical parameter using the standard deviation of the individual spacings and the overall mean basal spacing. Explicitly stated, $C.V. = 100\ (\sigma)/\bar{d}$ where σ equals the standard deviation and $\bar{d}$ is the mean basal spacing. A coefficient of variation of 0.50% or less was taken to indicate a well ordered non-interstratified clay. Greater values are characteristic of poorer order going to random interstratification. Recognizing that 0.50% is an arbitrary value, it is not meant to be an absolute criterion, but a reference value to which clays under examination can be uniformly compared.

2.6.4 Mass Attenuation Coefficients

The sample mass attenuation coefficient, μ_s, and mineral mass attenuation coefficients, μ_i are determined from X-ray fluorescence chemical analyses and ideal chemical formulae, respectively. The use of chemical data provides more reliable estimates of μ_s and μ_i than generally possible from X-ray diffraction measurements.

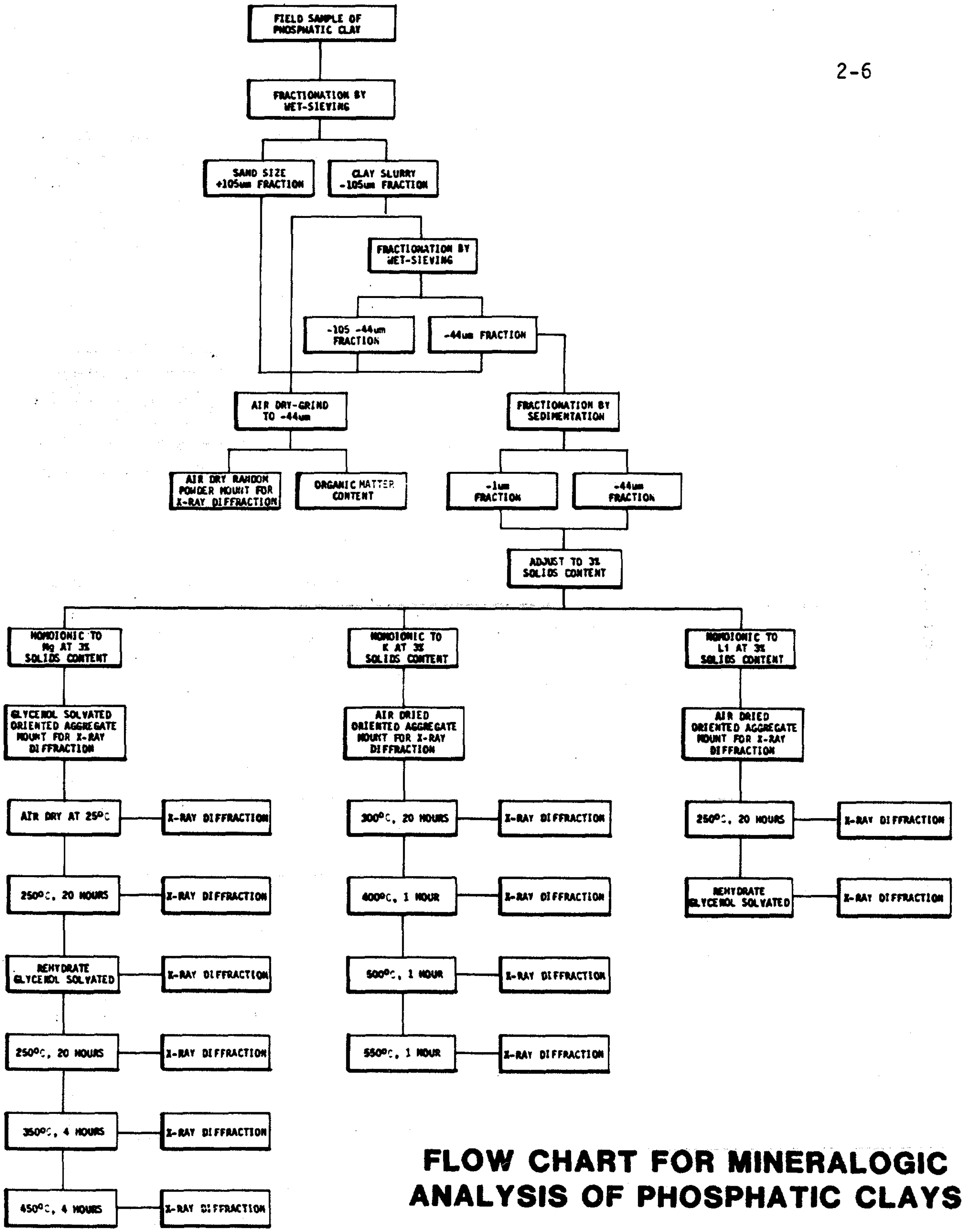

FLOW CHART FOR MINERALOGIC ANALYSIS OF PHOSPHATIC CLAYS

FIGURE 2-1

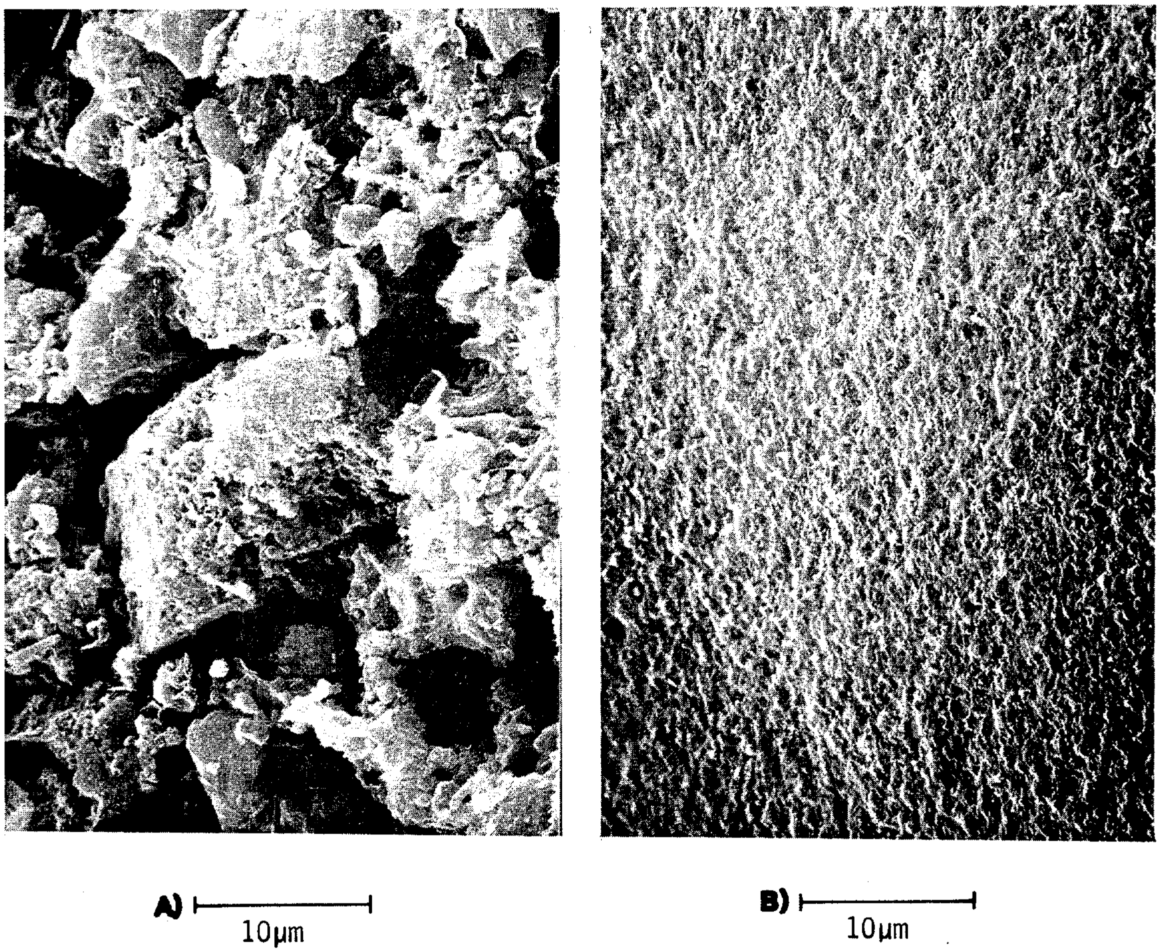

BOTTOM SURFACE

TOP SURFACE

SCANNING ELECTRON PHOTOMICROGRAPHS OF IMC CLAY FROM X-RAY DIFFRACTION ORIENTED AGGREGATE MOUNT

FIGURE 2-2

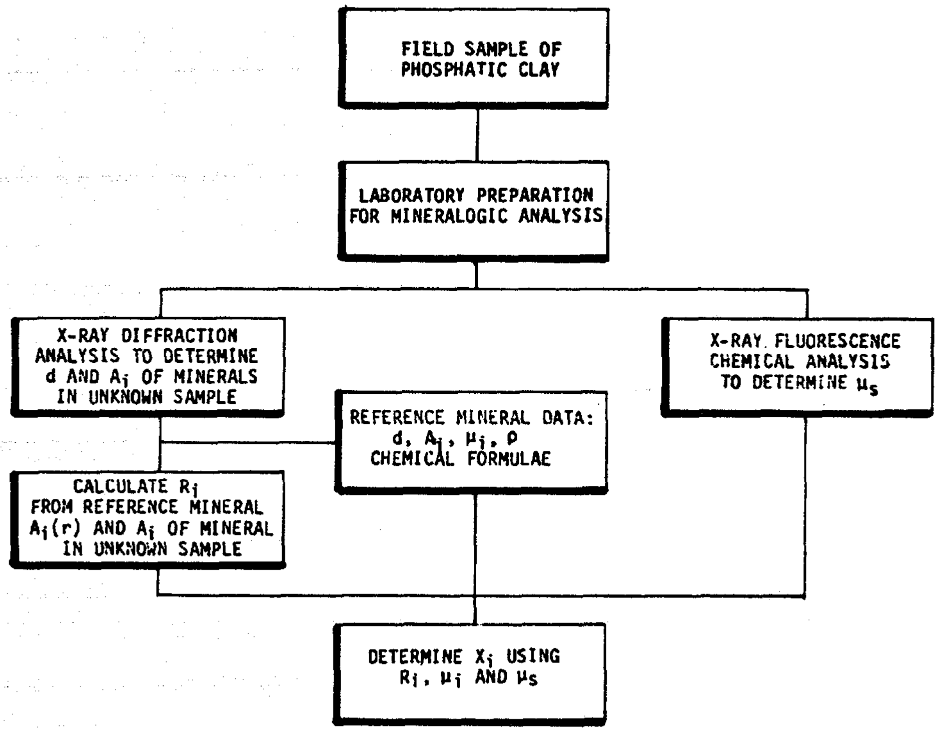

NOTATION: A_i=PEAK AMPLITUDE FOR MINERAL i IN UNKNOWN SAMPLE; d=BASAL SPACING; $A_i(r)$=PEAK AMPLITUDE FOR REFERENCE MINERAL i; R_i=RELATIVE PEAK AMPLITUDE RATIO, $R_i=A_i/A_i(r)$; μ_i=MASS ATTENUATION COEFFICIENT OF MINERAL i; ρ=SPECIFIC GRAVITY: μ_s=SAMPLE MASS ATTENUATION COEFFICIENT; AND X_i=WEIGHT FRACTION OF MINERAL i IN UNKNOWN SAMPLE, $X_i=R_i(\mu_s/\mu_i)$

FLOW CHART FOR MINERALOGIC QUANTITATIVE EVALUATION

FIGURE 2-3

Section 3

REFERENCE MINERALS

3.1 **Introduction**

Quantitative evaluation of the amount of specific minerals occurring in a soil by comparison of the diffraction peak amplitudes from X-ray diffraction analysis depends, in a large part, on the reference minerals used for comparison. Further, soils containing only two or three well crystallized mineral components give peak amplitudes that are more easily analyzed than soils with numerous mineral components and interstratifications (such as phosphatic clays), which give numerous superimposed peaks. The first requirement for meaningful quantitative mineralogic analyses, therefore, is to adequately define the peak amplitudes and basal spacings of reference minerals using the same equipment and procedures as used for the unknowns, whose minerals are to be determined. Specific reference minerals used for quantitative mineralogic analysis of phosphatic clays are presented below.

3.2 **Non-Clay Reference Minerals**

3.2.1 Characteristic Peak Amplitudes

Six non-clay reference minerals were selected for X-ray diffraction analysis: quartz, apatite, dolomite, wavellite, crandallite and potassium feldspar. Table 3-l summarizes the peak amplitudes, A, in counts per second (c/s) for specific X-ray diffraction peaks corresponding to, a particular atomic plane or basal spacing, d, in Angstroms (Å).

The quartz peak amplitude data are from the arithmetic average for each peak from three specimens from Central Florida.The coefficient of variation of the given mean peak amplitudes varied from 6 to 17%. Three reference peak amplitudes were used for quartz since all of the important quartz peaks are normally superimposed on clay mineral peaks producing some uncertainty in measuring the net peak amplitude. The basal spacings from the Central Florida reference quartz agree well with the ideal spacings of 4.26, 3.34 and 2.46 Å for quartz (Mitchell, 1976).

Two distinctive apatite peak amplitude values were selected from the arithmetic mean value for each peak from three different samples. The coefficient of variation of each peak amplitude was about 10%. The apatite samples were obtained from Central (Polk County) Florida and North (Hamilton County) Florida. The large geographic separation of the samples did not result in significantly different peak amplitudes.

One sample of dolomite from Central Florida was used for a reference mineral, but was slightly impure containing about 3% quartz and 8% apatite. The two major dolomite peak amplitude values summarized in Table 3-1 were corrected for these impurities.

The reference wavellite amplitude data was based upon very small samples that made analysis difficult. The available reference specimens were also impure, containing about 25% quartz. Removal of the quartz was not attempted because there would have been insufficient material for analysis. Three peaks are given for wavellite because of the pronounced tendency for preferred orientation. Averaging data from the three peaks tends to cancel orientation effects.

Basal spacings for crandallite are based on data available in the literature, The characteristic basal spacing for crandallite identification has been biased toward the sample from Alachua County, Florida described by Blanchard (1972). The reference data in Table 3-l are for a material that is 70% ideal crandallite and 30% ideal goyazite (hamlinite). Note that only the characteristic basal spacing is shown, since no sample was available to perform X-ray diffraction analyses to determine the peak amplitude.

The reference peak amplitude and basal spacing data for potassium feldspar are based upon X-ray diffraction traces from two microcline and one perthite sample.

3.2.2 Chemical Formulae

Chemical formulae for the reference non-clay minerals are shown in Table 3-l. The formulae represent an ideal composition, which is justified based upon X-ray diffraction data from phosphatic clays.

3.2.3 Mass Attenuation Coefficients

Mass attenuation coefficients, u , for the reference non-clay minerals are shown in Table 3-l. The coefficients were calculated using the ideal composition given in Table 3-l and elemental mass attentuation coefficients for CuKa radiation from the International Table for X-ray Crystallography (1974).

3.2.4 Specific Gravity

The specific gravity, P, selected for each reference non-clay mineral is shown in Table 3-l. The selected reference specific gravities are mean values obtained from the literature for each mineral.

3.3 Clay Reference Minerals

Satisfactory clay mineral reference specimens are difficult to obtain because of the tendency for clay minerals to exist as interstratifications of several phases. In other words, a single phase clay mineral is a rarity. In natural occurring sedimentary deposits, illite-smectite mixed layering is very common and mixed layered kaolinite-smectite has been reported. Palygorskite-smectite mixed layering has not been reported, but may be expected to occur based upon crystal-chemical considerations.

One of the requirements for identifying a clay mineral is that the sequence of basal spacings give a rational series of peaks whose coefficient of variation is less than 0.7%. For expandable mineral phases such as smectites, this introduces the experimental problem of defining a useable reproducible fully hydrated condition. Novich and Martin (1981) have established the optimum level of glycerol treatment for routine analysis. Fortunately, there exists a wide range of glycerol treatment levels that yield similar X-ray diffraction results. A solids content of. 3% was selected as the slurry concentration for preparation of oriented aggregates, which represents a compromise between obtaining good orientation and the "infinite thick" specimen desirable for quantitative analysis. All X-ray diffraction analyses, on the reference clay minerals were performed on oriented aggregate mounts homoionic to Mg and glycerol solvated.

3.3.1 Characteristic Peak Amplitudes

The reference clay mineral X-ray. diffraction peak amplitudes and basal spacings selected for total clay, smectite, illite, palygorskite and kaolinite are summarized in Table 3-3:

Pour smectite reference specimens were analyzed before selecting the best reference data for quantitative X-ray diffraction analysis of phosphatic clays. Table 3-2 summarizes data from four smectite clay reference specimens. The expansive character of the smectite clay minerals normally provides the basis for their positive identification. When air dried, the smectite minerals hive a basal spacing of l2-15Å. After treatment with glycerol the smectite minerals expand to a first order basal spacing d_{001} value of 17-18Å. When oven dried, d_{OOl} decreases to about 10Å due to the removal of interlayer water (Mitchell, 1976).

Specimen PC-2, was eliminated as a possible reference mineral because of: the extreme width of the first order peak (1.6); and the asymmetry of the basal spacing (2.3). which became more pronounced upon heat treatment. Strong evidence for interstratification was also evident in the X-ray diffraction data. The low coefficient of variation of 0.20% for sample PC-2 indicated that there was a good smectite phase present in addition to interstratified clay material. The Wyoming montmorillonite mineral was also excluded as a possible reference mineral since glycerol solvation of heated lithium (Li) saturated phosphatic clays have generally-indicated that isomorphous substitution in the smectite clay mineral phase of phosphatic clays is in the tetrahedral layer, which is not the case for montmorillonitic clays.

The Washington ferruginous smectite specimen gave no indication of interstratification and contained 10% quartz as the only impurity. Specimen PC-1 contained 4% quartz, 10% apatite and only a slight suggestion of interstratification. Based upon data from these two specimens, representative values for peak amplitude of 2000 counts/second and basal spacing of 17.8 Å were selected for smectite clay minerals.

Two illite clay specimens were examined with X-ray diffraction analyses. The illite clay minerals are typically characterized by a basal spacing (d_{001}) of 10 Å, which remains unchanged in the presence of glycerol and after oven drying. The d_{001} peak amplitude also becomes more intense after drying as interlayer water is removed (Mitchell, 1976). One reference illite sample contained some expandable layers. The other illite clay specimen from Pevear, Montana contained no expandable layers and 2% chlorite as the only impurity. No pure illite clay was located in Florida, so the Pevear specimen from Montana was considered the best illite reference. The basal spacing of 10.0 Å shown in Table 3-3 for the reference illite clay mineral agrees perfectly with the ideal value of 10.0 Å reported by Mitchell (1976).

Two of the three palygorskite specimens investigated for reference minerals contained considerable smectite. The palygorskite data in Table 3-3 was obtained from a clay specimen collected in Polk County, Florida and was free of any other detectable clay phase. The specimen was impure, however, containing 13% apatite and 1.5% quartz. The data summarized in Table 3-3 represents peak amplitudes corrected for the non-clay mineral impurities. The 10.5 Å palygorskite peak, when present, can be distinguished from the 10 Å illite peak and would represent a definite indication of palygorskite. The presence of a single peak between 10 and 10.5 Å would suggest the presence of illite, palygorskite, or both, but does not provide definitive identification. Palygorskite has a strong peak at 3.23Å. that becomes confused with other clay peaks as well as wavellite and feldspar. The 6.5 and 5.4Å palygorskite peaks are distinctive; unfortunately, these two peaks are not strong.

The kaolinite reference data in Table 3-3 is from a clay specimen from South Carolina that contained 6% mica as the only impurity. This kaolinite is considered a valid reference mineral, since previous research has shown that the South Carolina kaolinite is essentially identical to kaolinites found in Hamilton County, Florida. Further, relatively pure kaolinite samples have not been found in Central Florida. The measured basal spacing of 7.14Å also agrees well with the ideal 7.0Å value reported by Mitchell (1976).

All clay minerals have an X-ray diffraction peak at 4.45Å that clearly shows in random powder mounts. For clay specimens discussed in previous paragraphs, the 4.45Å peak gave an average amplitude of 90 counts/second with a coefficient of variation of 13%. The amplitude of the 4.45Å peak from a random powder mount is used as a measure of the total clay mineral content.

3.3.2 Chemical Formulae

The chemical formulae selected for each reference clay mineral are shown in Table 3-3. The starting composition for the clay minerals was the average composition for a species as given in Weaver and Pollard (1973) and then biased to include 4 to 5% Fe_20_3, which is common in phosphatic clays.

3.3.3 Mass Attenuation Coefficients

Mass attenuation coefficients, μ , for the reference clay minerals are shown in Table 3-3. The coefficients were calculated using the composition given in Table 3-3, elemental mass attenuation coefficients for CuKa radiation from the International Table for X-ray Crystallography (1974).

3.3.4 Specific Gravity

The specific gravity selected for each reference clay mineral was calculated from the composition given in Table 3-3 and the crystal dimensions of the unit cell.

Table 3-l

REFERENCE X-RAY DIPFRACTION DATA, MASS ATTENUATION COEFFECIENTS AND SPECIFIC GRAVITY FOR NON-CLAY MINERALS

Mineral	Basal Spacing, d(Å)	Peak Amplitude A (c/s)	Mass Attenuation Coefficient, $\mu(cm^2/g)$	Specific Gravity $\rho(g/cm^3)$
	4.26	745		
• Quartz: [1]	3.35	3400	36.38	2.66
SiO_2	2.46	305		
• Dolomite: [2]	2.89	1310	48.83	2.85
$CaMg(CO_3)_2$	2.19	330		
• Apatite: [3]	2.79	284	71.10	3.20
$Ca_5F(PO_4)_3$, 42.2%P_2O_5	2.69	130		
• Wavellite: [4]	8.6	260		
$(AlOH)_3(PO_4)_2 \cdot 5H_2O$,	8.4	340	28.33	2.33
34.5% P_2O_5	4.8	180		
• Crandallite: [5]				
$Ca_{0.7}Sr_{0.3}Al_3(PO_4)_2(OH)_5 \cdot H_2O$,	5.7	-*	44.7	2.9
	2.94	—		
7.26%SrO, 33.1% P_2O_5				
• K Feldspar: [6]				
$KAlSi_3O_8$, 16.9% K_2O	3.24	900	50.48	2.57

Notes:

[1] Average from three samples: clean surficial sand, Central Florida; leached zone sand, Central Florida; sand from Hawthorn Formation, Central Florida.

[2] One sample from Hawthorn Formation, Polk County, Florida.

[3] Average from three samples: white' pebble, Hamilton County, Florida; black pebble, Polk County, Florida; Hawthorn Formation, Polk County, Florida.

[4] Composite from two samples from Central Florida.

[5] Sample from Alachua County, Florida as reported in Blanchard (1972).

[6] Average from three samples from MIT mineral collection.

*A sample of crandallite was not available for X-ray diffraction analyses, hence, the peak amplitude is unknown,

Table 3-2

REFERENCE X-RAY DIFFRACTION PEAK AMPLITUDES AND BASAL SPACINGS FOR Mg SATURATED, GLYCEROL SOLVATED SMECTITE CLAY MINERALS

	First Order Basal Spacing d_{001}			Average Basal Spacing	
Sample	A (c/s)	Width @ A/2 ($2\theta^{\circ}$)	Asymmetry (Low/High)	d_{001} (Å)	C.V. (%)
Wyoming Montmorillonite	5,000	0.50	1.3	17.85	0.25
Washington Ferruginous Smectite	1,600	1.0	1.5	17.98	0.50
Polk County, Florida Smectite (PC-1)	2,500	1.2	1.4	17.82	0.68
Polk County, Florida Smectite (PC-2)	775	1.6	2.3	17.85	0.20

Where: A = peak amplitude in counts/second; d_{001} = first order basal spacing in Angstroms; and C.V. = coefficient of variation.

Table 3-3

REFERENCE MASS ATTENUATION COEFFICIENTS, SPECIFIC GRAVITY AND X-RAY DIFFRACTION PEAK AMPLITUDES AND BASAL SPACINGS FOR Mg SATURATED, GLYCEROL SOLVATED CLAY MINERALS

Mineral	Basal Spacing, d (Å)	Peak Amplitude, A (c/s)	Mass Attenuation Coefficient, μ (cm²/g)	Specific Gravity ρ(g/cm³)
● Total Clay	4.45	90	44.44*	—
● Smectite:	17.8	2000	41.81	2.78
$(Al_{3.35}Fe^{3}_{0.2}Mg_{0.35}Fe^{2}_{0.1})\cdot$				
$(Si_{7.7}Al_{0.3})O_{20}(OH)_4$				
● Illite				
$(Na_{0.07}K_{1.34})\cdot$	10.0	800	50.16	2.81
$(Al_{3.06}Fe^{3}_{0.45}Mg_{0.56}Fe^{2}_{0.07})\cdot$				
$(Si_{6.8}Al_{1.2})\ O_{20}(OH)_4$				
● Palygorskite:	10.5	625		
$(Mg_{1.96}Fe^{2}_{0.03}Al_{1.61}Fe^{3}_{0.37})\cdot$	6.5	60	41.34	2.09
$(Si_{7.79}Al_{0.21})O_{20}(OH)_2\ (OH_2)_4$	5.4	52		
● Kaolinite:	7.14	4000	30.84	2.61
$Al_8Si_8O_{20}(OH)_{16}$				

---

*Average total clay mass attenuation coefficient of 44.44 cm²/g selected from average of smectite, illite and palygorskite mass attenuation coefficients.

Section 4

MINERALOGY OF SELECTED PHOSPHATIC CLAYS

4.1 Introduction

The objective of the present mineralogic analysis is to quantitatively estimate the weight percentage of clay and non-clay minerals in twelve selected phosphatic clays, and establish correlations between mineralogic composition and physical properties (e.g., plasticity, viscosity, settling rate, final settled solids content), if possible. To achieve this objective over 200 X-ray diffraction traces after various pretreatments were obtained. Quantitative estimates of mineral species were then obtained by comparing the phosphatic clay sample X-ray diffraction traces with diffraction traces from reference mineral species and using sample mass attenuation coefficients determined from total chemical data. Since the clay mineral palygorskite has been correlated by previous research (Lamont et al. 1975) to poor settling characteristics, scanning electron microscope examinations were also performed on selected phosphatic clay samples to observe the morphology of the palygorskite clay mineral.

All mineralogic analyses performed on the phosphatic clays are presented and evaluated in this section. The relative peak amplitude ratios determined for each non-clay and clay specie are first presented. The reference mineral X-ray diffraction data summarized in Section 3 were used to convert the measured X-ray diffraction peak amplitudes to relative peak amplitude ratios. The total chemical composition of each phosphatic clay determined via X-ray fluorescence is then presented. Total chemical composition data was used to calculate sample mass attenuation coefficients. Finally, the quantitative mineralogic composition of each phosphatic clay is determined using the combined results from X-ray diffraction mineralogic and X-ray fluorescence chemical analyses,

4.2 Non-Clay Mineral X-ray Diffraction Analyses

The crystalline phases quartz, apatite, dolomite, feldspar, wavellite and crandallite account for the entire non-clay mineral X-ray diffraction trace with basal spacings between 1.45 and 17 Å in random powder mounts from the four size fractions of all phosphatic clay samples analyzed. Table 4-l summarizes mean relative peak amplitude ratios, R_i, for each non-clay mineral in the four size fractions analyzed. The mean relative peak amplitude is determined from the arithmatic average of the relative peak amplitude ratios from each characteristic basal spacing for a specific mineral. For example, the mean relative peak amplitude ratio for quartz is determined from the arithmetic average of relative peak amplitude ratios at characteristic basal spacings of 4.26, 3.35 and 2.46 Å.

4.2.1 Mean Relative Peak Amplitude Ratios

The mean relative peak amplitude ratios indicate that quartz and apatite occur in each clay sample in each size fraction. The apatite mean relative peak amplitude ratios are relatively high, and are the highest of the non-clay minerals for each size fraction. The apatite mean relative peak amplitude ratio is generally the highest in the +105 µm size fraction. In the -105 µm size fraction, the apatite mean relative peak amplitude ratio is reasonably consistent for all samples with a representative value of 34.4% and a standard deviation of 12.2%.

Quartz is the second most dominant non-clay mineral in the coarser size fractions of +105 and 105 - 44 µm, with average mean relative peak amplitude ratio values from all samples of 19.7 and 15.6%, respectively. In the finer size fractions, the quartz mean relative peak amplitude ratios are similar to other non-clay minerals except apatite, generally less than 5.0%.

Dolomite was detected in eleven of the twelve samples analyzed. The mean relative peak amplitude ratios for dolomite are typically less than 12.0% and are generally higher in the finer size fractions. The two samples and size fractions which yield the highest dolomite mean relative peak amplitude ratios, about 25 and 35% for. the Beker and Grace samples, respectively, in the -105 and -44 µm size fractions, are also the same samples and size fractions which yield the lowest apatite mean relative peak amplitude ratios.

Potassium feldspar was detected in the +105 µm size fractions where sufficient sample was available for analysis. The +105 µm size fraction average mean relative peak amplitude ratio from six samples was 3.5%. The feldspar mean relative peak amplitude ratios are generally higher in the larger size fractions (+105 µm and 105 - 44 µm) than in the finer size fractions. For the -105 µm and -44 µm size fractions, the mean relative peak amplitude ratio for feldspar actually represents an upper bound because no allowance was included to account for the presence of the clay mineral palygorskite. Less feldspar, therefore, may be present in the -105 µm and -44 µm size fractions of the Agrico, Hopewell, Occidental and USSAC samples than indicated by the given mean relative peak amplitude ratio.

Wavellite was detected in eight of the twelve samples. The wavellite mean relative peak amplitude ratios were generally higher in the finer size fractions with an overall average of 5.4%. Wavellite was only detected in the +105 µm size frac tion in two of six samples.

Crandallite was present in nine of the twelve samples. Since no reference crandallite sample was available, the X-ray of diffraction peak amplitude in counts per second is reported in Table 5-l rather than the relative peak amplitude ratio. Generally, the mineral crandallite occurs most in the finer size fractions.

Crandallite is a calcium-aluminum hydrous phosphate. When calcium is replaced by strontium, the mineral goyazite (hamlinite) results, which has essentially the same X-ray diffraction trace as crandallite. Based on the chemical composition reported by Blanchard (1972) for crandallite in Alachua County, Florida*, the crandallite in phosphatic clays may be expected to contain 70% crandallite and

---

*The only reference available for crandallite in Florida.

30% goyazite. Based on the X-ray fluorescence chemical analyses presented in Section 4.5.2, some strontium substitution for calcium must exist since the samples with the highest SrO content also display the highest crandallite peak amplitudes (Agrico, Brewster, CF, Occidental and Estech).

Random powder mount X-ray diffraction traces were not obtained for non-clay minerals in the -1 µm size fraction. Comparison of non-clay peaks in selected oriented aggregate specimens from -1 µm size fraction and from -44 µm size fraction are summarized in Table 4-2. As shown, dolomite and wavellite were eliminated in the -1 µm size fraction. Unfortunately, apatite and crandallite, both of which confuse clay peak interpretations, were reduced only slightly in the -1 µm size fraction. Quartz mean relative peak amplitude ratios were slightly reduced in the -1 µm size fraction to approximately 65% of the values occurring for the -44 µm size fraction.

4.2.2 Reliability of Mean Relative Peak Amplitude Ratio

The reliability of the mean relative peak amplitude ratios is indicated by the tabulation of individual relative peak amplitude ratios from the -105 µm size fraction in Table 4-3. The average coefficient of variation from the mean relative peak amplitude ratio on the individual samples was 9.3% for apatite with a range of coefficient of variation from the mean on any given sample ranging from 2.2 to 18.9%. The average coefficient variation from the mean relative peak amplitude ratio was 21.3% for quartz with the range for individual samples varying from 1.1 to 40.2%. The average coefficient of variation from the mean of the two dolomite peaks in any one sample was 18.0% while the range was between 3.9 and 42.1%.

The CF sample displayed the largest variability in the mean relative peak amplitude ratio for both quartz (40.2%) and apatite (18.9%). The coefficient of variation between the two dolomite peaks was the largest for the AMAX sample (42.1%). The largest variation between the three peaks for wavellite was 36.4% for the Estech sample. The +105 µm, 105 - 44 µm and -44 µm size fractions also gave comparable results for the average and range in coefficient of variation for each non-clay mineral. Crandallite relative peak amplitudes were not calculated and potassium feldspar has only one characteristic peak; hence no variability was calculated for these non-clay minerals.

Repetitive tests on separate samples from a single quartz sample established that the coefficients of variation to be expected experimentally should not exceed 7% for the total experimental error. The data summarized in Table 4-3 showed average coefficients of variation between 1.3 to 3.0 times the expected experimental error. This suggests that the larger coefficients of variations may result because the non-clay minerals in the phosphatic clays are not exactly identical to the reference minerals.

4.2.3 Summary

A summary of the non-clay mineral mean relative peak amplitude ratios is presented in Table 4-4. The mean relative peak amplitude ratios for the various size fractions and clay samples indicate the following significant findings:

- Apatite mean peak amplitude ratios are relatively high and are the highest of all non-clay minerals for all size fractions. No one clay, however, consistently yields the highest apatite mean relative peak ampitude ratio for all size fractions.
- Apatite, quartz and feldspar are more dominant in the +105 µm size fraction (sand particle size fraction). Average mean relative peak amplitude ratios are 52.5, 19.7 and 3.5%, respectively.
- Dolomite, wavellite and crandallite are relatively minor mineral species and occur mostly in the -105 µm size fraction (silt and clay particle size fraction). Mean relative peak amplitude ratios for wavellite and dolomite are 5.2 and 8.3%, respectively.

4.3 Total Clay X-Ray Diffraction Analyses

All clay minerals have an X-ray diffraction peak at 4.45 Å that clearly shows in random powder mounts. The amplitude of the 4.45 Å peak from a random powder mount, therefore, is a direct measure of the total clay mineral content of a specimen.

The relative peak amplitude ratios for total clay for various size fractions are summarized in Table 4-5. Although the total clay relative peak amplitude ratio is, as expected, highest in the -44 µm size fraction, the relative peak amplitude ratios are also high in the coarser +105 µm and 105 - 44 µm size fractions. This behavior clearly indicates strong aggregation of clay particles.

Phosphatic clay from Mobil is particularly strongly aggregated and yields the highest relative peak amplitude ratios for the +105 µm and 105 - 44 µm size fractions. Repeating the Mobil -44 µm wet sieving after 30 minutes at high speed in a Waring blender on a slurry adjusted to a pH of 10.0 with NaOH produced no significant change in the Mobil total clay relative peak amplitude ratios. Phosphatic clay from Agrico is also relatively strongly aggregated in the 105 - 44 µm size fraction in comparison to other phosphatic clays.

The random powder mount X-ray diffraction peak detected at 1.50Å indicated that the phosphatic clay samples contained dioctahedral clay; however, there was also a much smaller peak at 1.53Å. The abundant non-clay minerals made it impossible to unambiguously attribute some portion of the 1.53Å peak to trioctahedral clay species. Because the interfering non-clay minerals were only slightly reduced in the -1 µm size fraction, no improvement in possible assignment of triocathedral clay species was expected. A dioctahedral clay contains trivalent **cations** (Al^3, F_e^3, Cr^3) with only two-thirds of the catonic spaces **normally** filled. A trioctahedral clay contains divalent cations (Mg^2,Fe^2, Mn^2,Ni^2 with all cation sites normally filled. Dioctahedral smectite minerals include montmorillonite, beidellite and nontronite. Trioctahedral smectite minerals include hectorite and saponite. Generally, all of these minerals are rare, except for montmorillonite. Illite can occur as either dioctahedral or trioctahedral.

4.4 **Clay Mineral X-Ray Diffraction Analyses**

The clay minerals detected during X-ray diffraction analyses were: smectite, illite; palygorskite; kaolinite; and interstratified clay material. Relative peak amplitude ratios for the clay minerals in the -44 µm size fraction are presented in Table 4-6.

Samples for X-ray diffraction after -1 µm fractioning were selected to include the range of relative peak amplitude ratios. The phosphatic clay samples selected contained the maximum and minimum amount of: smectite (Hopewell and Estech); illite (Beker and Estech); palygorskite (Agrico and CF); and kaolinite (CF and Hopewell).

The -1 µm fractioning was performed to attempt to remove non-clay minerals and, hence, improve the X-ray diffraction peak amplitudes for interpretation of clay minerals. The comparison of relative peak amplitude ratios for clay minerals in the -1 µm and -44 µm size fraction on selected samples is presented in Table 4-7. As shown, all of the clay peak amplitude ratios were enhanced in the -1 um size fraction by factors of 1.44 to 2.27. As was shown in Table 4-3, however, the apatite X-ray diffraction peak amplitude ratios did not change significantly after -1 um fractioning, and the apatite peaks were a conspicuous feature in all X-ray diffraction traces.

4.4.1 Smectite Clay Minerals

Smectite clay minerals were detected in X-ray diffraction traces in all twelve phosphatic clays. The relative peak amplitude ratio averages 18.1% for the twelve samples and ranges from 4.3% for the Estech sample to 42.8% for the Hopewell sample.

Figures 4-l through 4-5 present X-ray diffraction traces for two hydration states for five of the six samples selected for -1 µm fractioning. The optimum hydration for measuring smectite basal spacings is obtained by the magnesium saturated glycerol solvated treatment. Conversely, dehydrated lithium saturated specimens heated at 250°C for 20 hours yield the least desirable X-ray diffraction trace.

Superimposed on Figures 4-l through 4-5 is a horizontal axis labelled S_1 through S_6 indicating the 2θ position for six orders of smectite basal spacing with a mean value of 18 Å*. The 18 Å basal spacing was an approximate reference to provide a consistent reference line for all samples. The actual basal spacing selected for smectite was 17.8 Å (Table 3-3). Also, note the amplitude scale change on each figure between 9^0 and 13^0 2θ. For 2θ values between 0^0 and 9^o-13^0 the scale on the right axis is the appropriate scale. For values above 9^o-13^0 2θ, the scale on the left axis is the appropriate scale. For very strong peaks, a section of the amplitude scale is omitted to effectively illustrate the essential features of each peak.

The X-ray diffraction trace for the Hopewell sample, which gave the highest smectite relative peak amplitude ratio, is shown on Figure 4-5. The X-ray diffraction trace for the Estech sample, which gave the lowest smectite relative peak amplitude ratio, is shown in Figure 4-4. The difference in the peak amplitude at the first order basal spacing, S_1, between the two samples is clear: for Hopewell A_{001} is ten times greater than for Estech.

For higher orders of smectite basal spacing only the 3rd and 6th orders are in an angular region of the X-ray diffraction traces relatively free from interference from other clay. diffraction peaks. The second order peak, S_2, commonly was a shoulder on the high angle side of the 10Å illite peak as shown in Figure 4-2 and 4-4 at about 9.5^0 2θ. The 4th order peak, S_4, coincides with the general clay prism peak at about 4.45Å, which for palygorskite does not decrease upon orientation as evident in Figure 4-l at about 19.5^0 2θ. The effect of kaolinite obscuring the 5th order, S_5, peak is obvious from comparing Figure 4-3 and 4-5 where both samples were high in smectite. Diffraction peaks from apatite and crandallite interfere with the 3rd to 6th order smectite peaks as shown in Figure 4-4 at about 30^0 2θ. In spite of these interferences, however, the higher orders were still observed.

A measure of the variation in mean basal spacing and deviations from the mean are given in Table 4-8. As shown, the smectite clay mineral mean basal spacing for all samples was greater than the 17.8Å basal spacing selected for the refer-

---

*The relation between basal spacing, d, and angle at which diffraction occurs, θ, is given by Bragg's law:

$$n\lambda = 2d \sin\theta$$

where: n = integral number of wave lengths
λ = wave length of incident X-ray
d = atomic plane spacing
θ = angle at which diffraction occurs

For smectite with an average basal (n = 1) spacing of 18Å the corresponding 20 angles for the first order basal reflection (n = 1) through the sixth order (n = 6) reflection are 4.87^0, 9.75^0, 14.64^0, 19.57^0, 24.53^0 and 29.54^0 20. The wave length of the CuKa X-ray is 1.5418 Å.

ence smectite. The average mean basal spacing from the twelve samples for the -44 um size fraction was 18.3Å with a range of 18.1 to 18.6Å. Mean basal spacings determined from -1 µm size fraction samples did not indicate significantly different mean values, and the coefficient of variation of the mean basal spacing increased in four of six samples.

The coefficient of variation of the mean basal spacing shown in Table 4-8 is a measure of the degree of disorder in the smectite mineral phase. The reliability of the coefficient of variation as a quantitative indication of disorder in the smectite phase must be tempered by non-clay and other clay mineral peak interferences. Novich and Martin (1981) showed that the common practice of omitting the S_1 peak when computing the mean spacing is erroneous, because for a properly prepared specimen the coefficient of variation of the mean basal spacing will decrease if the first order peak is included. Generally, a coefficient of variation greater than 0.50% indicates interstratification. The observed coefficients of variation of 1.1 to 3.2%, therefore, clearly indicate interstratification of the clay phases (i.e., illite-smectite, kaolinite-smectite).

4.4.1.1 Satellite Peak Behavior

The high coefficient of variation for the smectite clay phase is an indicator of interstratification. Further evidence of interstratification is provided by additional satellite peaks in the 20 range of 5.2 to 7.5^0 that are not associated directly with smectite or illite clay phases and whose position varies with hydration state.

Table 4-9 and 4-10 summarize the behavior of the smectite clay phase satellite peak positions for various treatments for the -44 µm and -1 µm size fractions for various treatments, respectively. The -44 um size fraction samples are arranged in five groups based upon the satellite peak position for magnesium saturated glycerol solvated specimens. As shown, only one of six potassium homoionic saturated specimens showed a satellite peak after heat treatment, while all magnesium homoionic saturated specimens showed satellite peaks.

The satellite peak behavior for -1 µm size fraction magnesium saturated glycerol solvated specimens and homoionic lithium saturated specimens is shown in Table 4-10. The X-ray diffraction traces for the homoionic lithium saturated specimens after heating at 250°C for 20 hours are also shown on Figures 4-1 through 4-5. The satellite peak at a spacing of 14Å at $6.3^0$20 for homoionic lithium saturated specimens after heating at 250°C for 20 hours is not pronounced for the Estech sample (Figure 4-4), is very questionable for the Agrico sample (Figure 4-1) and appears clearly for the Beker, CF and Hopewell samples.

Glycerol treatment of lithium saturated heated specimens fall into three categories. As shown in Table 4-10, samples from Agrico and CF expanded to yield a clearly defined 18Å peak. Specimens from AMAX, Beker and Hopewell indicated expansion but gave no definite peak. The lack of observed rehydration for the Estech sample may reflect the small amount of smectite clay minerals present, or that the smectite clay is a montmorillonite.

4.4.1.2 Summary

The X-ray diffraction analyses performed to determine the type and quantity of smectite clay minerals present within phosphatic clays indicate that smectite is clearly present in all twelve phosphatic clays tested. The large coefficients of variation determined for the smectite basal spacing indicate however, that the smectite, in the phosphatic clays is different from the reference smectite and that the clays are interstratified. The variation in behavior of the smectite peaks and satellite peaks between various phosphatic clay samples also indicates that the smectite minerals vary between clay samples and that the clays are interstratified. The relative peak amplitude ratios for smectite shown in Table 4-6, therefore, contain some inaccuracy.

The specific type of smectite clay present in the phosphatic clays was not identified as part of this study. As discussed in Section 3.3.1, however, the smectite clay in phosphatic clays is likely not montmorillonite based on the absence of expansion after glycerol solvation of heated lithium saturated phosphatic clays. Based on the common presence of iron in phosphatic clays, some researchers have implied that the smectite may be nontronite. No additional evidence was collected in this investigation, however, to substantiate this hypothesis,

4.4.2 Illite Clay Minerals

Illite was detected in all twelve clay samples. The relative peak amplitude ratio ranges from a low of 5.0% for the Estech phosphatic clay to a high of 17.5% for the Beker phosphatic clay sample, with an average of 10.6%. The illite relative peak amplitude ratios for the Agrico and Oxy samples were indeterminate due to high palygorskite peaks in the same 2θ angular region of the X-ray diffraction trace. Figure 4-l illustrates the high palygorskite peak- ~~am~~plitudes in the -1 μm size fraction of the Agrico sample near the 8° and 18° **2θ** region where the illite peaks occur. Conversely, the illite peak amplitudes are clearly visible for the -1 μm size fraction of the Beker sample at 8.9°, 17.9° and 26.8° 2θ in Figure 4-2. These reflection angles yield to a mean basal spacing of about 9.72 Å, which agrees more or less with the reference basal'spacing of 10.0Å . The coefficient of variation of the three peaks from the mean basal spacing is 0.35%.

4.4.3 Kaolinite Clay Minerals

Kaolinite was detected in eleven of twelve phosphatic clays. All kaolinite relative peak amplitude ratios, however, are relatively low, with an average of 1.0% and a range of 0.0% for the Grace sample to 2.3% for the CF sample. The low relative peak amplitude ratios indicate that the weight percent of kaolinite in phosphatic clay is small in comparison to smectite, illite and palygorskite clay minerals.

The maximum kaolinite relative peak amplitude ratio was found in the CF sample. Figure 4-3 illustrates the kaolinite peaks in the -1 μm size fraction of the CF sample at 12.4° and 24.9° **2θ**which correspond to the first and second order reflections for a mean basal spacing of 6.95 Å and a coefficient of variation of 0.20%. The kaolinite peaks for the -1 μm size fraction of the Estech sample, which indicates the second highest kaolinite relative peak amplitude ratio, are also clearly visible in Figure 4-4 at 12.3 and 25.1° 2θ.

The basal spacing of kaolinite is insensitive to drying or moderate heating, but is destroyed by heating to 500°C. The kaolinite phase in the Mobil sample was destroyed by heat at 450°C while the USSAC sample required 550°C to destroy the kaolinite phase. At 450°C the first order kaolinite peak was a clearly defined doublet in the USSAC sample with equal amplitudes at 7.5Å and 7.2Å. Heating to 500°C restored the single peak at 7.14Å with half the amplitude that was observed after heating at 300°C. The kaolinite in the Agrico, Brewster and Occidental samples was destroyed at 500°C as typically occurs for kaolinite.

4.4.4 <u>Palygorskite Clay Minerals</u>

Palygorskite was detected in X-ray diffraction traces in ten of twelve phosphatic clays. Palygorskite relative peak amplitude ratios ranged from 0.0% in the CF and Brewster samples to 26.4% in the Agrico sample. The average palygorskite relative peak amplitude ratio was 11.1% for the twelve samples tested.

A comparison of Figures 4-1 and 4-3 illustrates X-ray diffraction traces for samples with the maximum and minimum amount of palygorskite, respectively. The -1 µm size fraction X-ray diffraction trace for the CF sample (Figure 4-3) indicates no palygorskite peaks. The -1 µm size fraction X-ray diffraction trace for the Agrico sample (Figure 4-1) clearly indicates palygorskite peaks at 8.4°, 13.7° , 16.3°, and 27.3° **2θ.** These peaks yield the three characteristic basal spacings of 10.4, 6.5 and 5.4 Å.

4.4.4.1 Palygorskite Spiking

The Brewster and CF phosphatic clay samples did not contain palygorskite clay minerals as indicated by X-ray diffraction analyses. To determine ‘the minimum amount of palygorskite detectable with X-ray diffraction analyses, palygorskite spiking was performed on the CF sample.

Palygorskite was added to a slurry of CF phosphatic clay to produce palygorskite contents of 10.9 and 24.5% by weight assuming that no palygorskite was present in the original sample. Three specimens were then prepared for X-ray diffraction analyses from each spiked slurry and the original unspiked sample. Each specimen was X-rayed four times. No differences in the X-ray diffraction traces were observed between specimens at the same palygorskite concentration. Very slow scanning produced no significant improvement in counting statistics. The measured maximum, minimum and mean peak amplitudes for the three characteristic palygorskite peaks are summarized in Table 4-11.

Based on the X-ray diffraction data summarized in Table 4-11, it appears that X-ray diffraction analyses can detect palygorskite contents of 10%. The data for the 10.5Å position in the original CF slurry was not from a peak, but rather was produced by the broad flat high background between the 18Å smectite and 10Å illite peaks. All data for the 10.9 and 24.5% palygorskite additions produced discrete peaks.

The weight percent palygorskite in each spiked sample was calculated using the X-ray diffraction peak amplitudes summarized in Table 4-11, reference palygorskite data shown in Table 3-3 and the CF sample mass attenuation coefficient determined from X-ray fluorescence analyses. The sample spiked with 10.9% palygorskite was found to actually contain 16.2 ± 3% palygorskite and the sample spiked with 24.5% palygorskite was found to actually contain 26.6 ± 5% palygorskite. Assigning all of the excess palygorskite content found by calculation as the original undetected palygorskite content of the CF sample indicates that the CF sample may contain: 3.7 ± 4.1*% palygorskite using peak amplitudes from all three basal spacings; or 5.7 ± 2.1*% palygorskite using the 10.5 Å peak amplitudes only. An X-ray diffraction detection limit of 5% for palygorskite, therefore, appears reasonable.

4.4.4.2 Scanning Electron Microscope Examination

Scanning electron microscope examinations were performed on the reference mineral palygorskite and seven phosphatic clay samples. The scanning electron microscope examinations were performed to visually observe the relative quantity of palygorskite in each clay sample and determine the general crystal morphology of the palygorskite clay mineral. Typically, palygorskite displays a long, fibrous morphology with a length of 4-5 µm and width of about 100 Å (Mitchell, 1976). A total of 25 scanning electron photomicrographs are presented for the seven clay samples studied. The photomicrographs presented represent a small fraction of the total area visually examined for a particular sample.

The -1 µm size fraction of the palygorskite reference clay was prepared from a slurry (Section 2.3) and displayed typical brush heap morphology at a magnification of 2,000X as shown in Figure 4-6A. Increasing the magnification to 20,000X (Figure 4-6C) reveals that the individual fibers are narrow, long and flexible as typical for the morphology of palygorskite. The non fibrous lumps in Figures 4-6A and 4-6B contained high concentrations of calcium and phosphorous as determined by energy dispersive analyses by X-ray (EDAX) which were presumed to be apatite.

Scanning electron photomicrographs of the Agrico sample, which contained the greatest amount of palygorskite, are shown in Figure 4-7. Figures 4-7A and 4-7B are from fractured lump samples (Section 2.3) and Figure 4-7C is from a slurry sample. As shown, long fibrous palygorskite is prevalent in the Agrico sample. In Figures 4-7A and 4-7B, the palygorskite fibers appear to be coating other clay minerals. Gel was not observed during the examination.

No evidence of palygorskite was apparent in the Brewster specimen prepared from a fractured lump (Section 2.3) below a magnification of 10,000X, which suggests that palygorskite is not abundant. Long fibers were very rare as shown by the photomicrographs in Figure 4-8, which agrees with the absence of palygorskite in

---

* ± one standard deviation.

the X-ray diffraction trace. Very stubby fibers, however, were common. Adequate chemical composition of the stubby fibers was impossible to obtain because of their small size and scattered distribution. Since palygorskite was not detected by X-ray diffraction of the Brewster clay, the stubby fibers may be wavellite and not palygorskite. The light appearing grains in Figure 4-8B were apatite based upon similar morphology to apatite grains of sufficient size to permit reliable chemical data. From the center of Figure 4-8A and spreading to the right there also appears to be considerable gel.

No evidence for palygorskite from scanning electron microscope examinations was found on the fractured lump specimen prepared from CF clay. The long fiber palygorskite shown in Figure 4-9 was a rare occurrence, in the slurry preparation from CF clay. The general impression from all areas examined was gel as illustrated by Figure 4-9B. Palygorskite clay was also not detected in X-ray diffraction traces from the CF clay samples.

Fractured lump sample preparations from Mobil phosphatic clay contained abundant long fibrous palygorskite as evident in Figure 4-10. Very little evidence for gel was observed in the sample. X-ray diffraction analyses on Mobil clay indicated a relatively low palygorskite relative peak amplitude ratio of 7.2%. The abundant palygorskite visually observed in the photomicrographs, however, indicates that a higher value may be more appropriate.

Smectite, gel, and palygorskite were all abundant in the Occidental sample. Figure 4-11A shows a typical smectite morphology. Abundant gel is obvious in Figure 4-11C. The substrate in Figure 4-12C also is gel. Palygorskite was present in the Occidental samples as very long fibers as shown in Figures 4-12B and 4-12C. The rather short palygorskite fibers in Figure 4-12A were also palygorskite in contrast to the stubby fibers in the Brewster sample (compare Figure 4-8A and 4-12B).

Figure 4-13 illustrates photomicrographs from USSAC phosphatic clay prepared from fractured lumps (Figure 4-13A) and from slurry (Figures 4-13B and 4-13C). The clay minerals smectite and palygorskite are shown in Figure 4-13A, while Figures 4-13B and 4-13C prominently illustrate the non-clay mineral wavellite. The wavellite crystals are lath shaped with very straight edges. In comparison to palygorskite, the wavellite laths are wider, larger and straighter. The difference in morphology between palygorskite and wavellite is clearly illustrated in the lower half of Figure 4-13C where palygorskite fibers are covering a bundle of wavellite laths. Some gel was also observed in the USSAC samples, but was not a significant constituent.

In summary, the scanning electron microscope examinations indicate that gel was particularly abundant in the Occidental, CF and IMC samples, but is a minor constituent in the Agrico, Mobil and USSAC samples. Chemically the gel had no distinctive feature being composed of clay minerals and apatite. Fine grained crystalline material suspended in the gel may have contributed to the overall gel chemistry.

The difficulty in locating palygorskite in the CF and Brewster clay samples during scanning electron microscope examinations is consistent with the absence of palygorskite in the X-ray diffraction trace. The visually observed relative order of abundance of palygorskite in the photomicrographs of Agrico, Occidental, USSAC and Mobil in comparison to the CF and Brewster samples is also consistent with X-ray diffraction analyses. The palygorskite typically displayed long, fibrous morphology. Some short, stubby palygorskite was also found in the Occidental sample. In all samples the palygorskite was found to be coating other clay minerals or amorphous gel, rather than existing as individual aggregates of palygorskite.

X-ray diffraction analyses indicated that USSAC clay was relatively high in wavellite, which agrees with visual observation of relatively numerous amounts of wavellite bundles in the photomicrographs. The lack of wavellite observations during examination of the Occidental sample, which the X-ray diffraction analyses indicate contains the highest amount of wavellite, is attributed to the abundent gel present in the Occidental sample. The similarity in wavellite content between the Brewster and USSAC clay samples based on X-ray diffraction analyses (Table 4-l) indicates that the stubby fibers in Figure 4-8 are wavellite rather than palygorskite.

4.5 **Chemical Composition**

The total chemical compositions of the phosphatic clay samples were determined with X-ray fluorescence as described in Section 2.5. Organic matter contents were determined with the Walkley-Black method described in Section 2.4.

4.5.1 Organic Matter Content

Organic matter contents determined for the twelve phosphatic clay samples are summarized in Table 4-12 and illustrated in Figure 4-14. The organic matter contents are the arithmetic mean from two determinations. The coefficient of variation from the mean was generally less than 0.10%.

The maximum organic matter content of 3.0% was measured on the CF sample and the minimum value of 0.3% was measured on the Hopewell sample. The average organic matter content from all twelve samples is 1.3 ± 1.0*%. When the CF, Beker and Occidental samples are deleted from the average, the mean organic matter content reduces considerably to 0.7 ± 0.2*%. The CF, Beker and Occidental samples yield obviously higher (about 400% higher) organic matter contents than the remaining nine clay samples, with a mean value of 2.8 ± 0.2*%.

---

*± one standard deviation.

4.5.2 Total Chemical Composition

The total chemical compositions of the phosphatic clays were determined from X-ray fluorescence chemical analyses on the -44 um size fraction*. The various oxides detected and weight percent of each oxide in the clay samples are presented in Table 4-13. As shown, the summation of the constituents averages 100.79% with a relatively small coefficient of variation of 0.73%.

Based on the mean weight percent of each oxide, four constituents comprise 72.8% of the phosphatic clays: S_iO_2, Al_20_3, Ca0 and P_20_5. The variation from the mean of each oxide is significant, as s own by coefficients of variation of 13.2 to 72.5%, indicating that an "average" total chemical composition for the phosphatic clays is not meaningful.

4.5.3 Mass Attenuation Coefficient

Sample mass attenuation coefficients, μ_s, are shown in Table 4-13 for each clay. The coefficients were calculated from total chemical data using elemental mass attenuation coefficients for CuKa radiation given in the International Tables for X-ray Crystallography$_2$ (1974). The sample mass attenuation coefficients range from 49.5 to 58.9 cm^2/g with a mean value of 52.8 cm^2/g. The coefficient of variation of 6.1% is relatively low, and suggests that the mean value may be used for other phosphatic clays with reasonable reliability.

4.6 **Quantitative Mineralogic Evaluation**

4.6.1 Methodology

To convert relative peak amplitude ratios, R_i, into quantitative estimates of weight fraction, X_i, for a given mineral requires the following assumptions:

- the reference minerals used to determine the relative peak amplitude ratios, R_i, and mass attenuation coefficients, u_i, derived from ideal chemical composition are identical to the mineral phase in the unknown sample; and
- the total chemical composition and calculated sample mass attenuation coefficients, μ_s, are correct for the unknown sample.

For multicomponent mixtures, the equation to compute the weight fraction, X_i, of a given component is in its simplest form:

$$X_i = R_i (\mu_s/\mu_i) \qquad (1)$$

---

*The Grace sample was received after chemical analyses were performed; hence no chemical composition was determined for the Grace phosphatic clay.

For eleven of twelve clays studied, the chemical composition determined in Table 4-13 for the -44 µm size fraction permitted a reliable calculation for the value of u_s. Using sample mass attenuation coefficients, relative peak amplitude ratios in Tables 4-l and 4-6 and mineral mass attenuation coefficients in Tables 3-l and 3-3, the -44 µm weight fraction of each mineral, except crandallite*, is easily calculated.

The significance of the mass attenuation coefficient is illustrated in Figure 4-15 for a simple two component mixture of apatite and quartz. For a mixture of mineral phases, the summation of all components should equal 100%, hence:

$$1.00 = \sum X_i \tag{2}$$

Further, the sample mass attenuation coefficient, μ_s is equal to the sum of the contribution from each component:

$$\mu_s = \sum \mu_i X_i \tag{3}$$

Applying Equations 1, 2 and 3 to a quartz-apatite binary mixture permits calculation of the relative peak amplitude ratio, R_i, for any weight fraction, X_i, as follows:

$$R_q = X_q \mu_q / (X_q(\mu_q - \mu_a) + \mu_a) \tag{4}$$

$$R_a = X_a \mu_a / (X_a(\mu_a - \mu_q) + \mu_q) \tag{5}$$

where R_q and R_a are the relative peak amplitude ratios for quartz and apatite, respectively, and μ_q and μ_a are the mass attenuation coefficients for quartz and apatite, respectively.

As shown in Figure 4-15, the deviation from linearity between R_i and X_i is significant. For example, a quartz-apatite mixture with 50% quartz by weight yields a quartz relative peak amplitude ratio, R_q, of 33.8% whereas the apatite relative peak amplitude ratio, R_a, is 66.2%.

4.6.2 Mineralogic Composition of -44 µm Size Fraction

The mineralogic composition computed for the -44 µm size fraction of each clay using the methodology described above is presented in Table 4-14. The total chemical composition data (Table 4-13) permitted calculation of the sample mass attenuation coefficient, hence no assumption regarding the summation of the mineral species was necessary. For the Grace clay sample, the mean sample mass attenuation coefficient determined from the other eleven clays of 52.84 cm^2/g was used to calculate the weight fractions of each mineral.

---

*Since no reference mineral for crandallite is available, no relative peak amplitude ratios were determined for crandallite.

The crandallite weight fraction was calculated assuming that all of the SrO determined from chemical analyses (Table 4-13) was in the crandallite and that the composition of the crandallite in the sample was 70% ideal crandallite and 30% goyazite. Crandallite clearly was indicated by X-ray diffraction data for the Agrico, Brewster, CF, Occidental and Estech samples. No X-ray diffraction evidence for crandallite was obtained on specimens from the Beker, Grace and Hopewell samples. For the remaining samples, a trace of crandallite was probable based upon X-ray diffraction data.

4.6.2.1 Non-Clay Minerals

The non-clay minerals account for 35.6 to 58.9% of the -44 μm size fraction of phosphatic clay material. The mean summation of non-clay minerals from the twelve samples is 48.2% with a coefficient of variation of 15.4%. The mean value, therefore, is reasonably reliable to allow the conclusion that non-clay minerals, on the average, account for about 50% of the minerals within phosphatic clays.

The dominant non-clay mineral is clearly apatite. The apatite weight fraction varies from 6.6 to 40% with a mean value of 26.3%, or about 54% of the mean summation of all non-clay minerals. The apatite weight fraction coefficient of variation of 40.5%, however, precludes selecting one reliable mean apatite weight fraction as typical for phosphatic clays, although all phosphatic clays contain some apatite. The apatite weight fraction is real, because there is good correlation between the chemically determined P_2O_5 content and the X-ray diffraction apatite weight fraction. The correlation for the actual data, shown in Figure 4-16, yields a slope of 2.28 which is within 3.8% of the ideal slope of 2.37 used for ideal apatite with 42.2% P_2O_5. The correlation coefficient, r, of 0.87 indicates that 76% of the P_2O_5 variation is accounted for by the apatite content. The intercept for this regression, however, implies 5.57% apatite occurs for 0% P_2O_5. A more physically satisfactory regression constrained through the origin yields a slope of 2.78, which implies an apatite P_2O_5 content of 36.0%. Using a multivariate analysis to determine the correlation between the P_2O_5 content and the X-ray diffraction weight fraction of apatite, wavellite and crandallite, all of which contain P_2O_5, indicates the relation:

$$W_{P_2O_5}=0.251(X_a)+0.111(X_w)+1.523(X_c) \qquad (6)$$

where X_a, X_w, and X_c, are the apatite, wavellite and crandallite weight fraction, respectively. The correlation was restrained to provide a zero intercept*. The calculated correlation coefficient for the relation is 0.997, indicating that more than 99% of the variation in the P_2O_5 content is explained by considering all three minerals.

---

*The correlation from multivariate analyses not constrained to provide a zero intercept is: $W_{P_2O_5} = 0.993 + 0.215\ (X_a) + 0.102\ (X_w) + 1.655\ (X_c)$ with a correlation coefficient of 0.968. For 0% apatite. wavellite and crandallite, this correlation implies the occurrence of 0.99% P_2O_5.

The quartz content of -44 µm phosphatic clay particle size fraction ranged from 2.4 to 8.0% by weight, with a mean value of 5.5% (see Table 4-14). The dolomite content was more variable ranging from a low of 0% to a high of 38% with a mean value of 8.7%. The correlation between dolomite and the MgO content of the samples is shown in Figure 4-17. The correlation coefficient of 0.96 indicates that 92% of the MgO variation is accounted for by the dolomite content. The slope of the regression line between the dolomite and MgO contents is within 1% of the slope expected for ideal dolomite composition with 21.7% MgO.

Crandallite and feldspar are relatively small constituents in the -44 µm size fraction, comprising 0.0 to 3.5% and 0.0 to 0.4% of the clay samples, respectively. The wavellite content of the clays is 0.0% for six of the clays and ranges from 9.6 to 19.0% with a mean value of 12.9% for the remaining six clays.

4.6.2.2 Clay Minerals

The clay mineral smectite was present in all samples and was the most abundant clay mineral in eight of the twelve samples. The smectite content varied over a wide range from 6.0 to 51.0%, with a mean value of 22.3%.

Illite was present in all samples. The illite content varied from 4.5 to 18.0% with a mean value of 10.3%. Illite weight fractions determined from the X-ray diffraction (analyses correlated reasonably with the chemically determined K_2O content. The relationship shown in Figure 4-18, has a correlation coefficient of 0.82 and a slope of 13.5 which agrees within 7.7% with the slope of 12.5 for ideal illite with 8.0% K_20. The observed slope of 13.5 suggests that either the illite in the phosphatic clays contains only 7.4% K_20, instead of 8.0%, or that the refer-, ence amplitude for illite should be larger by about 6.0%. The 10 Å) illite peak was indeterminant in the Agrico and Occidental samples, although the 5 Å peak was present. The weight percent of illite in these samples shown in Table 4-14 and Figure 4-18, therefore, was calculated from the K_2O content assuming ideal illite with a K_2O content of 8.0%.

Palygorskite was the most abundant clay phase in four of the ten samples as detected by X-ray diffraction analyses. The palygorskite weight fraction varied considerably from 0.0 to 35.0%, with an average of 14.1%. As discussed in Section 4.4.4.1, the CF and Brewster samples may actually contain as much as 5% palygorskite.

Kaolinite is a minor clay phase in all samples. The kaolinite content varied from 0.0 to 3.8% with a mean value of 1.8%.

4.6.2.3 Total Clay Content

The weight fraction of total clay calculated from the 4.45 Å clay prism peak generally exceeds the total clay content calculated from the summation of individual clay minerals. The weight fraction of total clay calculated from the 4.45 Å peak varied from 50 to 89%, with a mean value of 70.1%.

The summation of individual clay mineral phases yielded total clay contents of 25.1 to 85.3%, with a mean value of 48.5%. The two samples with the highest summation of clay minerals, AMAX and Hopewell, were also the highest in smectite content. Three samples, Brewster, Grace and Estech, indicate very low clay mineral summations. The very low clay mineral summation for these samples is ascribed to interstratificatied clay material and/or amorphous clay material that gave no X-ray diffraction peaks at basal spacings characteristic of specific clay minerals, but did contribute to the total clay 4.45 Å peak.

4.6.2.4 Total Mineral Summation

The total mineral summation for each sample based on the non-clay mineral summation and clay mineral summation from individual clay phases is presented in Table 4-14. Six of twelve samples (Agrico, Beker, IMC, Mobil, Oxy, USSAC) give a total mineral summation close to l00%, which suggests that the reference minerals can be applied to these phosphatic clays. The six samples give a mean total mineral summation of 99.5% with a coefficient of variation of 5.7%. Four samples, Brewster, CF, Estech and Grace yield relatively low total mineral summations of 82.7, 80.6, 84.7 and 73.2%, respectively. If the Brewster and CF samples are assumed to contain 5%. palygorskite, the individual mineral summations of these samples improve to 87.7 and 85.6%. (Based on palygorskite spiking, the CF sample probably contains 5% palygorskite and the 85.6% summation is a more appropriate value.) Two samples, AMAX and Hopewell, yield high total mineral summations of 121.4 and 120.9%, respectively.

Table 4-14 also presents the total mineral summation based on non-clay individual mineral summation and total clay determined from the 4.45 Å peak. Five of twelve samples (AMAX, Beker, Estech, Grace and Hopewell) give a summation close to 100% whereas the other seven samples yield summations in excess of 120%. The Beker sample is the only clay which consistently yielded a total mineral summation of about 100% based on both total clay and individual clay mineral summations.

The scatter in the summations in Table 4-14 is indicative of the degree of accuracy of the methodology used to quantify the mineralogic composition of phosphatic clays; i.e., reliability of reference minerals and mass attenuation coefficients, interpretation of XRD traces complicated by peak interferences, clay phase interstratification and detection limits. Table 4-15 was prepared from Table 4-14 in an attempt to normalize the mineralogic composition to a 100% summation. This was done for the sake of consistency with the understanding that results in Table 4-15 are in no way more accurate than those in Table 4-14.

Although the mineralogic composition in Tables 4-14 and 4-15 is specifically for the -44 µm size fraction, the corresponding particle sizes generally comprise more than 90% by weight of phosphatic clays. Hence, composition of the -44 µm size fraction can also be used to represent the composition of bulk phosphatic clay.

4.6.3 Mineralogic Composition of 105-44 µm Size Fraction

The mineralogic composition of the 105-44 µm size fraction is presented in Table 4-16. Sufficient' material for' X-ray diffraction analysis was only available from nine of twelve clay samples after sample preparation. Since the sample mass attenuation coefficients for the 105-44 µm size fraction materials were not determined, the weight fraction for each mineral was calculated assuming that the minerals detected by X-ray diffraction accounted for 100% of the specimen.

The total clay content in the 105-44 µm size fraction was determined based on the 4.45 Å peak. A total clay mass attenuation coefficient of 44.44 cm^2/g was assumed based on the arithmetic mean from the smectite, illite and palygorskite clay mass attenuation coefficients (Table 3-3)*. The individual clay mineral phases in the 105-44 um size fraction were not determined.

4.6.3.1 Non-Clay Minerals

The results achieved with this procedure indicate that apatite is the dominant non-clay mineral in five of the nine samples analyzed. The apatite content ranged from 15.4 to 36.5% with a mean value of 23.2%. The quartz content is generally highest or second highest of the non-clay minerals with a range of 5.6% to 55.9% and a mean value of 24.3%. Wavellite varied considerable from 0% to 45.6% with a mean value of 12.5%.

The non-clay minerals dolomite, feldspar and crandallite were all relatively minor components in the 105-44 µm size fraction. Dolomite ranged from 0% to 9.8% and averaged 3.1%. Feldspar was present in six of nine samples, with a weight fraction varying from 0 to 12.3% and averaging 3.7%. Crandallite was detected in only one sample in the 105-44 µm size fraction.

In summary, the 105-44 µm size fraction generally contains approximately three times more quartz than the finer -44 µm size fraction. The occurrence of apatite is approximately the same in both size fractions. Wavellite and crandallite are slightly more prevalent in the 105-44 µm size fraction whereas the dolomite content is substantially lower. The feldspar, while still a minor component in the 105-44 µ size fraction, is more prevalent than in the -44 µm size fraction.

4.6.3.2. Total Clay Content

The total clay 4.45 Å peak was detected in eight of nine 105-44 µm size fraction specimens. The total clay contents determined from this characteristic peak ranged from 0% to 71.7% and averaged 31.3%. The presence of clay in the 105-44 µm size fraction indicates that the clays are aggregated.

---

*The mineral mass attenuation coefficient for kaolinite was not included in the arithmetic average since kaolinite was found to be a minor clay mineral in the -44 µm size fraction.

4.6.3.3 Reliability of Mineral Summation

The summation of the individual mineral weight fractions for each sample based on recalculated sample mass attenuation coefficients and measured mean relative peak amplitude ratios are presented in Table 4-16. The sample mass attenuation coefficients were calculated using: the reference non-clay mineral mass attenuation coefficients given in Table 3-l and an average value of 44.44 cm^2/g for total clay; and weight fractions determined assuming that the detected minerals accounted for 100% of the sample.

As shown, for six of the clay samples (Agrico, AMAX, IMC, Mobil, Occidental and USSAC), the calculated summation is not significantly different from the assumed summation of 100%. For three clay samples, Beker, CF and Hopewell, the calculated summations are substantially lower than the assumed summation. Overall, however, the mineralogic composition for the 105-44 um size fraction is considered representative.

4.6.4 Mineralogic Composition of +105 μm Size Fraction

The mineralogic composition of the +105 μm size fraction, or sand size fraction, is presented in Table 4-17. Sufficient material for X-ray diffraction analysis was only available from six of twelve clay samples after sample preparation. Since the sample mass attenuation coefficients for the +105 μm size fraction materials were not determined, the weight fraction for each mineral was calculated assuming that the minerals detected by X-ray diffraction accounted for 100% of the specimen.

The total clay content in the +105 μm size fraction was determined based on the 4.45 Å peak. A total clay mass attenuation coefficient of 44.44 cm^2/g was assumed based on the arithmetic mean from the smectite, illite and palygorskite clay mass attenuation coefficients (Table 3-3)*. The individual clay mineral phases in the +105 μm size fraction were not determined.

4.6.4.1 Non-Clay Minerals

The results achieved with this procedure indicate that apatite is the dominant non-clay mineral in four of the six samples analyzed. The apatite content varied from 20.1 to 67.5% with a mean value of 46.1%. Where apatite is not the major nono-clay mineral, the quartz content is highest of the non-clay minerals. The quartz content varies significantly, with a range of 6.6% to 64.4% and a mean value of 33.3%. The +105 μm size fraction generally contains approximately twice and six times more apatite and quartz, respectively, than the finer -44 μm size fraction.

---

*The mineral mass attenuation coefficient for kaolinite was not included in the arithmetic average since kaolinite was found to be a minor clay mineral in the -44 μm size fraction.

The non-clay minerals dolomite, feldspar, wavellite and crandallite were all relatively minor components in the +105 µm size fraction. Dolomite was detected in three of six samples with a gross average weight fraction of 1.6%. Feldspar was present in all six samples, with a weight fraction varying from 1.0 to 9.8% and averaging 4.3%. Crandallite was not detected in the +105 µm size fraction. Wavellite was detected in two of six samples. Except for feldspar, all these minor non-clay minerals are less prevalent in the +105 µm size fraction than in the -44 µm fraction.

4.6.4.2 Total Clay Content

The total clay 4.45 Å peak was detected in three of six +105 um size fraction specimens. The total clay contents determined from this characteristic peak were 11.9, 15.3 and 42.3% for the Agrico, CF and Mobil smaples, respectively. The presence of clay in the +105 µm size fraction indicates that the clays are strongly aggregated, particularly in Mobil phosphatic clay.

4.6.4.3 Reliability of Mineral Summation

The summation of the individual mineral weight fractions for each sample based on recalculated sample mass attenuation coefficients and measured mean relative peak amplitude ratios are presented in Table 4-17. The sample mass attenuation coefficients were calculated using: the reference non-clay mineral mass attenuation coefficients given in Table 3-l and an average value of 44.44 cm^2/g for total clay; and weight fractions determined assuming that the detected minerals accounted for 100% of the sample.

As shown, for four of the clay samples (Agrico, CF, Mobil and Occidental), the calculated summation agrees well with the assumed summation of 100%. For two clay samples, AMAX and Hopewell, the calculated summations are 20 and 28%, respectively, below the assumed summation. Overall, however, the weight fractions presented in Table 4-17 are considered representative.

4.6.5 Overall Mineralogic Composition of Phosphatic Clays

Based on grain size distribution curves presented in Volume 1, the size fraction composition of phosphatic clays by weight can be represented by the following statistical parameters:

	Weight Fraction		
Size Fraction (µm)	**Average (%)**	**Standard Deviation (%)**	**Coefficient of Variation (%)**
+105	**2.8**	**4.7**	**167.9**
105-44	**5.7**	**3.7**	**64.9**
-44	**91.5**	**4.8**	**5.2**

Using the above statistics characterizing the grain size distribution and the corresponding mineralogic composition statistics presented in Tables 4-15, 4-16 and 4-17, the overall mineralogic composition of phosphatic clays are found to be characterized by the following statistical values:

	Weight Fraction		
Mineral	Average (%)	Standard Deviation (%)	Coefficient of Variation (%)
Quartz	7.2	2.9	40.3
Dolomite	8.0	10.6	132.5
Apatite	26.2	10.2	38.9
Wavellite	6.5	6.4	98.5
Crandallite	1.2	0.9	75.0
Feldspar	0.4	0.5	125.0
Total Clay	50.4	7.7	15.3

Assuming that the occurrence of specific clay minerals is in direct proportion to the relative weight fraction determined on the -44 µm particle size, the following statistical values are found to characterize their occurrence.

	Weight Fraction		
Clay Mineral	Average (%)	Standard Deviation (%)	Coefficient of Variation (%)
Smectite	22.3	8.4	37.7
Illite	11.3	4.3	38.1
Palygorskite	14.6	9.5	65.1
Kaolinite	2.2	2.2	100.0

4.7 **Summary**

The crystalline phases quartz, apatite, dolomite, feldspar, wavellite and crandallite were found to account for the entire non-clay mineral X-ray diffraction trace for the twelve phosphatic clays analyzed. Quantitative mineralogic evaluations indicate that non-clay minerals account on the average for 50% by weight of phosphatic clays with a range of 35% to 60%. Quantitative mineralogic analyses also reveal the following findings:

- Apatite is clearly the dominant non-clay mineral. The apatite weight fraction varies from 6.6 to 40% with an overall mean value of 26.2%, or about 53% of the mean summation of all non-clay minerals. A good correlation exists between the chemically determined P_2O_5 content and the apatite content. The apatite content was found to account for 76% to 98% of the variation in the P_20_5 content. (All of the variation in the P_20_5 content is accounted for if the wavellite and crandallite contents are considered additionally.) The P_2O_5 content of phosphatic clays ranged from 4.6 to 17.9% with a mean value of 9.9%.

- The non-clay minerals quartz, dolomite and wavellite are relatively small constituents. Each typically constitutes 6 to 8% of the weight of phosphatic clays, although the wavellite and dolomite contents vary substantially over a wide range. Crandallite and feldspar are minor constituents, each typically constituting less than 1% of phosphatic clays.

The crystalline clay phases smectite, illite, palygorskite and kaolinite were detected in X-ray diffraction traces. Quantitative mineralogic analyses indicate that clay minerals generally account for 40.0 to 65% by weight of phosphatic clays. The clay mineral smectite was the most abundant clay mineral in eight of twelve samples. The smectite content ranged from 6.0 to 51.0%, with a mean value of 22.3%. Palygorskite was the most abundant clay mineral in the remaining four samples and constituted 0.0 to 35.0% of the -44 µm size fraction with an overall average of 14.6% for the full range of particle sizes. Illite was present in all samples and comprised 4.5 to 18.0% of the -44 µm size fraction, with a gross mean value of 11.3%. Kaolinite was a minor clay phase in all samples, generally constituting less than 3% of the phosphatic clay samples.

The results obtained from mineralogic analyses on clay phases present within phosphatic clays also reveal the following findings:

- The clay mineral phase is often strongly aggregated as evidenced by relatively high total clay contents in the +105 µm and 105 - 44 µm size fraction. The Mobil phosphatic clay is particularly strongly aggregated and the Agrico phosphatic clay is also strongly aggregated.
- Palygorskite spiking indicated that the minimun X-ray diffraction detection limit for palygorskite is 5-10%. Phosphatic clays shown with 0% palygorskite, therefore, may contain 5-10% palygorskite. Palygorskite generally occurs as very elongated particles with some evidence of relatively stubby particle occurrences.
- The large coefficients of variation determined for different smectite basal spacings indicate that smectite in the phosphatic clays is different from the reference smectite and that interstratification exists. The weight fraction determined for the various clay minerals is complicated by clay phase interstratification, peak interferences and the presence of amorphous gel. The total clay content calculated from the 4.45 Å clay peak generally exceeds the total clay content calculated from the summation of individual clay minerals. The difference in calculated total clay contents is ascribed to interstratified clay material and/or amorphous clay material that gave no X-ray diffraction peaks at basal spacings characteristic to specific clay minerals, but did contribute to the total clay 4.45 Å peak.

Overall, the main objective of the mineralogic analyses: to quantitatively determine the weight fraction of specific minerals within phosphatic clays, has been achieved with reasonable success. Six of twelve samples gave a total mineral summation close to 100%, which suggests that the reference minerals can be applied to phosphatic clays. The largest sources of uncertainty found to affect the summation of the estimated weight fractions are the as yet unidentified type of interstratified clay and the presence of amorphous gel within phosphatic clays.

Table 4-1

MEAN RELATIVE PEAK AMPLITUDE RATIOS FOR NON-CLAY MINERALS IN VARIOUS SIZE FRACTIONS

		Mean Relative Peak Amplitude Ratio, R_i (%)												Statistics	
Mineral	Size Fraction (μm)	Agrico	AMAX	Beker	Brewster	CF	Estech	Grace	Hopewell	IMC	Mobil	OXY	USSAC	Average, R_i (%)	Standard Deviation, σ_{R_i} (%)
Quartz	+105	27.4	11.6	n	n	3.9	n	n	38.0	n	9.5	28.2	n	19.77	13.31
	105 - 44	10.7	23.7	26.1	n	1.8	n	n	29.2	17.8	4.1	15.8	11.5	15.63	9.55
	-105	1.5	9.8	4.9	3.2	2.6	0.6	2.7	5.0	5.4	1.5	3.1	3.2	3.70	2.35
	-44	3.1	4.8	5.7	3.7	2.5	1.5	3.3	5.5	5.4	3.5	3.8	3.3	3.84	1.28
Apatite	+105	49.0	55.0	n	n	78.1	n	n	23.2	n	46.7	63.2	n	52.53	18.33
	105 - 44	27.9	26.7	28.0	n	22.9	n	n	20.6	35.0	23.6	42.6	31.7	28.77	6.82
	-105	49.5	25.8	19.2	41.3	32.6	50.9	10.0	26.9	33.4	41.6	40.5	41.3	34.42	12.23
	-44	48.3	30.6	15.9	48.6	33.9	48.3	8.8	25.8	35.0	43.5	37.9	46.2	35.23	13.14
Dolomite	+105	0.0	0.0	n	n	3.3	n	n	0.9	n	3.7	0.0	n	1.32	1.73
	105 - 44	0.7	9.6	2.9	n	2.4	n	n	0.6	1.2	6.1	0.0	0.0	2.61	3.25
	-105	2.4	12.1	24.2	4.3	10.0	0.0	35.4	0.0	1.8	6.7	0.8	2.0	8.31	11.01
	-44	2.9	8.8	24.7	2.9	10.0	0.0	35.0	0.0	3.8	5.7	0.8	2.1	8.06	10.88
Feldspar	+105	1.8	1.1	n	n	5.3	n	n	8.0	n	0.9	4.2	n	3.55	2.81
	105 - 44	i	3.8	6.3	n	1.1	n	n	8.9	4.0	0.0	2.4	i	4.42	2.80
	-105*	2.7	2.2	i	i	0.0	1.1	0.0	1.1	0.0	0.0	2.2	2.0	1.13	1.09
	-44*	0.6	i	0.4	0.4	0.0	0.0	0.0	0.6	i	0.0	1.1	2.2	0.53	0.69
Wavellite	+105	0.0	5.0	n	n	0.0	n	n	2.1	n	0.0	0.0	n	1.18	2.05
	105 - 44	3.0	14.4	0.0	n	4.0	n	n	4.4	0.0	0.0	5.0	37.3	7.57	12.00
	-105	d	6.8	d	6.7	d	6.6	0.0	6.5	0.0	0.0	11.3	9.5	5.27	4.26
	-44	0.0	5.7	0.0	6.8	0.0	6.2	0.0	5.4	0.0	0.0	11.0	7.2	3.52	3.93
Crandallite**	+105	0	0	n	n	0	n	n	0	n	0	0	n	0.00	0.00
	105 - 44	0	0	0	n	0	n	n	0	16	0	0	i	2.00	5.66
	-105	20	10	0	18	20	32	i	0	6	0	12	10	11.64	10.19
	-44	18	0	0	18	20	36	0	0	0	4	12	0	9.00	11.80

---

*Upper bound for mean relative peak amplitude ratio with no allowance for palygorskite.

**Peak amplitude, A, in counts/second since no reference peak amplitude for crandallite is available.

n = insufficient material available for analysis after sample preparation.

d = mineral detected, but peak too vague to establish amplitude.

i = presence or absence of mineral indeterminate from X-ray diffraction trace.

Table 4-2

COMPARISON OF NON-CLAY MINERAL MEAN RELATIVE PEAK AMPLITUDE RATIOS IN ORIENTED AGGREGATE MOUNTS

	Ratio of Mean Relative Peak Amplitude Ratios, $\bar{R}_i(-1\ \mu m)/\bar{R}_i(-44\ \mu m)$						Statistics	
Mineral	Agrico	AMAX	Beker	CF	Estech	Hopewell	Average	Standard Deviation
Quartz	0.74	0.49	0.90	0.50	i	0.60	0.65	0.17
Dolomite	0.00	0.00	0.00	0.00	0.00	np	0.00	0.00
Apatite	0.90	0.76	1.05	0.69	0.81	1.00	0.87	0.14
Wavellite	np	0.00	np	np	0.00	0.00	0.00	0.00
Crandallite	0.83	np	np	1.20	0.81	np	0.95	0.22

---

np = mineral specie not originally present in the -44 μm size fraction.
i = presence or absence of mineral indeterminate in the -1 μm size fraction.

Table 4-3

INDIVIDUAL RELATIVE PEAK AMPLITUDE RATIOS FOR NON-CLAY MINERALS IN THE -105 μm SIZE FRACTION

Mineral	Basal Spacing, d (Å)	Relative Peak Amplitude Ratio, R_i (%)											
		Agrico	AMAX	Beker	Brewster	CF	Estech	Grace	Hopewell	IMC	Mobil	Oxy	USSAC
Quartz	4.26	1.36	11.8	5.37	3.76	1.88	0.81	1.68	5.64	5.64	1.34	4.03	3.49
	3.35	1.18	10.9	4.59	2.50	2.12	0.47	2.65	4.18	3.88	1.65	2.65	2.88
	2.46	1.97	6.6	4.59	3.28	3.80	i	2.62	5.25	6.56	i	2.62	3.28
	$\bar{R}_i$	1.50	9.77	4.85	3.18	2.60	0.64	2.65	5.02	5.36	1.50	3.10	3.22
	C.V. (%)	27.6	28.5	9.3	20.0	40.2	37.6	1.1	15.1	25.4	14.7	26.0	9.6
Dolomite	2.89	2.29	15.7	27.9	3.66	9.01	0.0	37.4	0.0	1.68	5.7	0.76	1.68
	2.19	2.42	8.5	20.6	4.85	10.9	0.0	33.3	0.0	1.82	7.8	i	2.42
	$\bar{R}_i$	2.36	12.1	24.2	4.26	9.96	0.0	35.3	0.0	1.75	6.75	0.76	2.05
	C.V. (%)	3.9	42.1	21.3	19.8	13.4	—	8.2	—	5.7	22.0	—	25.5
Apatite	2.79	45.1	25.4	16.9	39.4	28.2	46.5	9.2	26.1	33.8	40.1	38.7	39.4
	2.69	53.9	26.2	21.5	43.1	36.9	55.4	10.8	27.7	33.1	43.1	42.3	43.1
	$\bar{R}_i$	49.50	25.80	19.20	41.25	32.55	50.95	10.00	26.90	33.45	37.53	40.5	41.25
	C.V. (%)	12.6	2.2	16.9	6.3	18.9	12.4	11.3	4.2	1.5	13.0	6.3	6.3
Wavellite	8.6	d	8.46	d	6.9	d	6.9	0.0	6.0	0.0	0.0	14.6	11.5
	8.4	d	6.47	d	5.3	d	4.1	0.0	7.1	0.0	0.0	8.2	7.1
	4.8	d	5.56	d	7.9	d	8.9	0.0	5.6	0.0	0.0	11.1	10.0
	$\bar{R}_i$	—	6.83	—	6.70	—	6.63	0.0	6.53	0.0	0.0	11.3	9.53
	C.V. (%)	—	21.7	—	19.6	—	36.4	—	12.5	—	—	28.4	23.5

---

i = presence or absence of mineral indeterminate from X-ray diffraction trace.

d = mineral detected, but peak too vague to establish amplitude.

$\bar{R}_i$ = arithmetic average of individual relative peak amplitude ratios from listed characteristic basal spacings.

C.V. = cofficient of variation of individual relative peak amplitude ratios from average, $\bar{R}_i$.

Arithmetic average of the coefficients of variation for each mineral from the 12 samples are: 21.3% for quartz; 18.0% for dolomite; 9.3% for apatite; and 23.7% for wavellite.

Table 4-4

SUMMARY OF NON-CLAY MINERAL SIZE FRACTION OCCURRENCE AND MEAN RELATIVE PEAK AMPLITUDE RATIO

Mineral	Frequency of Occurrence* (%)	Major Occurrence Size Fraction**		Minor Occurrence Size Fraction**	
		Size (μm)	$\bar{R}_i$† (%)	Size (μm)	$\bar{R}_i$† (%)
Quartz	100	+105	19.77	-105	3.70
Apatite	100	+105	52.53	-105	34.42
Dolomite	92	-105	8.31	+105	1.32
Feldspar	100	+105	3.55	-105	1.13
Wavellite	67	-105	5.27	+105	1.18
Crandallite	75	-105	11.64††	+105	0.00††

---

*Frequency of occurrence determined from ratio of number of samples where mineral was detected to total number of samples.

**Major and minor occurrence size fraction based on +105 μm and -105 μm division only. This size division corresponds approximately to the division between sand size particles (+74 μm) and silt and clay size particles (-74 μm).

†Average mean relative peak amplitude ratio from twelve phosphatic clay samples.

††Peak amplitude, A, in counts per second, since no reference peak amplitude for crandallite is available.

Table 4-5

RELATIVE PEAK AMPLITUDE RATIO FOR TOTAL CLAY IN VARIOUS SIZE FRACTIONS

Mineral	Size Fraction (μm)	Relative Peak Amplitude Ratio, R_i (%)												Statistics	
		Agrico	AMAX	Beker	Brewster	CF	Estech	Grace	Hopewell	IMC	Mobil	Oxy	USSAC	Average, R_i (%)	Standard Deviation, σ_{R_i} (%)
Total Clay	+105	8.9	0.0	n	n	11.1	n	n	0.0	n	33	0.0	n	8.83	12.83
	105 - 44	52	8.9	11.0	n	13.3	n	n	0.0	31	64	24	36	26.58	21.06
	-105	51	53	44	62	71	36	33	58	67	58	62	58	54.42	11.70
	-44	62	53	49	62	75	36	42	62	67	56	60	67	57.58	11.08

n = insufficient material available for analysis after sample preparation.

Table 4-6

RELATIVE PEAK AMPLITUDE RATIOS FOR CLAY MINERALS IN THE -44 μm SIZE FRACTION

Mineral	Basal Spacing, d (Å)	Relative Peak Amplitude Ratio, R_i (%)												Statistics	
		Agrico	AMAX	Beker	Brewster	CF	Estech	Grace	Hopewell	IMC	Mobil	Oxy	USSAC	Average, R_i (%)	Standard Deviation, σ_{R_i} (%)
Smectite	18.0	9.0	27.8	21.0	11.3	24.3	4.3	5.5	42.8	26.8	13.8	13.3	17.3	18.10	11.07
Illite	10.0	i	15.6	17.5	9.4	8.1	5.0	6.3	15.0	11.2	8.5	i	10.0	10.66	4.14
Palygorskite	10.5	26.4	16.8	10.0*	0.0	0.0	7.2	8.0	16.0	12.0	7.2*	16.8	13.6	11.17	7.49
Kaolinite	7.14	1.9	0.4	0.7	0.9	2.3	2.0	0.0	0.20	1.2	0.2	1.5	1.0	1.03	0.77

---

*10.5 Å palygorskite peak indeterminant; R_i based on average from 6.5 and 5.4 Å peaks.
i = presence or absence of mineral indeterminate from X-ray diffraction trace.

Table 4-7

COMPARISON OF CLAY MINERAL RELATIVE PEAK AMPLITUDE RATIOS IN THE -44 μm AND -1 μm SIZE FRACTIONS

	Ratio of Relative Peak Amplitude Ratios, R_i(-1 μm)/R_i(-44 μm)						Statistics	
Mineral	Agrico	AMAX	Beker	CF	Estech	Hopewell	Average	Standard Deviation
Smectite	2.00	1.51	1.44	2.29	1.51	1.24	1.67	0.40
Illite	i	1.48	1.25	1.85	1.38	1.25	1.44	0.25
Palygorskite	1.85	1.33	np	np	1.44	1.50	1.53	0.22
Kaolinite	2.63	3.13	2.29	2.83	1.75	1.00	2.27	0.78

---

np = mineral specie not present in the -44 μm size fraction.
i = presence or absence of mineral indeterminate in the -1 μm size fraction.

Table 4-8

MEAN BASAL SPACING FOR MAGNESIUM SATURATED GLYCEROL SOLVATED SMECTITE CLAY MINERALS

	-44 µm Size Fraction		-1 µm Size Fraction	
Sample	Mean Basal Spacing, d Å	C. V. (%)	Mean Basal Spacing, d Å	C. V. (%)
Agrico	18.3	2.0	18.1	1.4
AMAX	18.2	1.5	18.3	1.8
Beker	18.3	2.2	18.2	2.8
Brewster	18.2	1.7	ns	ns
CF	18.3	1.1	18.3	1.9
Estech	18.3	1.9	18.6	2.2
Grace	18.1	2.4	ns	ns
Hopewell	18.4	1.5	17.8	1.2
IMC	18.2	1.1	ns	ns
Mobil	18.1	1.3	ns	ns
Oxy	18.6	3.2	ns	ns
USSAC	18.3	1.7	ns	ns

---

ns = No -1 µm size fraction sample prepared for X-ray diffraction analysis.
C. V. = coefficient of variation.

Table 4-9

BEHAVIOR OF SMECTITE CLAY MINERAL SATELLITE PEAKS IN THE -44 μm SIZE FRACTION

	Satellite Peak Position, d (Å)				
	Mg Saturated	K Homoionic		Mg Homoionic	
Sample	Glycerol Solvated	300°C for 20 Hours	450°C for 1 Hour	300°C for 20 Hours	400°C for 1 Hour
Agrico	11.8	i	i	ne	ne
Mobil	11.8	i	i	ne	ne
Grace	11.8	ne	ne	17.0	14.7
IMC	11.8	ne	ne	16.0	ne
AMAX	12.5	ne	ne	13.8	12.5
Beker	12.5	ne	ne	ne	ne
CF	12.5	i	i	ne	ne
Brewster	13.0	i	i	ne	ne
USSAC	13.0	13.0	14.0	ne	ne
Hopewell	13.0	ne	ne	i	11.8
Oxy	13.6	i	i	ne	ne
Estech	14.2	ne	ne	13.4-11.8	14.0-12.4

---

i = Treatment examined, but no peak observed.
ne = Treatment not examined.

Table 4-10

BEHAVIOR OF SMECTITE CLAY MINERAL SATELLITE PEAKS IN THE -1 μm SIZE FRACTION

	Satellite Peak Position for Mg Saturated Gylcerol Solvated Specimens, d (Å)					Satellite Peak Position for L_i Saturated Homionic Specimens, d (Å)	
Sample	25°C	250°C for 20 Hours	Rehydrate, Glycerol Solvated at 25°C	250°C for 20 Hours	350°C for 4 Hours	250°C for 20 Hours	Rehydrate Glycerol Solvated at 25°C
Agrico	14.7	i	15.0	i	i	14.0	18.0
AMAX	12.8	13.2	12.8	13.8-12.3	i	11.0	e
Beker	12.2	13.3-11.8	11.8	13.4-11.8	11.6-10.6	14.0-12.0	e
CF	13.0	11.8	13.0	13.2-11.8	14.7	14.0	18.0
Hopewell	i	12.1	i	12.1	i	17.0	e
Estech	13.6-12.3	13.6	i	14.0	13.8	14.0	i

---

i = Treatment examined, but no peak observed.
e = Expansion occurred, but no peak observed.

Table 4-11

PEAK AMPLITUDES FOR PALYGORSKITE SPIKING ON CF PHOSPHATIC CLAY

Palygorskite Added By Weight, %	Basal Spacing, d (Å)	Peak Amplitude, A (c/s)		Statistics	
		Maximum	Minimum	Mean Peak Amplitude, A (c/s)*	C. V. (%)
0.0	10.5	62	55	59.6	3.7
0.0	6.5	0	0	0	0
0.0	5.4	0	0	0	0
10.86	10.5	100	88	93.9	4.1
10.86	6.5	12	4	6.8	33.8
10.86	5.4	10	4	7.4	23.0
24.49	10.5	160	146	153.5	3.7
24.49	6.5	12	8	10.5	16.2
24.49	5.4	16	10	13.6	14.7

---

*Mean peak amplitude, A, determined from arithmetic average of 12 determinations, four X-ray diffraction traces on three mounts per sample.

Table 4-12

ORGANIC MATTER CONTENTS OF PHOSPHATIC CLAYS

Sample	Organic Matter Content, OC (%)
Agrico	0.6
AMAX	0.9
Beker	2.6
Brewster	0.8
CF	3.0
Estech	0.9
Grace	1.4
Hopewell	0.3
IMC	0.8
Mobil	0.8
Oxy	2.9
USSAC	0.5

Table 4-13

TOTAL CHEMICAL COMPOSITION FOR -44 μm SIZE FRACTION

	Weight Percent, W_i (%)											Statistics		
Oxide	Agrico	AMAX	Beker	Brewster	CF	Estech	Hopewell	IMC	Mobil	Oxy	USSAC	Mean, W_i (%)	Standard Deviation	C.V. (%)
SiO_2	32.0	38.3	34.0	31.1	33.0	22.2	44.0	38.7	29.8	34.9	34.8	33.0	6.3	19.1
Al_2O_3	14.1	14.2	10.8	16.5	16.6	17.5	15.3	15.7	13.0	17.6	15.5	15.2	2.0	13.2
Fe_2O_3	3.79	3.87	3.29	2.58	4.00	3.17	4.74	5.08	6.70	3.50	3.80	4.05	1.12	27.7
TiO_2	0.47	0.55	0.32	0.56	0.52	0.36	0.55	0.53	0.44	0.55	0.55	0.49	0.084	17.1
Cr_2O_3	0.029	0.034	0.017	0.033	0.029	0.027	0.038	0.029	0.022	0.022	0.028	0.028	0.0060	21.4
ZrO_2	0.006	0.027	0.006	0.008	0.009	0.010	0.020	0.009	0.007	0.010	0.010	0.011	0.0065	58.6
CaO	17.3	13.4	15.7	15.6	13.4	22.1	10.6	11.5	16.2	12.2	13.8	14.7	3.2	21.8
MgO	3.79	4.46	8.05	2.85	4.40	1.45	3.17	2.96	3.80	2.50	2.60	3.64	1.71	47.0
MnO	0.01	0.03	0.02	0.01	0.02	0.03	0.03	0.02	0.08	0.02	0.02	0.026	0.019	72.5
SrO	0.098	0.067	0.023	0.115	0.121	0.256	0.027	0.066	0.066	0.107	0.081	0.093	0.063	67.4
Na_2O	0.55	0.37	0.35	0.53	0.45	0.44	0.35	0.58	0.55	0.50	0.59	0.48	0.091	19.1
K_2O	0.36	1.06	1.10	0.96	0.61	0.46	1.22	0.98	0.96	0.62	1.01	0.85	0.29	33.6
Rb_2O	0.002	0.007	0.006	0.005	0.004	0.003	0.006	0.006	0.007	0.003	0.005	0.005	0.002	34.6
P_2O_5	11.6	8.05	4.62	11.8	7.13	17.9	7.53	8.04	10.5	10.4	11.1	9.9	3.5	35.2
LOI	16.5	16.3	22.4	18.4	20.9	13.9	13.2	17.5	17.6	17.6	16.3	17.3	2.7	15.4
SUM	100.60	100.73	100.70	101.50	100.19	100.01	101.78	101.70	99.73	101.53	100.19	100.79	0.73	0.73
μ_s(cm^2/g)	54.7	52.0	50.9	51.3	50.6	58.6	50.1	52.4	58.9	49.5	52.2	52.84	3.23	6.12

LOI = Loss on ignition or weight loss during heating from 110° to 900°C.
μ_s = Calculated sample mass attenuation coefficient.
SUM = Summation of constituents.

Table 4-14

MINERALOGIC COMPOSITION OF -44 μm SIZE FRACTION OF PHOSPHATIC CLAYS

	Weight Fraction, X_i (%)												Statistics		
Mineral	Agrico	AMAX	Beker	Brewster	CF	Estech	Grace*	Hopewell	IMC	Mobil	Oxy	USSAC	Mean, W_i (%)	Standard Deviation	C.V. (%)
Non-Clay Minerals															
Quartz	4.7	6.9	8.0	5.2	3.5	2.4	4.8	7.6	7.8	5.7	5.2	4.7	5.5	1.7	31.5
Dolomite	3.3	9.4	26.	3.1	10.4	0.	38.	0.	4.1	6.9	0.8	2.3	8.7	11.7	134.4
Apatite	37.	22.	11.	35.	24.	40.	6.6	18.	26.	36.	26.	34.	26.3	10.6	40.5
Wavellite	0.	10.5	0.	12.3	0.	13.	0.	9.6	0.	0.	19.	13.	6.5	7.1	110.0
Crandallite**	1.4†	0.9	0.3	1.6†	1.7†	3.5†	0.	0.4	0.9	0.9	1.5†	1.1	1.2	0.9	76.4
Feldspar	0.	0.	0.4	0.4	0.	0.	0.	0.	0.	0.	0.	0.	0.07	0.16	233.6
Summation	46.4	49.7	45.7	57.6	39.6	58.9	49.4	35.6	38.8	49.5	52.5	55.1	48.2	7.4	15.4
Clay Minerals															
Smectite	11.7	34.	25.	14.	29.	6.0	6.8	51.	33.	19.	16.	22.	22.3	13.0	58.4
Illite	4.5††	16.	18.	9.6	8.2	5.8	6.7	15.	12.	10.	7.8††	10.	10.3	4.2	40.9
Palygorskite	35.	21.	12.	0.	0.	10.2	10.3	19.	15.	10.	20.	17.	14.1	9.5	67.5
Kaolinite	3.4	0.7	1.2	1.5	3.8	3.8	0.	0.3	2.0	0.4	2.4	1.7	1.8	1.4	76.5
Summation	54.6	71.7	56.2	25.1	41.0	25.8	23.8	85.3	62.0	39.4	46.2	50.7	48.5	19.0	39.3
Total Clay	82.	63.	56.	71.	89.	50.	51.	71.	82.	75.	70.	81.	70.1	12.8	18.3
Total Mineral Summation, S_1	101.0	121.4	101.9	82.7	80.6	84.7	73.2	120.9	100.8	88.9	98.7	105.8	96.7	15.2	15.8
Non-clay Mineral and Total Clay Summation, S_2	128.4	112.7	101.7	128.6	128.6	108.9	100.4	106.6	120.8	124.5	122.5	136.1	118.3	11.9	10.1

---

*Weight fraction for Grace phosphatic clay calculated using mean sample attenuation coefficient, μ_s, from other eleven samples of 52.84 cm^2/g.

**Crandallite weight fraction calculated assuming all SrO determined in chemical analyses to be in crandallite composed of 70% ideal crandallite and 30% goyazite.

†Crandallite peak clearly indicated in X-ray diffraction trace.

††Illite weight fraction calculated assuming all KrO determined in chemical analyses to be accounted for by illite.

Table 4-15

NORMALIZED MINERALOGIC COMPOSITION OF -44 μm SIZE FRACTION OF PHOSPHATIC CLAYS

	Weight Fraction, X_i (%)												Statistics		
Mineral	Agrico	AMAX	Beker	Brewster	CF	Estech	Grace*	Hopewell	IMC	Mobil	Oxy	USSAC	Mean, W_i (%)	Standard Deviation	C.V. (%)
Quartz	4.7	6.1	7.9	5.2	3.5	2.4	4.8	7.1	7.7	5.7	5.2	4.4	5.4	1.6	30.4
Dolomite	3.3	8.3	25.6	3.1	10.4	0.0	38.0	0.0	4.1	6.9	0.8	2.2	8.5	11.6	135.9
Apatite	36.6	19.5	10.8	35.0	24.0	40.0	6.6	16.9	25.8	36.0	26.0	32.1	25.8	10.7	41.5
Wavellite	0.0	9.3	0.0	12.3	0.0	13.0	0.0	9.0	0.0	0.0	19.0	12.3	6.2	6.9	111.5
Crandallite	1.4	0.8	0.3	1.6	1.7	3.5	0.0	0.4	0.9	0.9	1.5	1.0	1.2	0.9	78.0
Feldspar	0.0	0.0	0.4	0.4	0.0	0.0	0.0	0.0	0.0	0.0	0.0	0.0	0.1	0.2	200.0
Clay	54.0	56.0	55.0	42.4	60.4	41.1	50.6	66.6	61.5	50.5	47.5	48.0	52.8	7.6	14.5

Note: Results obtained from Table 4-14 as follows:

- Where $S_1 < 100\%$ and $S_2 > 100\%$ (Brewster, CF, Estech, Grace, Mobil, Oxy), use identical non-clay mineral composition as in Table 4-14 and adjust total clay weight fraction to yield a summation of 100%.
- Where $S_1 > 100\%$ and $S_2 > 100\%$ (Agrico, AMAX, Beker, Hopewell, IMC, USSAC), normalize all weight fractions based on the particular summation (i.e., S_1 or S_2) that is closer to 100%.

Table 4-16

MINERALOGIC COMPOSITION OF 105-44 μm SIZE FRACTION OF PHOSPHATIC CLAYS

	Sample Designation												Statistics		
Mineral	Agrico	AMAX	Beker	Brewster	CF	Estech	Grace	Hopewell	IMC	Mobil	Oxy	USSAC	Average, %	Standard Deviation	C.V. (%)
Mean Relative Peak Amplitude Ratios, R_i (%)															
Quartz	10.7	23.7	26.1	n	1.8	n	n	29.2	17.8	4.1	15.8	11.5	15.63	9.55	61.1
Apatite	27.9	26.7	28.0	n	22.9	n	n	20.6	35.0	23.6	42.6	31.7	28.78	6.82	23.7
Dolomite	0.7	9.6	2.9	n	2.4	n	n	0.6	1.2	6.1	0.0	0.0	2.61	3.25	124.5
Feldspar	0.0	3.8	6.3	n	1.1	n	n	8.9	4.0	0.0	2.4	0.0	2.94	3.13	106.3
Wavellite	3.0	14.4	0.0	n	4.0	n	n	4.4	0.0	0.0	5.0	37.3	7.57	12.00	158.6
Crandallite	0.0	0.0	0.0	n	0.0	n	n	0.0	16.0	0.0	0.0	0.0	1.78	5.33	299.8
Total Clay	52.0	8.9	11.0	n	13.3	n	n	0.0	31.0	64.0	24.0	36.0	26.69	21.21	79.5
Weight Fraction, X_i (%)															
Quartz	14.9	32.5	46.5	n	5.6	n	n	55.9	22.9	5.6	24.2	11.0	24.3	17.8	73.1
Apatite	19.8	18.7	25.5	n	36.5	n	n	20.2	23.0	16.5	33.3	15.4	23.2	7.3	31.5
Dolomite	0.7	9.8	3.9	n	5.6	n	n	0.8	1.1	6.2	0.0	0.0	3.1	3.5	112.1
Feldspar	0.0	3.7	8.1	n	2.5	n	n	12.3	3.7	0.0	2.7	0.0	3.7	4.1	110.8
Wavellite	5.4	25.3	0.0	n	16.0	n	n	10.8	0.0	0.0	9.8	45.6	12.5	15.0	119.6
Crandallite	0.0	0.0	0.0	n	0.0	n	n	0.0	16.7	0.0	0.0	0.0	1.9	5.6	301.8
Total Clay	59.2	10.0	16.0	n	33.8	n	n	0.0	32.6	71.7	30.0	28.0	31.3	22.6	72.3
Calculated Sample Mass Attenuation Coefficient μ_s (cm^2/g)	47.70	43.39	48.15	—	51.53	—	—	44.34	49.04	48.67	49.96	40.32	47.01	3.58	7.6
Summation of Weight Fraction Based on Calculated μ_s and Measured R_i	94.3	87.1	74.3	—	45.5	—	—	63.7	105.0	97.8	89.8	116.5	86.0	21.8	25.3

---

n = Insufficient material available for mineralogic analysis after sample preparation.

Table 4-17

MINERALOGIC COMPOSITION OF +105 μm SIZE FRACTION OF PHOSPHATIC CLAYS

	Sample Designation												Statistics		
Mineral	Agrico	AMAX	Beker	Brewster	CF	Estech	Grace	Hopewell	IMC	Mobil	Oxy	USSAC	Average, %	Standard Deviation	C.V. (%)
Mean Relative Peak Amplitude Ratios, R_i (%)															
Quartz	27.4	11.6	n	n	3.9	n	n	38.0	n	9.5	28.2	n	19.77	13.31	67.3
Apatite	49.0	55.0	n	n	78.1	n	n	23.2	n	46.7	63.2	n	52.53	18.33	34.9
Dolomite	0.0	0.0	n	n	3.3	n	n	0.9	n	3.7	0.0	n	1.32	1.73	131.1
Feldspar	1.8	1.1	n	n	5.3	n	n	8.0	n	0.9	4.2	n	3.55	2.81	79.2
Wavellite	0.0	5.0	n	n	0.0	n	n	2.1	n	0.0	0.0	n	1.18	2.05	173.7
Crandallite	0.0	0.0	n	n	0.0	n	n	0.0	n	0.0	0.0	n	0.0	0.0	—
Total Clay	8.9	0.0	n	n	11.1	n	n	0.0	n	33.0	0.0	n	8.83	12.83	145.3
Weight Fraction, X_i (%)															
Quartz	44.9	24.5	n	n	6.6	n	n	64.4	n	14.9	44.4	n	33.3	21.7	65.2
Apatite	41.1	59.5	n	n	67.5	n	n	20.1	n	37.5	50.9	n	46.1	16.9	36.7
Dolomite	0.0	0.0	n	n	4.2	n	n	1.1	n	4.3	0.0	n	1.6	2.1	131.0
Feldspar	2.1	1.7	n	n	6.4	n	n	9.8	n	1.0	4.7	n	4.3	3.4	79.0
Wavellite	0.0	14.3	n	n	0.0	n	n	4.6	n	0.0	0.0	n	3.2	5.8	182.9
Crandallite	0.0	0.0	n	n	0.0	n	n	0.0	n	0.0	0.0	n	0.0	0.0	—
Total Clay	11.9	0.0	n	n	15.3	n	n	0.0	n	42.3	0.0	n	11.6	16.5	142.4
Calculated Sample Mass Attenuation Coefficient μ_s (cm^2/g)	51.89	56.13	—	—	62.52	—	—	44.51	—	53.48	54.72	—	53.88	5.87	10.9
Summation of Weight Fraction Based on Calculated μ_s and Measured R_i	87.1	80.2	—	—	101.8	—	—	72.2	—	93.8	95.6	—	88.5	10.9	12.3

n = Insufficient material available for mineralogic analysis after sample preparation.

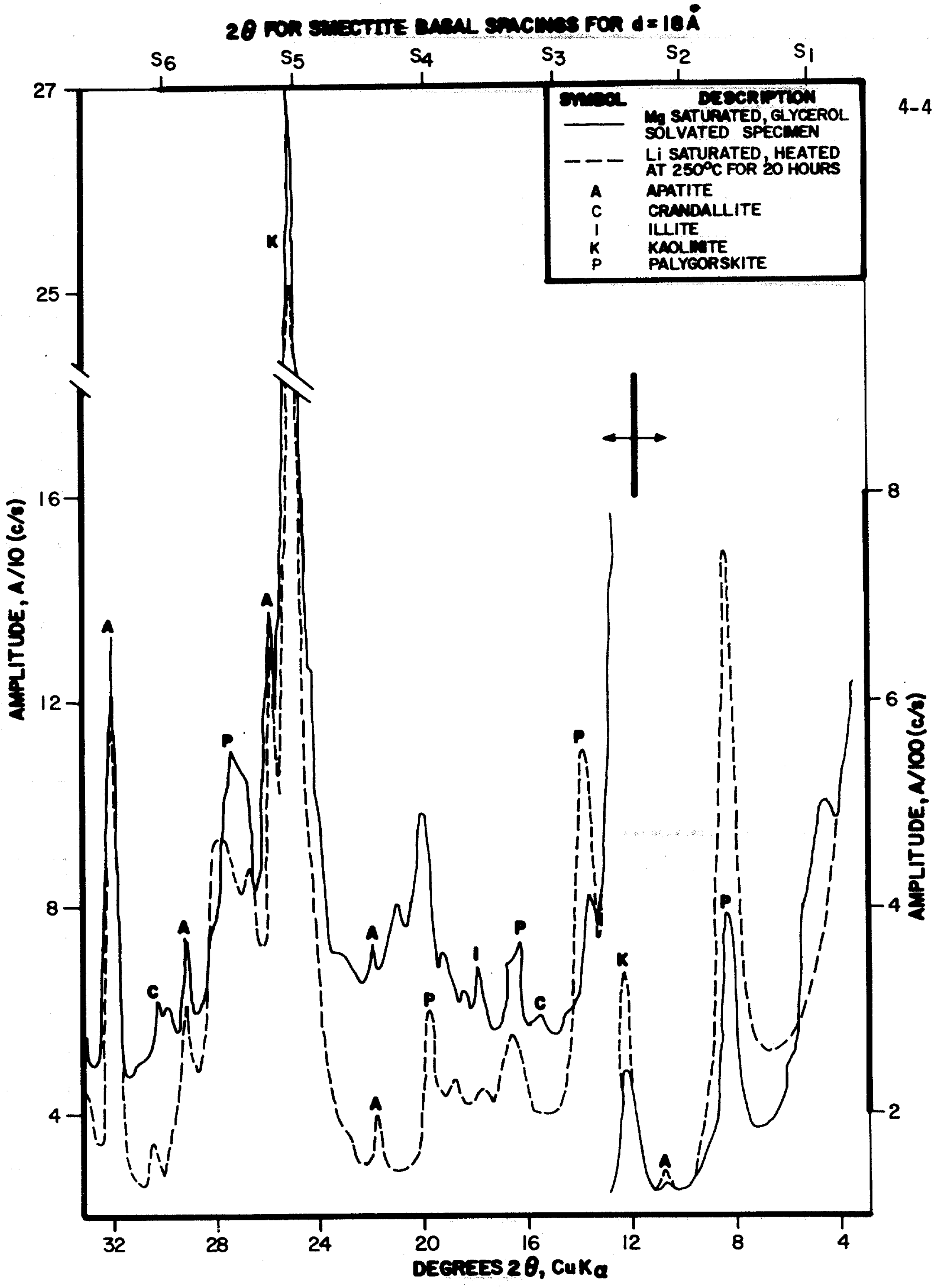

AGRICO X-RAY DIFFRACTION TRACE FOR -1µm SIZE FRACTION

FIGURE 4-1

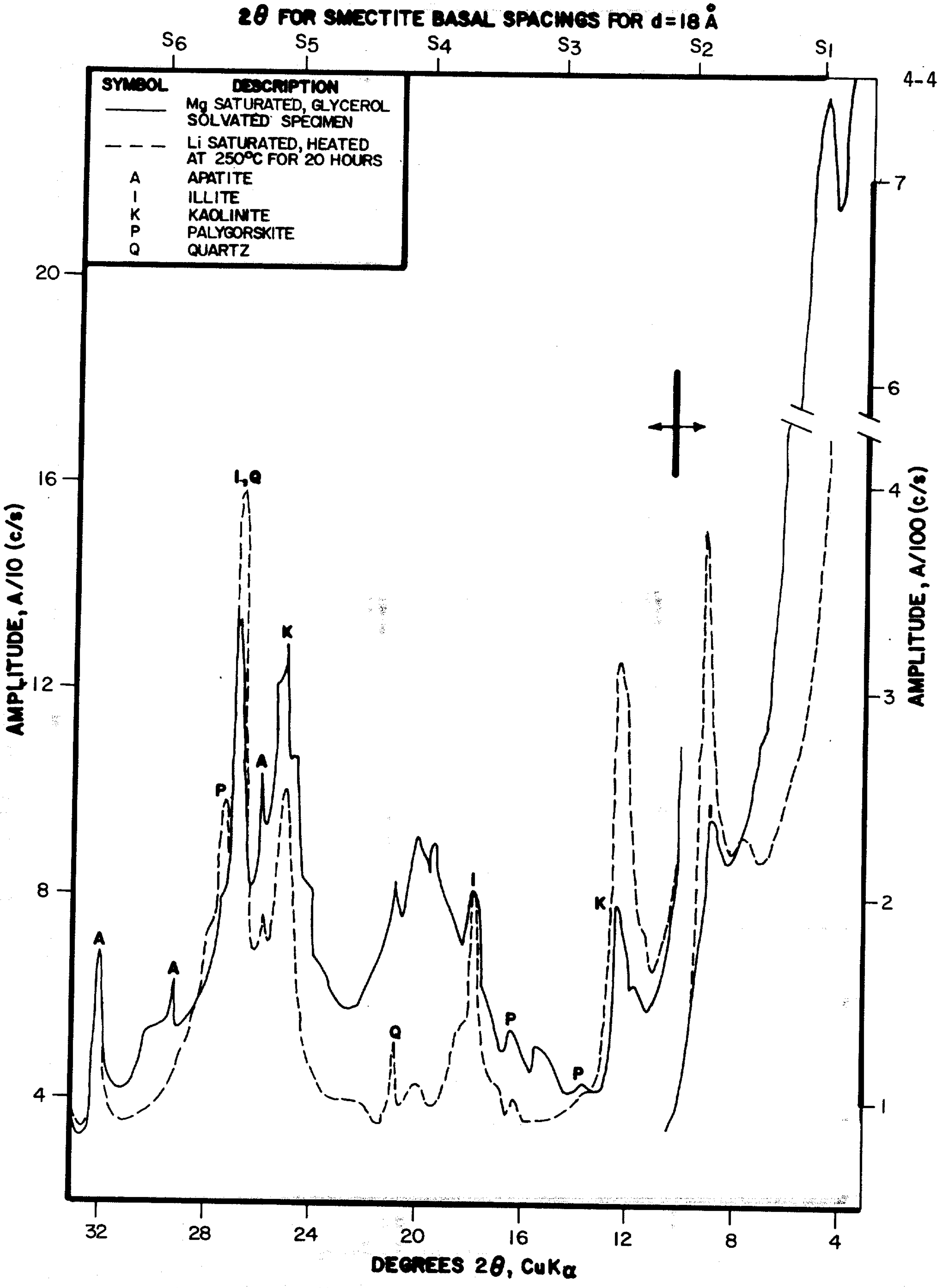

BECKER X-RAY DIFFRACTION TRACE FOR -1μm SIZE FRACTION

FIGURE 4-2

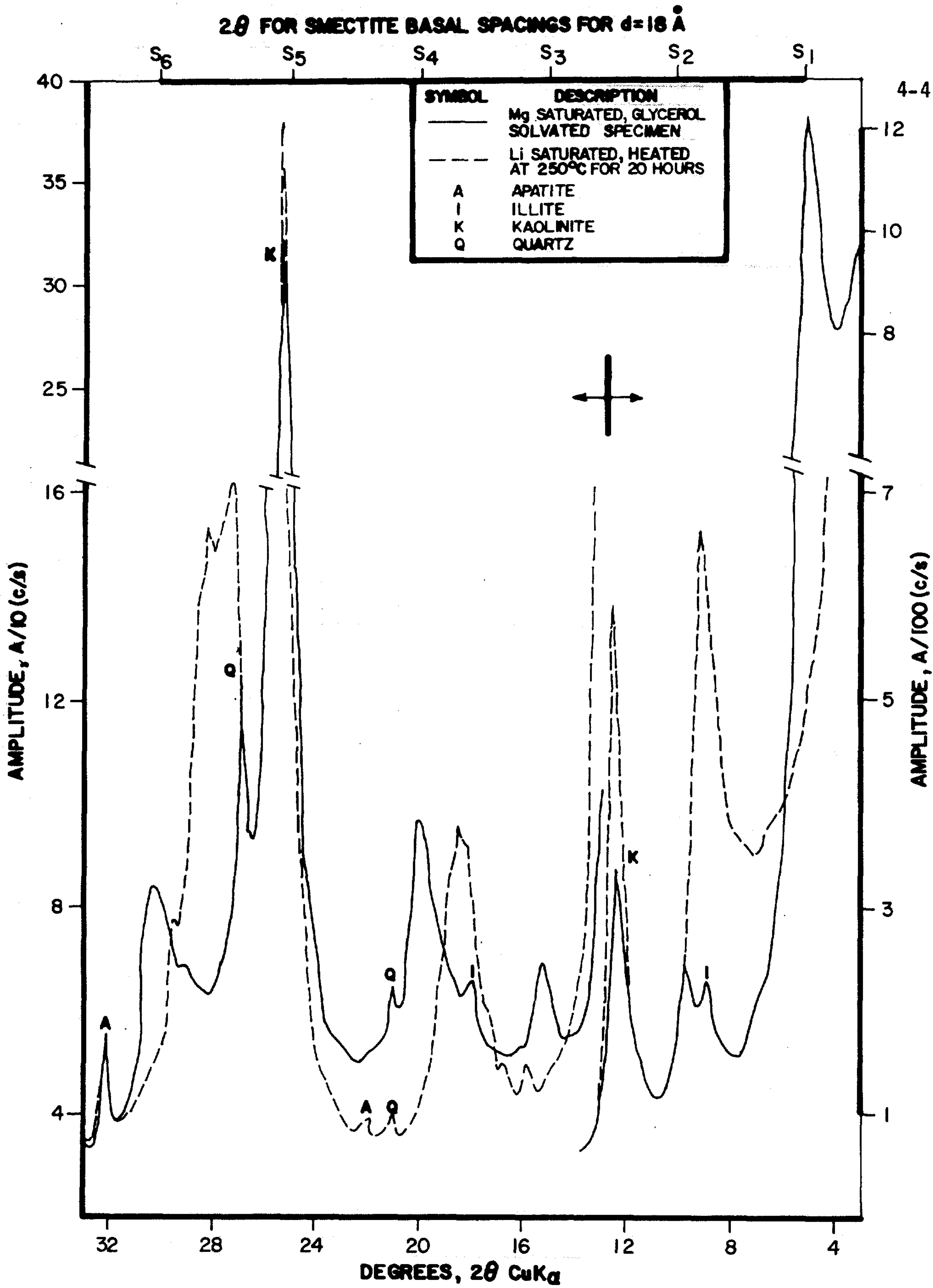

CF X-RAY DIFFRACTION TRACE FOR -1μm SIZE FRACTION

FIGURE 4-3

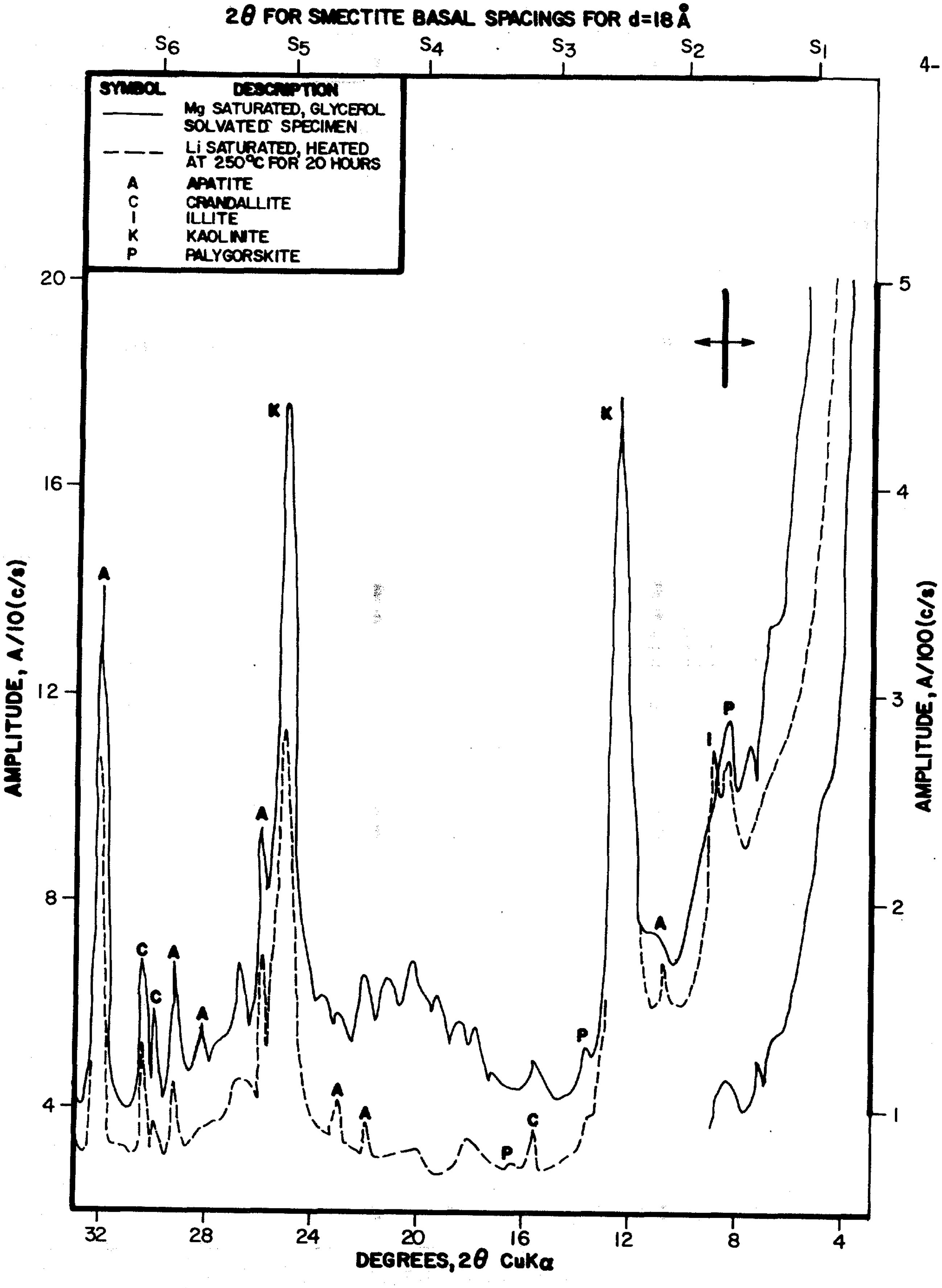

ESTECH X-RAY DIFFRACTION TRACE FOR -1um SIZE FRACTION

FIGURE 4-4

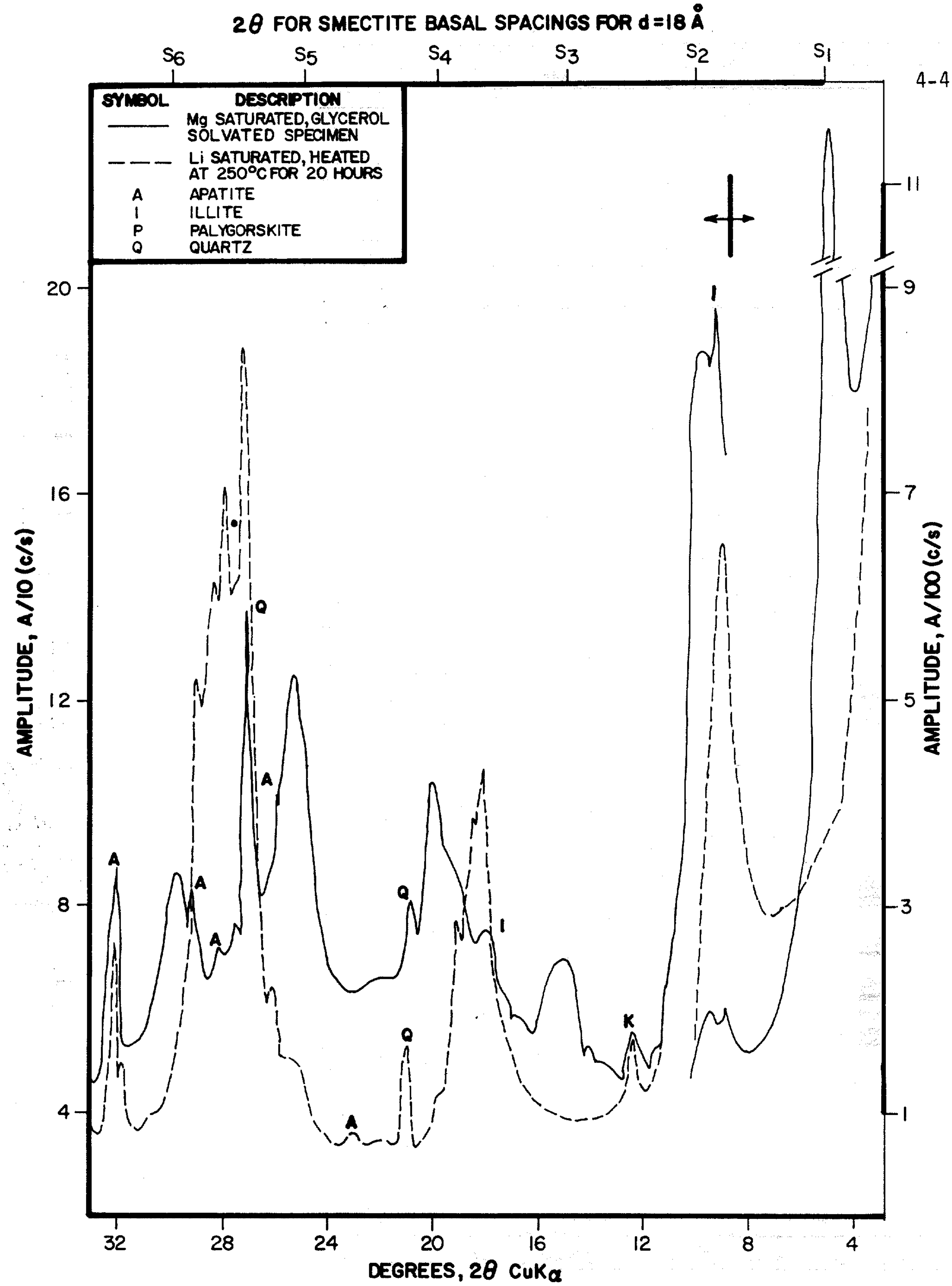

HOPEWELL X-RAY DIFFRACTION TRACE FOR -1μm SIZE FRACTION

FIGURE 4-5

FIGURE 4-6

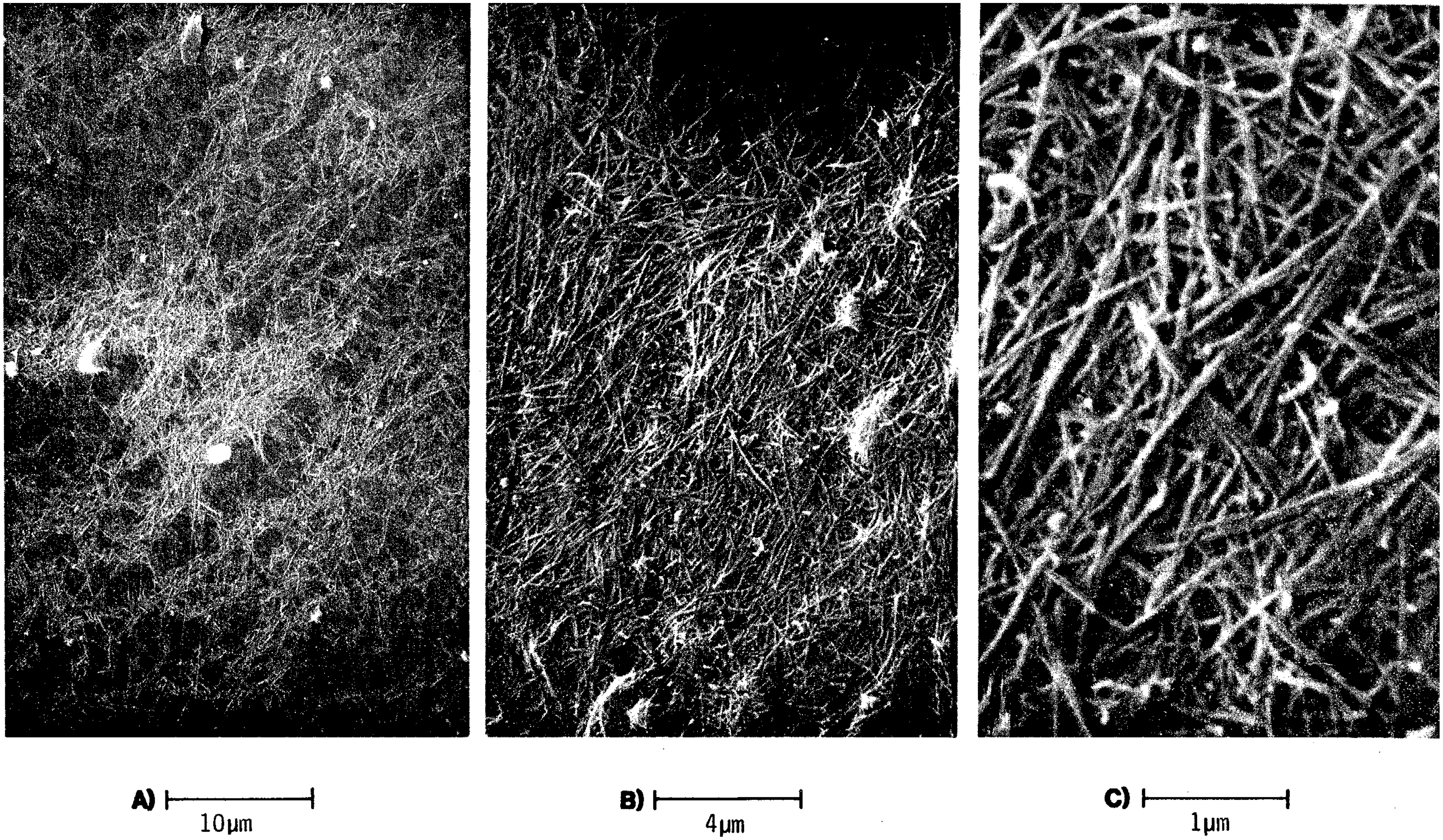

SCANNING ELECTRON PHOTOMICROGRAPHS
OF REFERENCE PALYGORSKITE CLAY

FIGURE 4-7

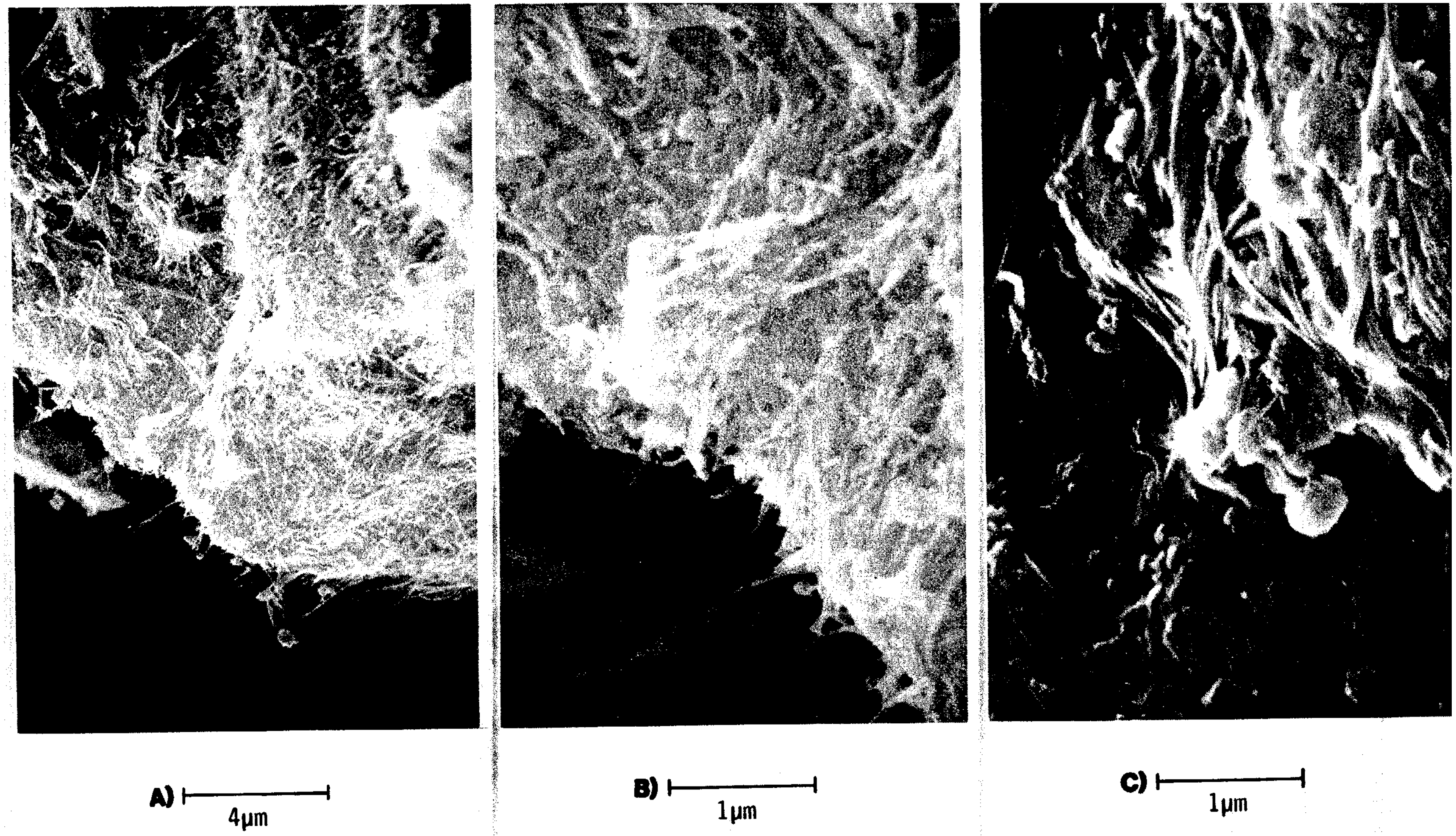

SCANNING ELECTRON PHOTOMICROGRAPHS OF AGRICO CLAY

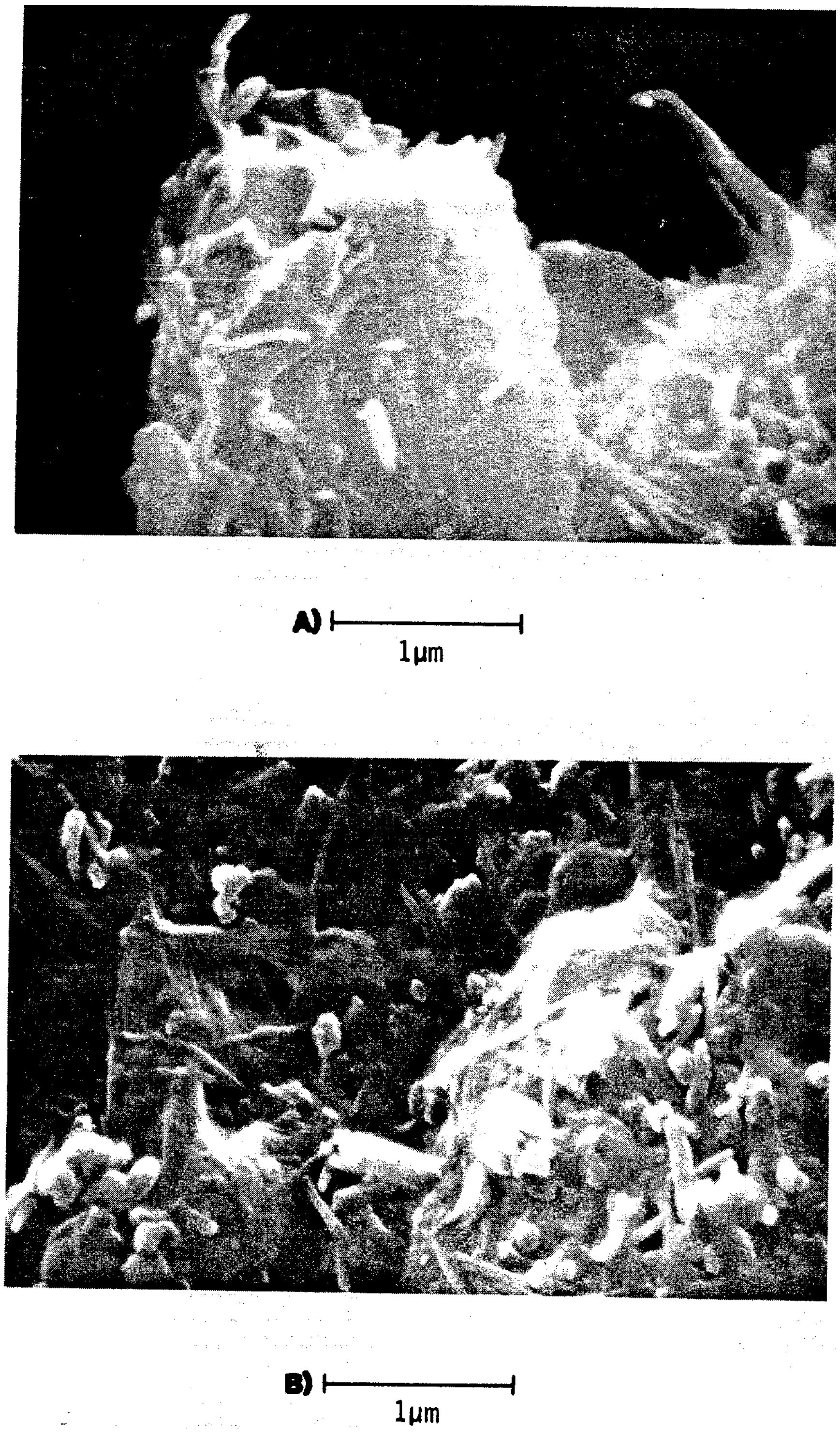

SCANNING ELECTRON PHOTOMICROGRAPHS
OF BREWSTER CLAY

FIGURE 4-8

FIGURE 4-9

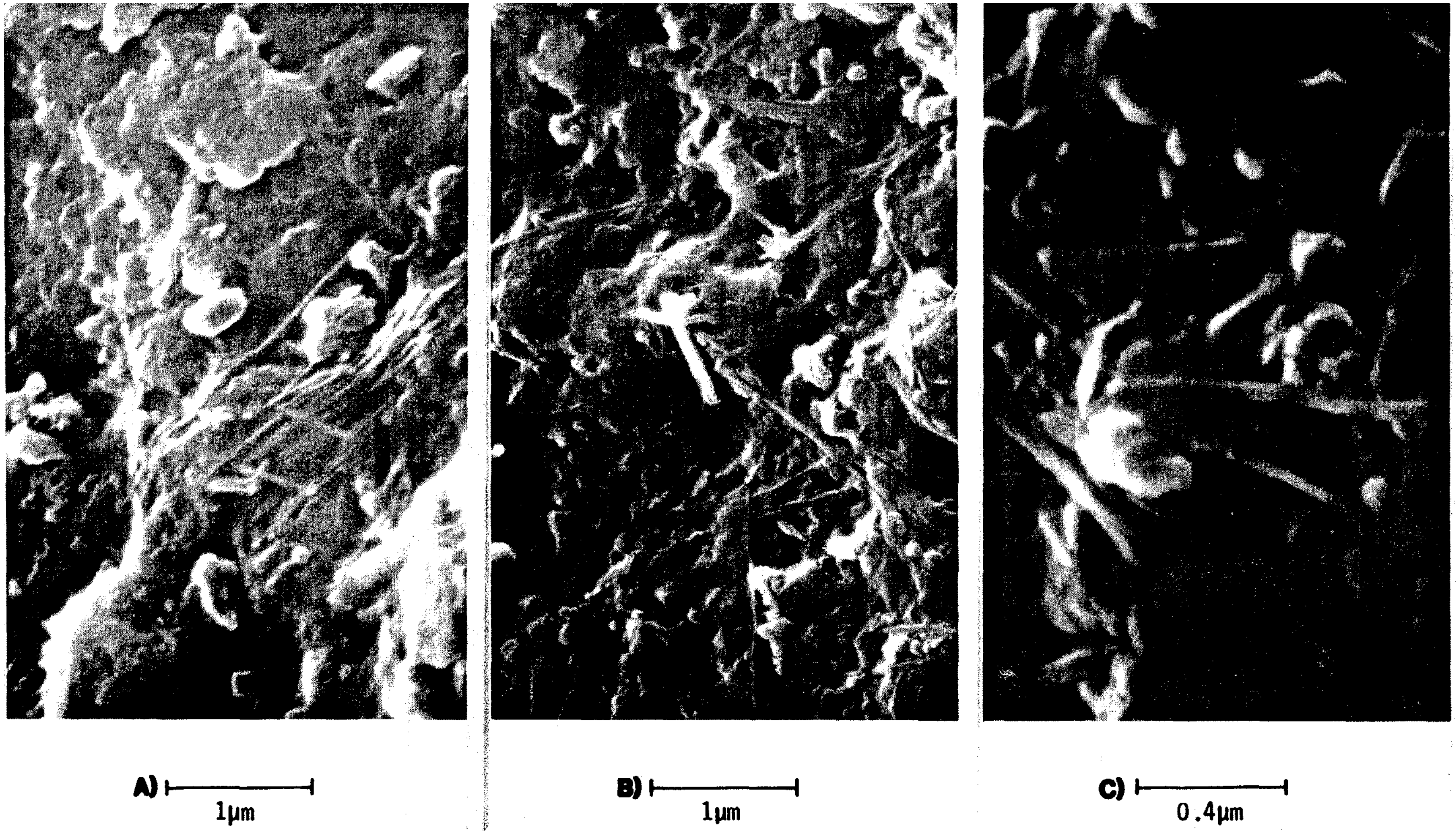
A) 1µm

B) 1µm

C) 0.4µm

SCANNING ELECTRON PHOTOMICROGRAPHS OF CF CLAY

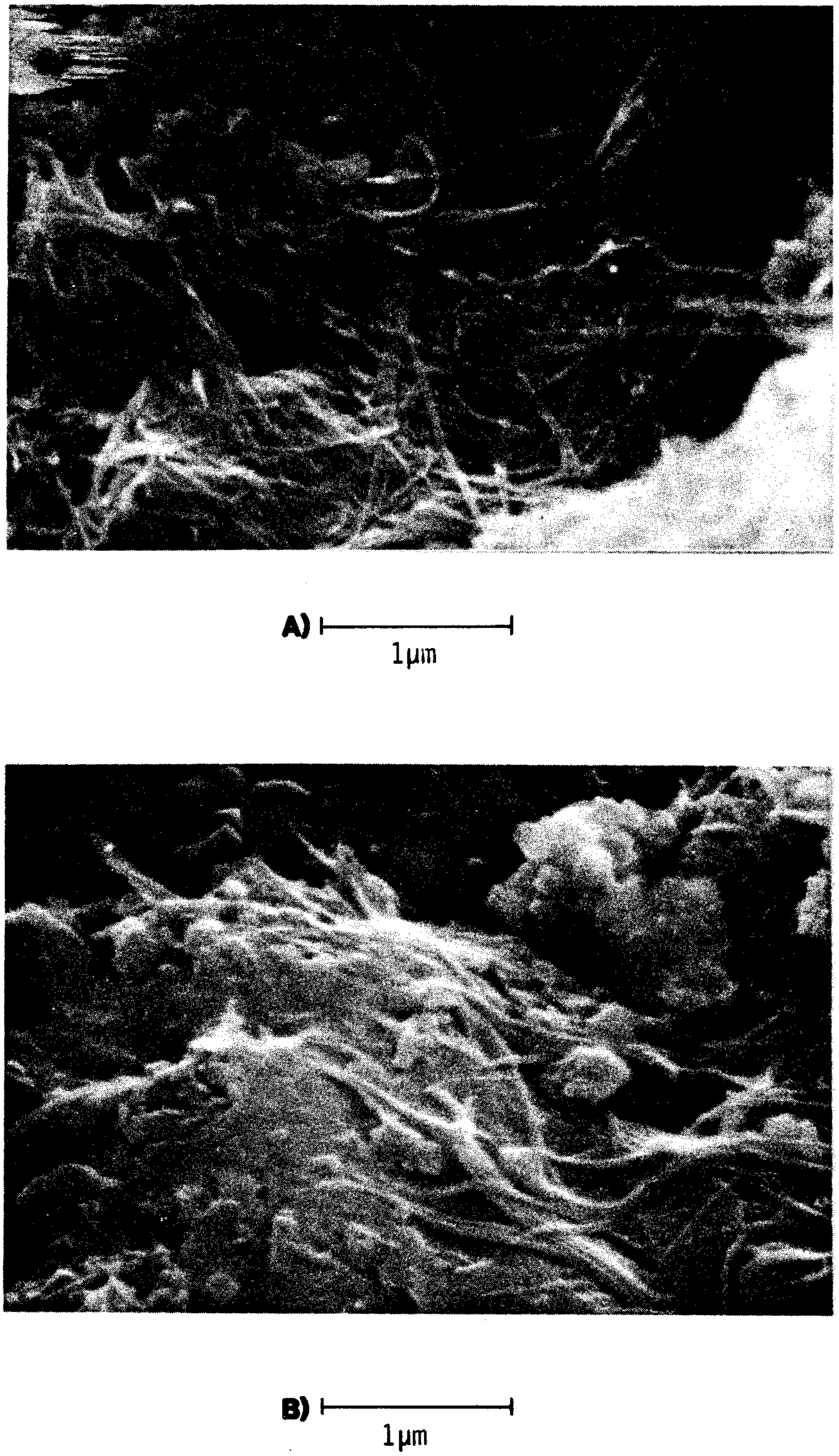

SCANNING ELECTRON PHOTOMICROGRAPHS OF MOBIL CLAY

FIGURE 4-10

FIGURE 4-11

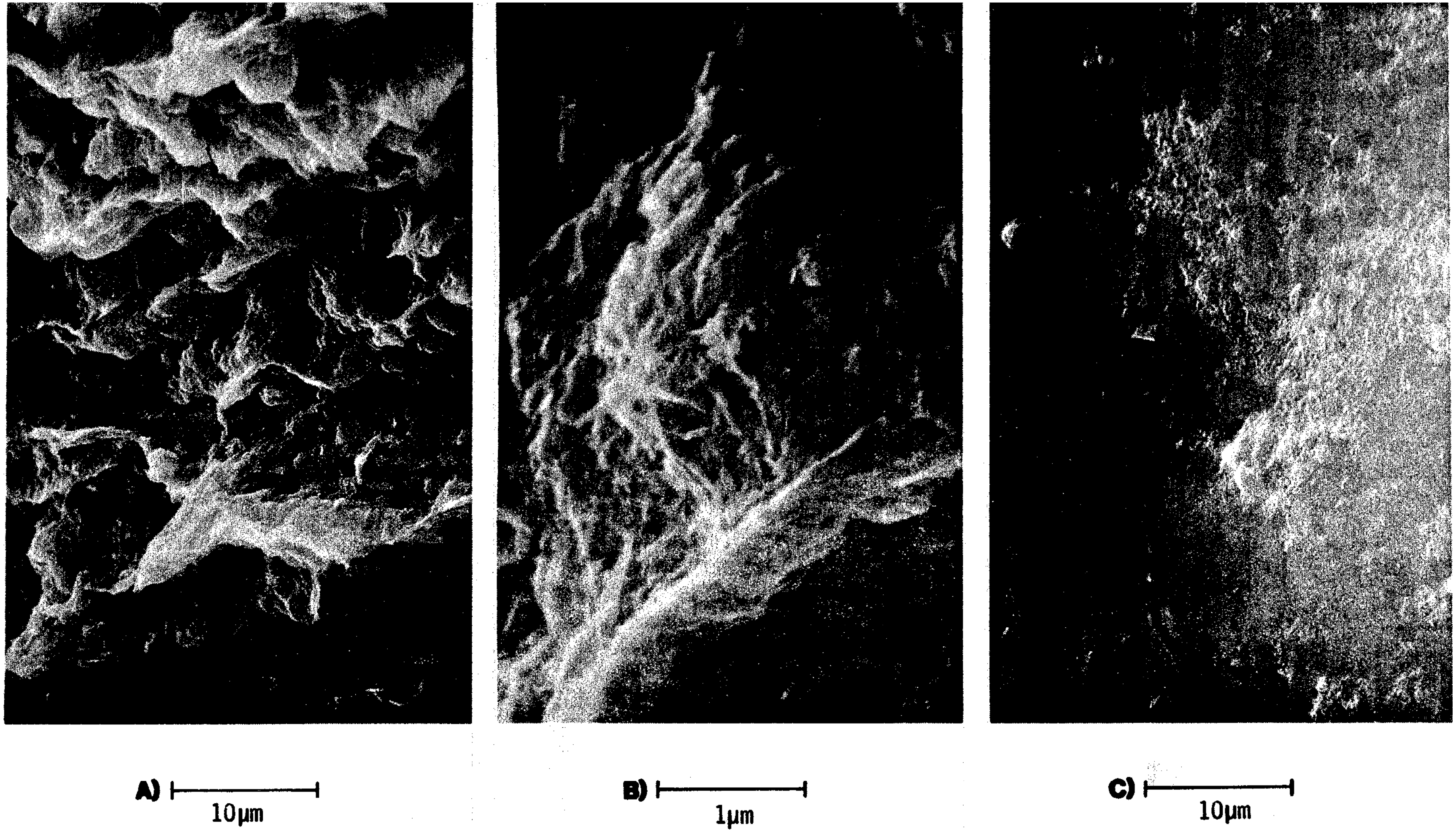

SCANNING ELECTRON PHOTOMICROGRAPHS OF OCCIDENTAL CLAY

FIGURE 4-12

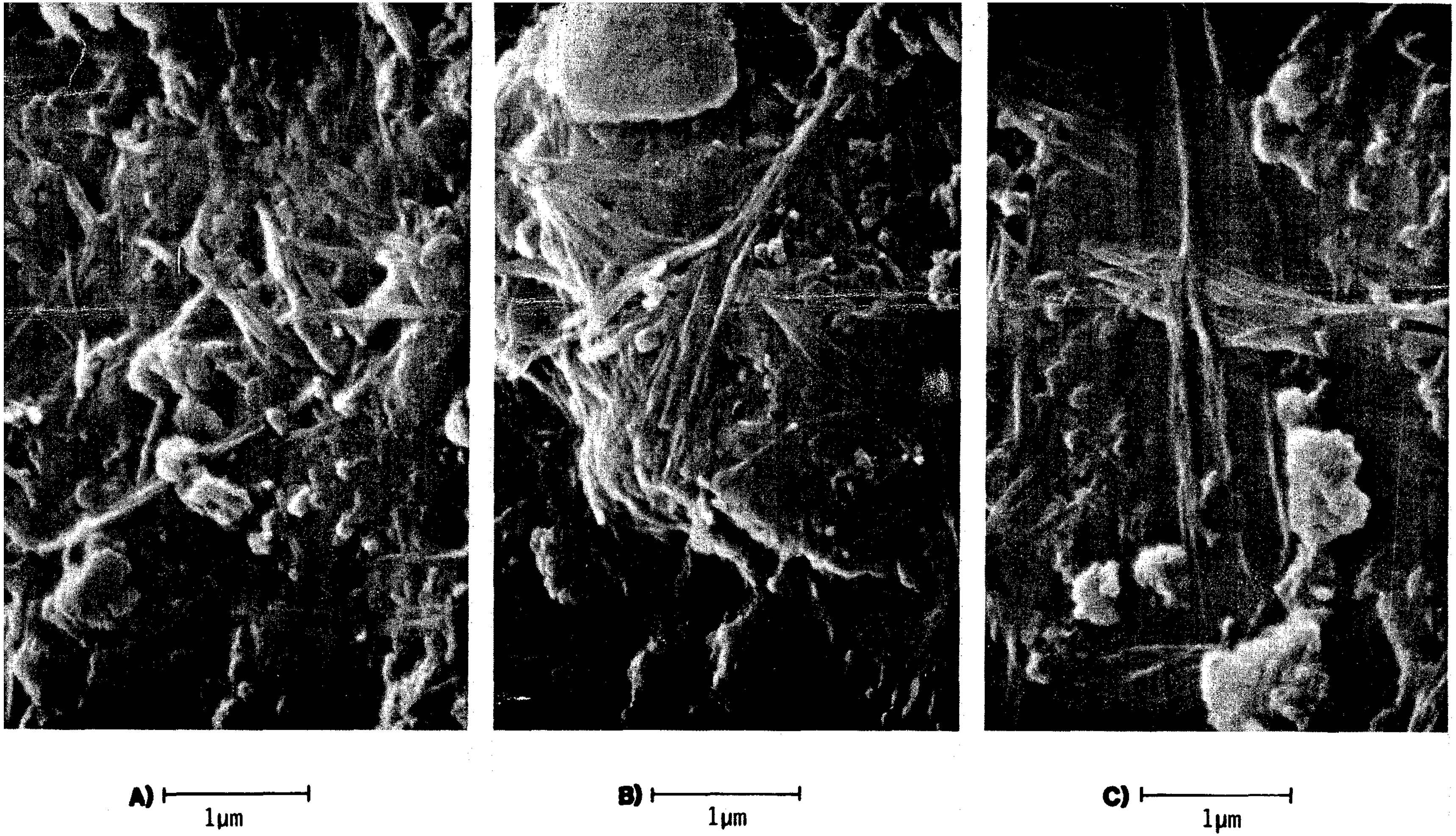

SCANNING ELECTRON PHOTOMICROGRAPHS OF OCCIDENTAL CLAY

FIGURE 4-13

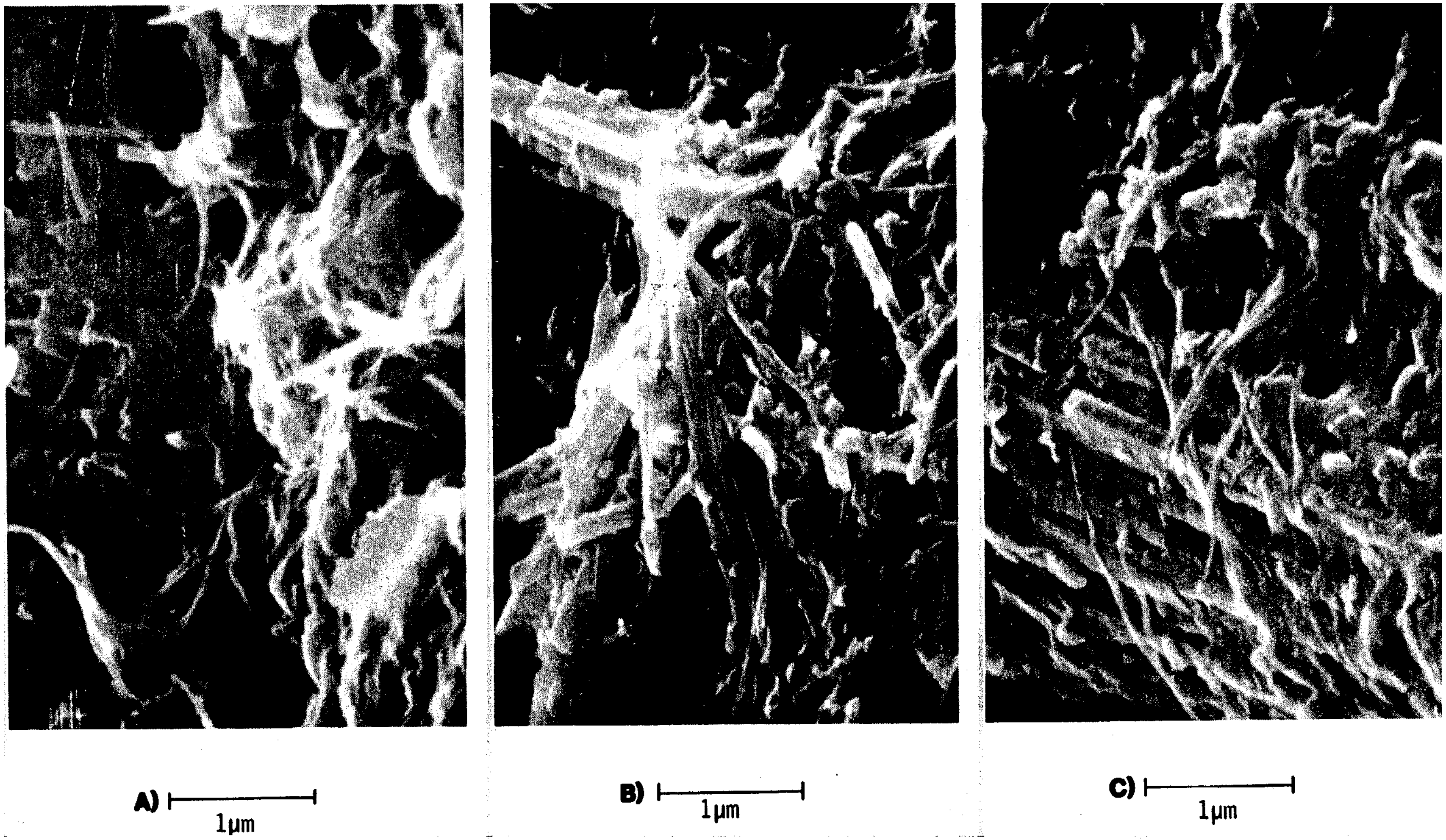

SCANNING ELECTRON PHOTOMICROGRAPHS OF USSAC CLAY

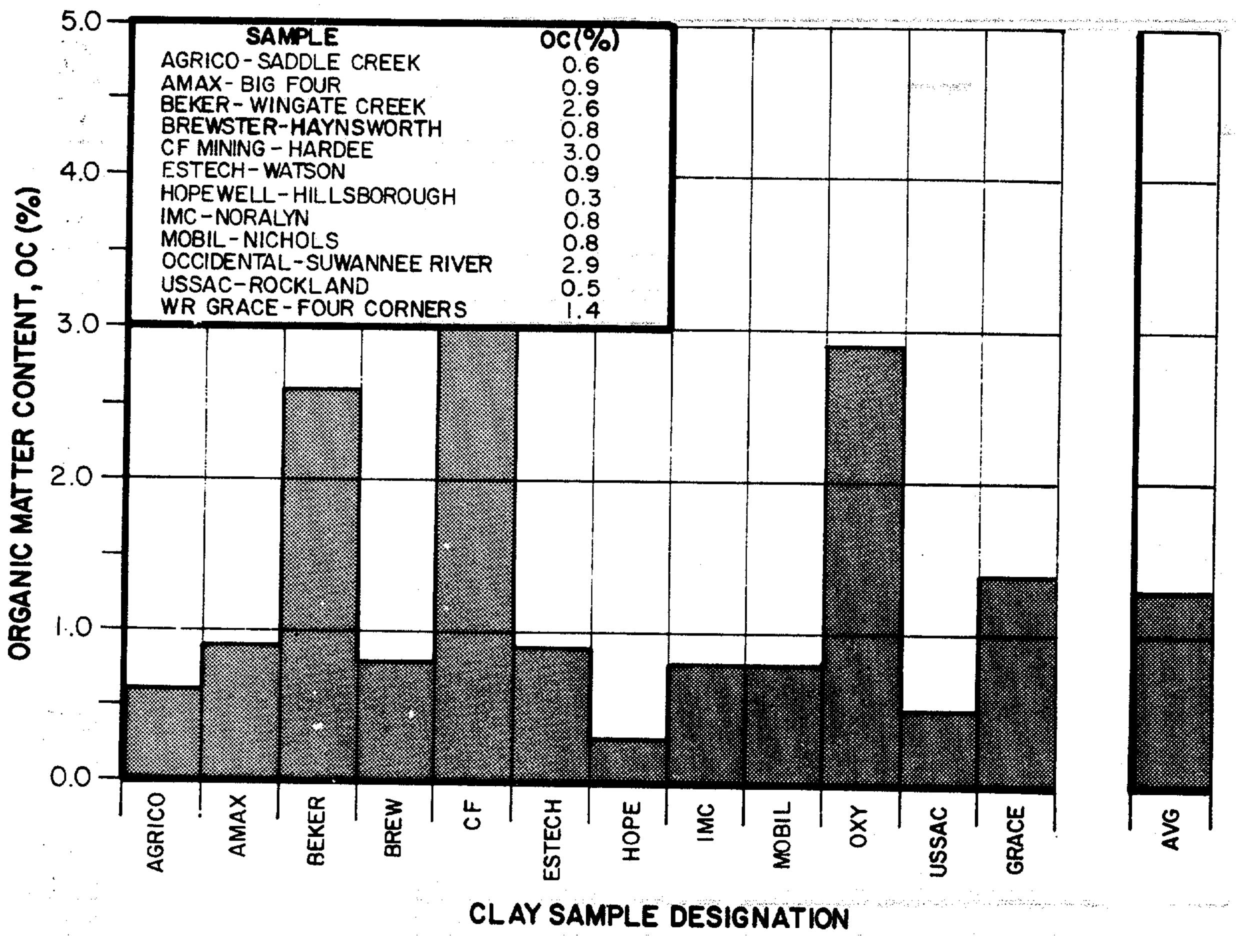

SAMPLE	OC(%)
AGRICO-SADDLE CREEK	0.6
AMAX-BIG FOUR	0.9
BEKER-WINGATE CREEK	2.6
BREWSTER-HAYNSWORTH	0.8
CF MINING-HARDEE	3.0
ESTECH-WATSON	0.9
HOPEWELL-HILLSBOROUGH	0.3
IMC-NORALYN	0.8
MOBIL-NICHOLS	0.8
OCCIDENTAL-SUWANNEE RIVER	2.9
USSAC-ROCKLAND	0.5
WR GRACE-FOUR CORNERS	1.4

ORGANIC MATTER CONTENT

FIGURE 4-14

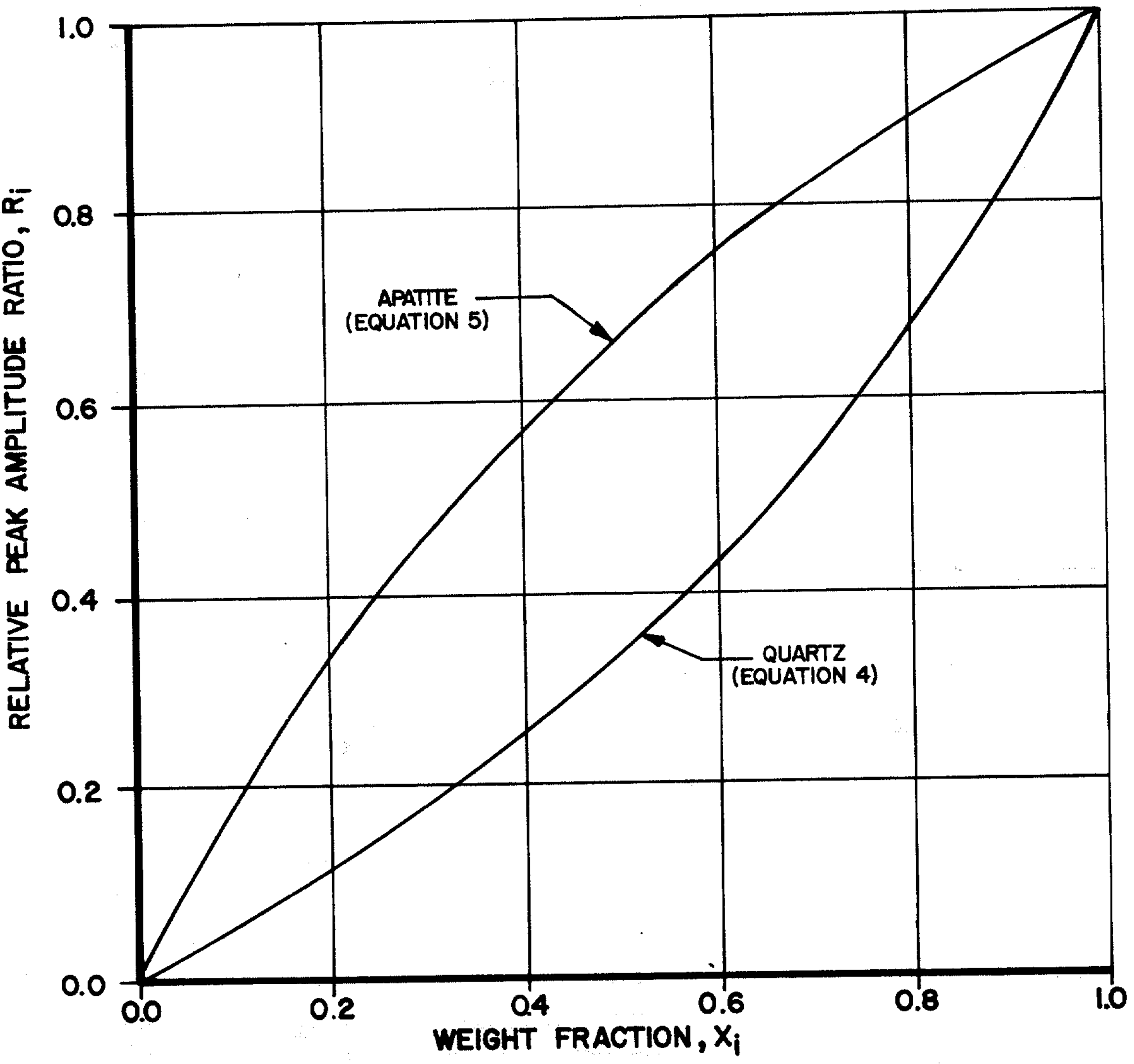

CALCULATED RELATIVE PEAK AMPLITUDE RATIO FOR QUARTZ - APATITE MIXTURE

FIGURE 4-15

FIGURE 4-16

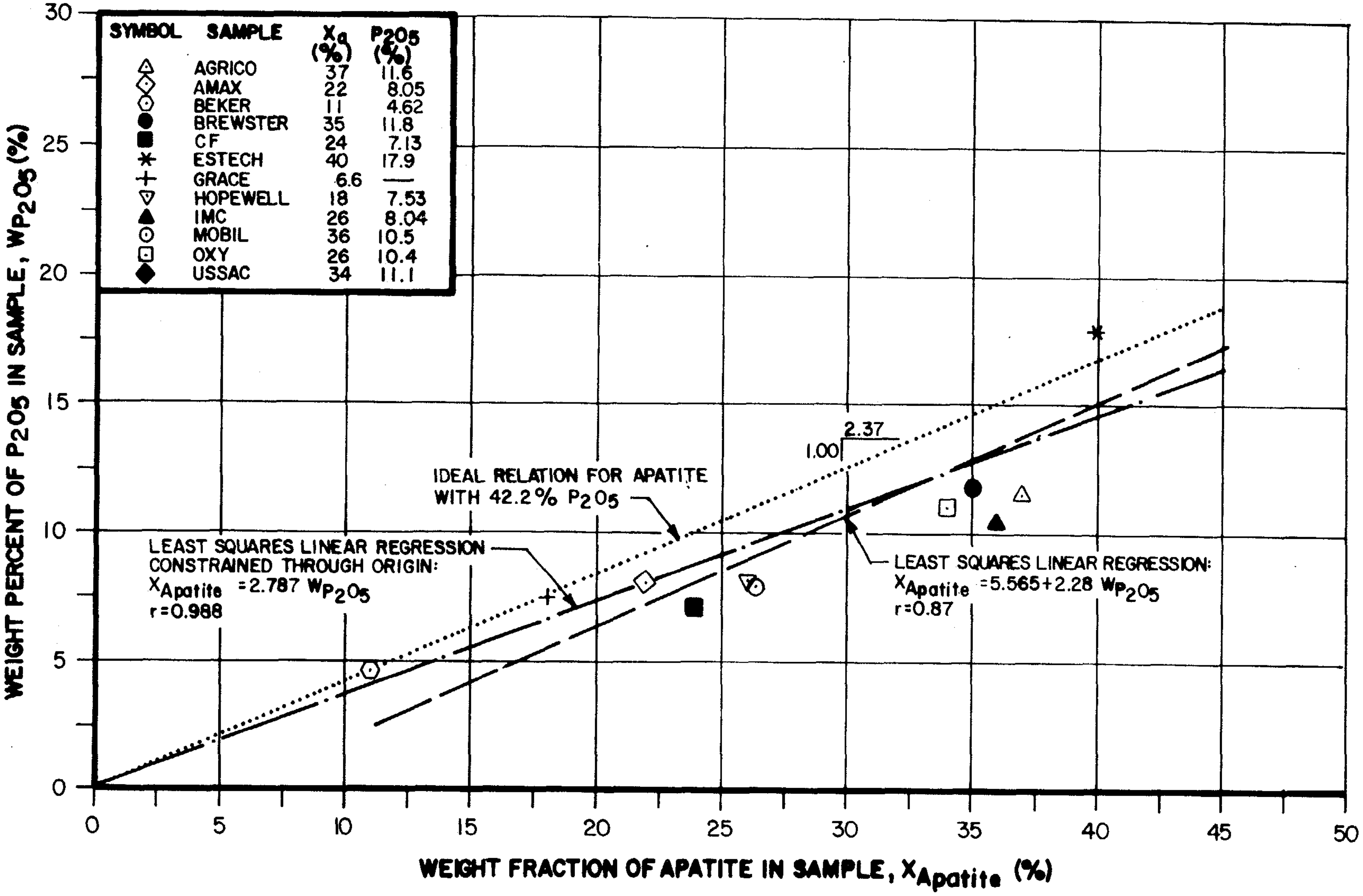

CORRELATION BETWEEN P_2O_5 CONTENT AND APATITE CONTENT

FIGURE 4-17

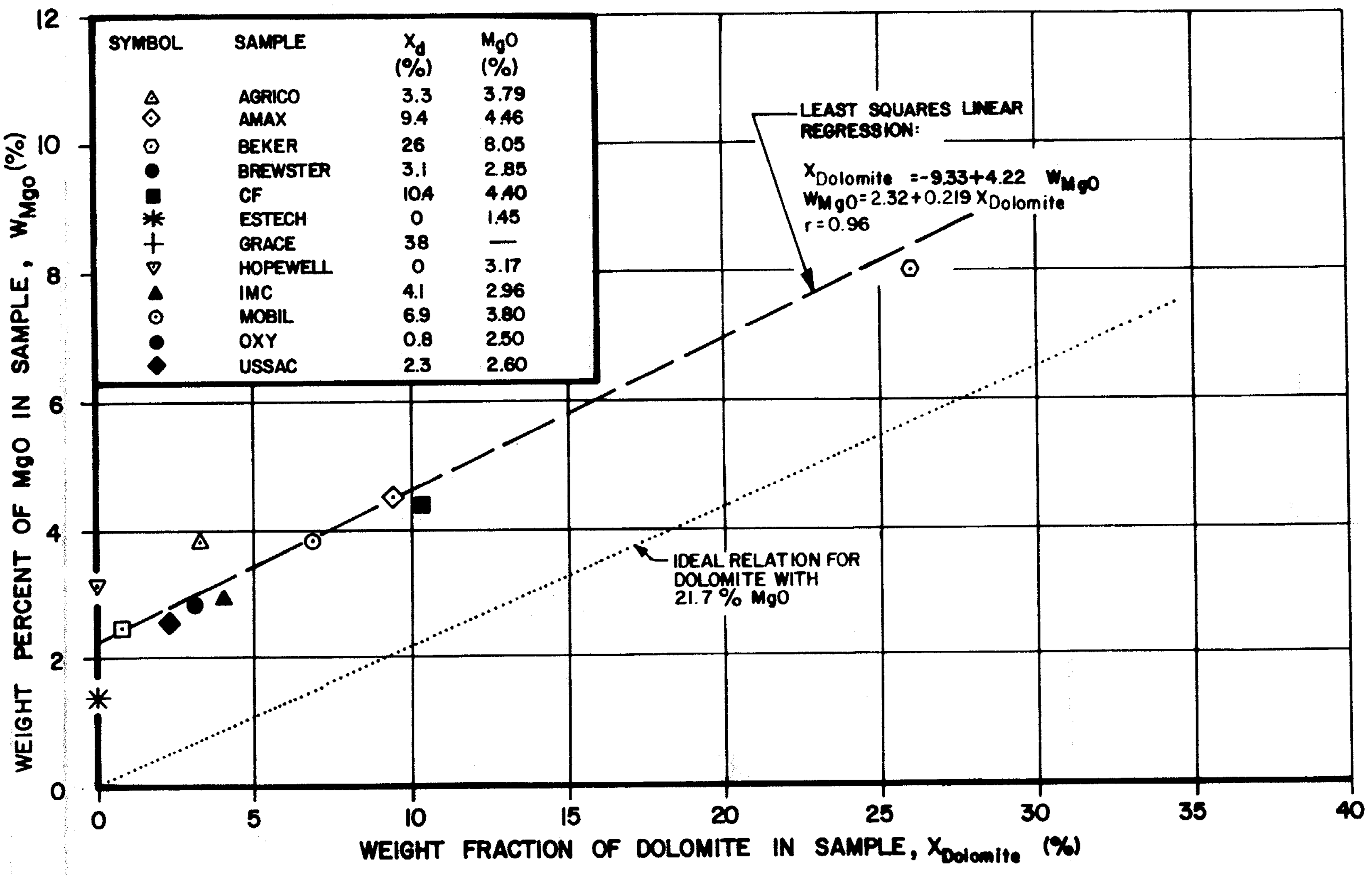

CORRELATION BETWEEN MgO CONTENT

AND DOLOMITE CONTENT

FIGURE 4-18

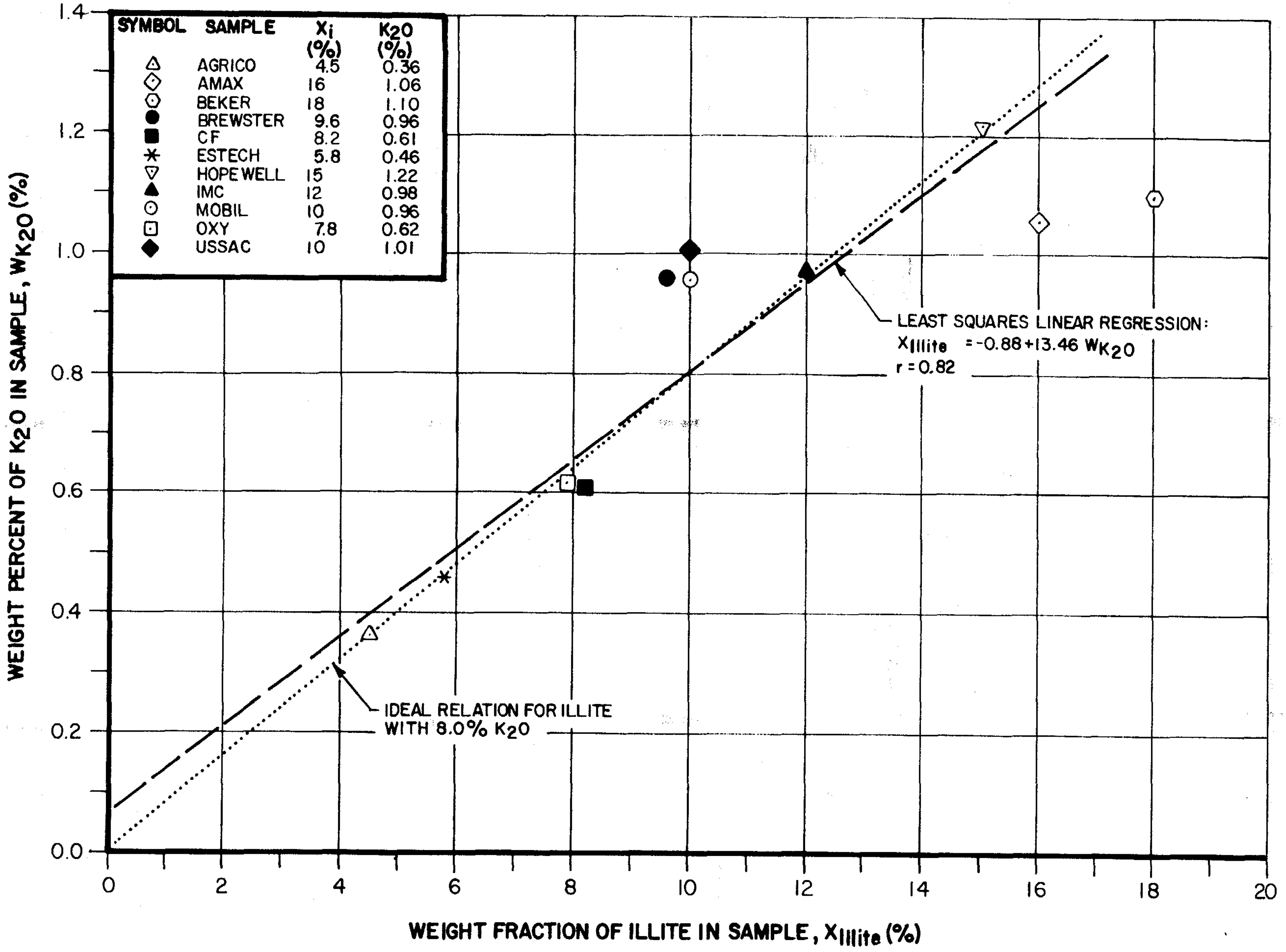

SYMBOL	SAMPLE	X_i (%)	K_2O (%)
△	AGRICO	4.5	0.36
◇	AMAX	16	1.06
⬡	BEKER	18	1.10
●	BREWSTER	9.6	0.96
■	CF	8.2	0.61
✱	ESTECH	5.8	0.46
▽	HOPEWELL	15	1.22
▲	IMC	12	0.98
⊙	MOBIL	10	0.96
⊡	OXY	7.8	0.62
◆	USSAC	10	1.01

CORRELATION BETWEEN K_2O CONTENT AND ILLITE CONTENT

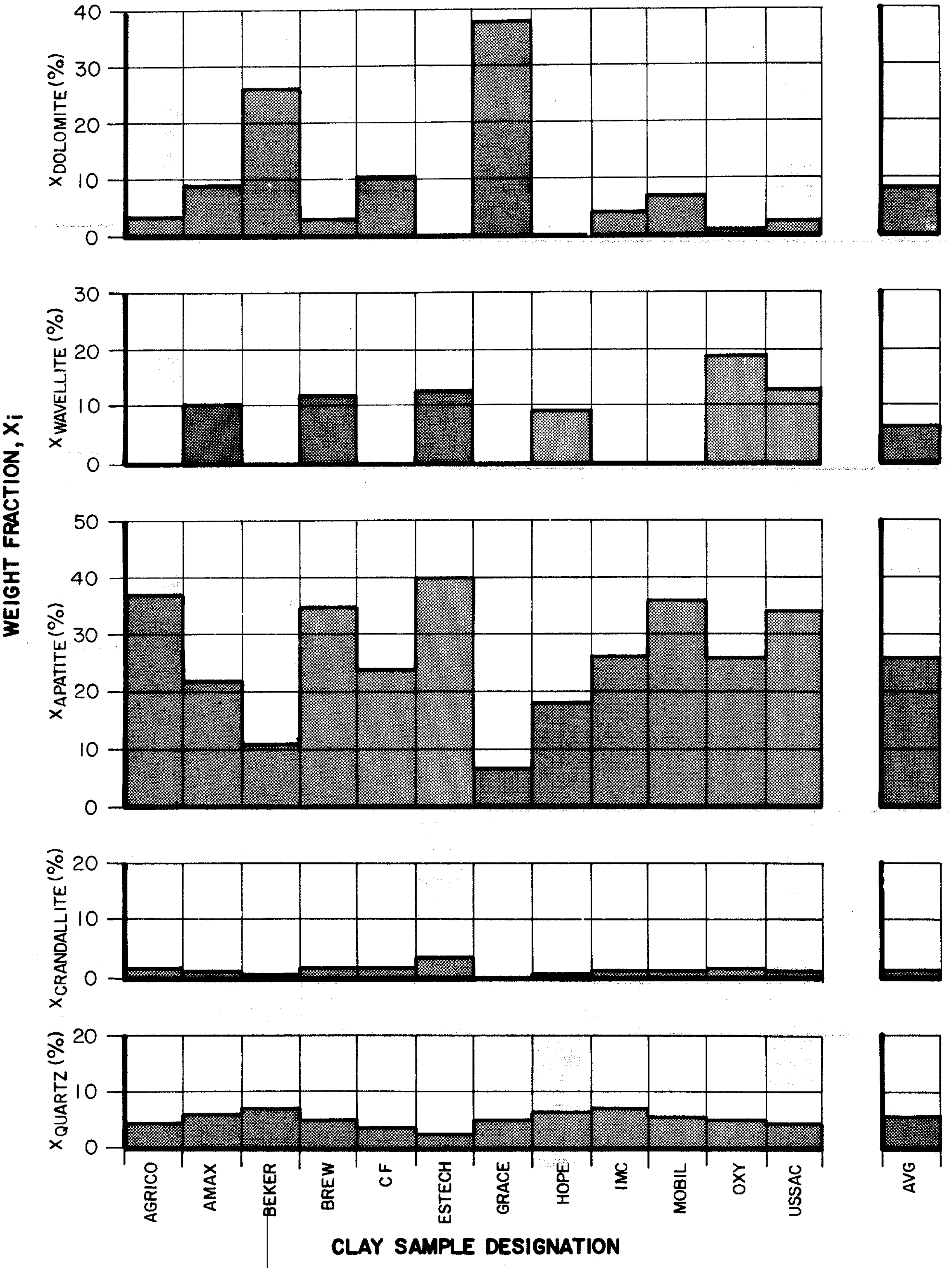

WEIGHT FRACTION OF NON-CLAY MINERALS IN -44μm SIZE FRACTION

FIGURE 4-19

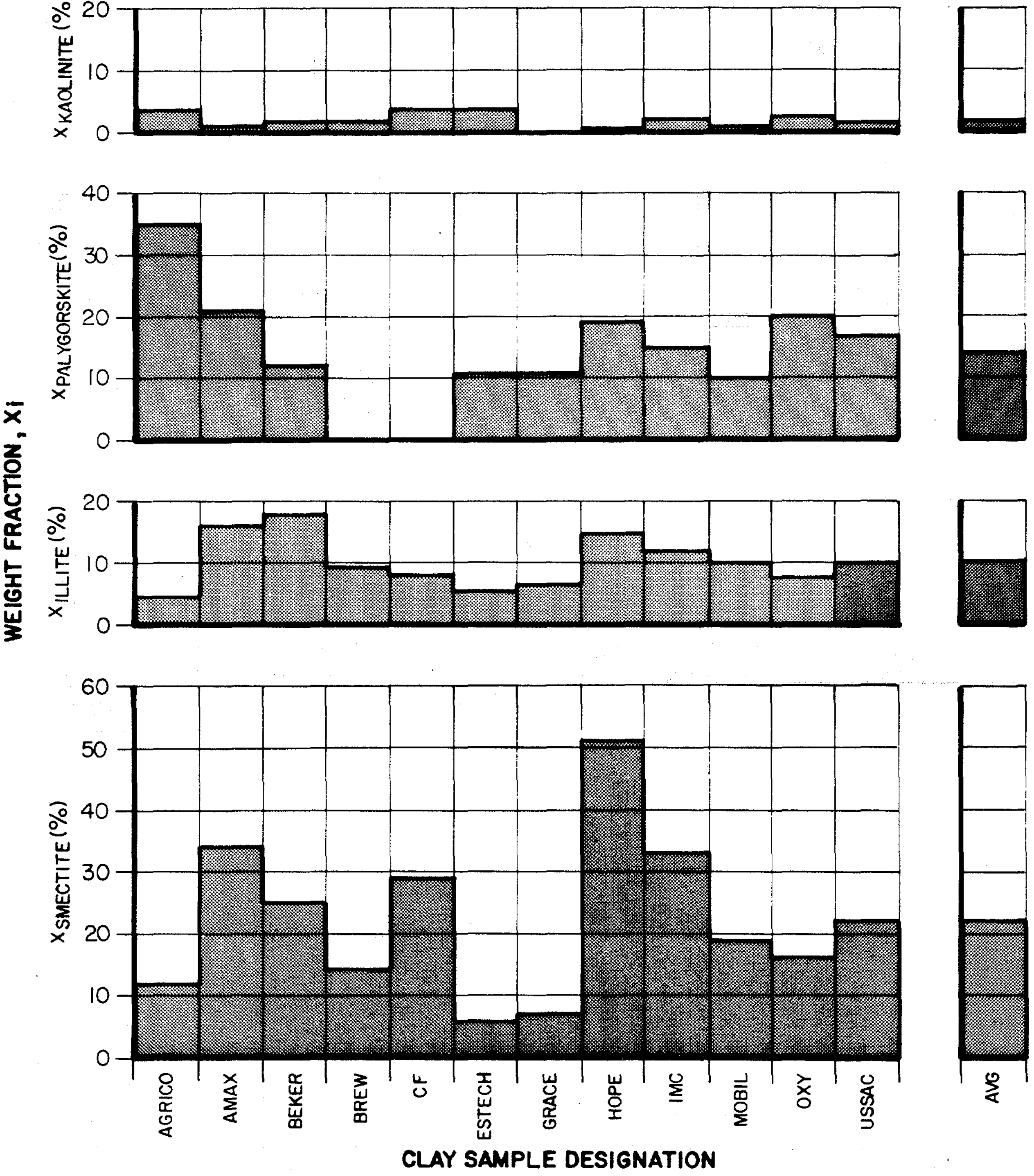

WEIGHT FRACTION OF CLAY MINERALS IN −44μm SIZE FRACTION

FIGURE 4-20

Section 5

MINERALOGY OF SELECTED SAND TAILINGS

5.1 **Introduction**

One sample of sand tailings from the Agrico-Saddle Creek Mine and two samples of sand tailings from the CF Mining-Hardee County Mine were selected for mineralogic analysis. The sand tailings were used to prepare samples for evaluation of the settling, consolidation and shear strength behavior of sand-clay mixes. X-ray diffraction analyses were performed to determine the mineral species present in each sand tailings.

5.2 **Physical Characteristics of Sand Tailings**

The particle size distribution for each sand tailings sample is presented in Figure 5-l. As shown, the sand tailings are similar in gradation with 1% of the sand tailings by dry weight finer than the 74 µm particle size. The uniformity coefficient, C_u*, for the sand tailings ranges from 1.8 to 2.0, indicative of poorly graded uniform sands. The sand tailings classify as SP soils according to the Unified Soil Classification System.

Microscopic examination of the samples showed features typical of Florida sand tailings. Angularity of the quartz varied from well rounded to sharp angular. Many of the quartz grains were aggregates of quartz cemented with quartz. The quartz in the three samples was very similar. Apatite in the CF samples was predominately black apatite. A high proportion of apatite in the Agrico sample was white grains that were well rounded and shiny.

The average specific gravity, p, from two determinations on each sand tailings sample is shown on Figure 5-l and listed in Table 5-l. The measured range of values of 2.690 to 2.859 are above the reference specific gravity for quartz of 2.66. Other minerals, most likely apatite (feed phosphate), therefore, are present within the sand tailings in significant quantities.

5.3 **X-Ray Diffraction Analyses**

X-ray diffraction of random powder mounts of sand tailings ground to pass a sieve with 44 µm openings indicated that quartz and apatite were the major crystalline phases. The Agrico sand tailings also contained a trace of feldspar not detected in either CF sample. Using the reference peak amplitudes and basal spacings in Table 2-l for quartz, apatite and feldspar, the relative peak amplitude ratios, R, summarized in Table 5-l were determined from X-ray diffraction analyses.

---

*The uniformity coefficient $C_u = D_{60}/D_{10}$ where D_{60} = particle size at which 60% of the soil is finer by dry weight and D_{10} = particle size at which 10% of the soil is finer by dry weight.

As shown, the three samples display a wide range of quartz and apatite relative peak amplitude ratios. The samples with the highest measured specific gravities also indicate the highest apatite relative peak amplitude ratios. The relative peak amplitude, ratios have a coefficient of variation between 5 and 10% based upon six repetitive tests on random powder mounts from the CF-l sample.

5.4 **Quantitative Mineralogic Composition**

To convert the relative peak amplitude ratios, R_i, into quantitative estimates of the weight fraction, X_i, of a given mineral in the sample, it is necessary to assume that:

- the reference quartz, apatite and feldspar minerals are identical to minerals occurring within the sand tailings;
- the minerals shown in Table 5-1 account for 100% of the respective sand tailings sample; and
- the reference mineral mass attenuation coefficients presented in Table 3-l are the same as occur for minerals within the sand tailings.

The X-ray diffraction analyses for sand tailings indicate that the composition is very closely a quartz-apatite binary mixture, except for the trace of feldspar in the Agrico sample. The weight fraction for each mineral component, X_i, therefore, can be determined as outlined below.

For a quartz-apatite binary mixture, the summation of the mineral phases must equal 100%, hence:

$$1.00 = \sum X_i = (X_q{*} + X_a{*}) \qquad (1)$$

Further, the sample mass attenuation coefficient, u_s, is equal to the sum of the contribution from each mineral component:

$$\mu_s = \sum \mu_i X_i = (\mu_q {*} X_q + \mu_a {*} X_a) \qquad (2)$$

Using the calculated sample mass attenuation coefficient, u_s and relative peak amplitude ratios, R_i, the weight fraction for a given mineral is calculated in its simplest form as:

$$X_i = R_i(\mu_s/\mu_i) \qquad (3)$$

---

*Where X_q = weight fraction of quartz; X_a = weight fraction of apatite; μ_q = mass attenuation coefficient for quartz; and μ_a = mass attenuation coefficient for apatite.

For a quartz-apatite mixture, Equation 3 is applied twice to determine X_q and X_a as follows:

$$X_q = \frac{R_q}{\mu_q} \quad (\mu_q X_q + \mu_a X_a) \qquad \textbf{(4a)}$$

$$X_a = \frac{R_a}{\mu_a} \quad (\mu_q X_q + \mu_a X_a) \qquad \textbf{(4b)}$$

Solving for X_q using Equations 1, 4a and 4b yields the expression:

$$X_q = \frac{R_q}{\mu_q} \quad (\mu_q X_q + (1.00 - X_q)\mu_a) \qquad \textbf{(5)}$$

The weight fraction of quartz and apatite in the two CF sand tailings samples calculated from Equations 1 and 5 are presented in Table 5-2. As shown, the CF samples yield quartz contents of 85.4 and 93.5% and apatite contents of 14.6 and 6.5%. The calculated specific gravities from the mineralogic composition in Table 5-2 and reference specific gravities in Table 3-1 yield values in excellent agreement with measured specific gravities.

The Agrico sand tailings sample contains a trace of feldspar. Equation 3 is applied three times, therefore, to determine X_q, X_a and X_f* as follows:

$$X_q = \frac{R_q}{\mu_q} \quad (\mu_q X_q + \mu_a X_a + \mu_f{}^* X_f) \qquad \textbf{(6A)}$$

$$X_a = \frac{R_a}{\mu_a} \quad (\mu_q X_q + \mu_a X_a + \mu_f X_f) \qquad \textbf{(6B)}$$

$$X_f = \frac{R_f}{\mu_f} \quad (\mu_q X_q + \mu_a X_a + \mu_f X_f) \qquad \textbf{(6C)}$$

Solving this series of equations yields the mineralogic composition for the Agrico sand tailings presented in Table 5-2. As shown, the Agrico sand tailings contains a significant component of apatite (38.6%), 60.4% quartz and 1.0% feldspar. The calculated specific gravity also agrees well with the measured value.

---

*Where X_f = weight fraction of feldspar; and μ_f = mass attenuation coefficient for feldspar.

Table 5-1

SAND TAILINGS X-RAY DIFFRACTION RELATIVE PEAK AMPLITUDE RATIOS

Sample	Designation	Measured Specific Gravity ρ (g/cm^3)	Relative Peak Amplitude Ratio, R_i (%)		
			Quartz	Apatite	Feldspar
CF Mining - Hardee No. 1	CF-1	2.719	75	26.9	0
CF Mining - Hardee No. 2	CF-1	2.690	88	8.1	0
Agrico-Saddle Creek	AGR	2.859	44	55	0.9

Table 5-2

SAND TAILINGS MINERALOGIC COMPOSITION

Sample	Designation	Measured Specific Gravity, ρ (g/cm^3)	Calculated Specific Gravity, ρ (g/cm^3)	Weight Fraction, X_i (%)		
				Quartz	Apatite	Feldspar
CF Mining - Hardee No. 1	CF-1	2.719	2.739	85.4	14.6	0.0
CF Mining - Hardee No. 2	CF-2	2.690	2.695	93.5	6.5	0.0
Agrico-Saddle Creek	AGR	2.859	2.868	60.4	38.6	1.0

FIGURE 5-1

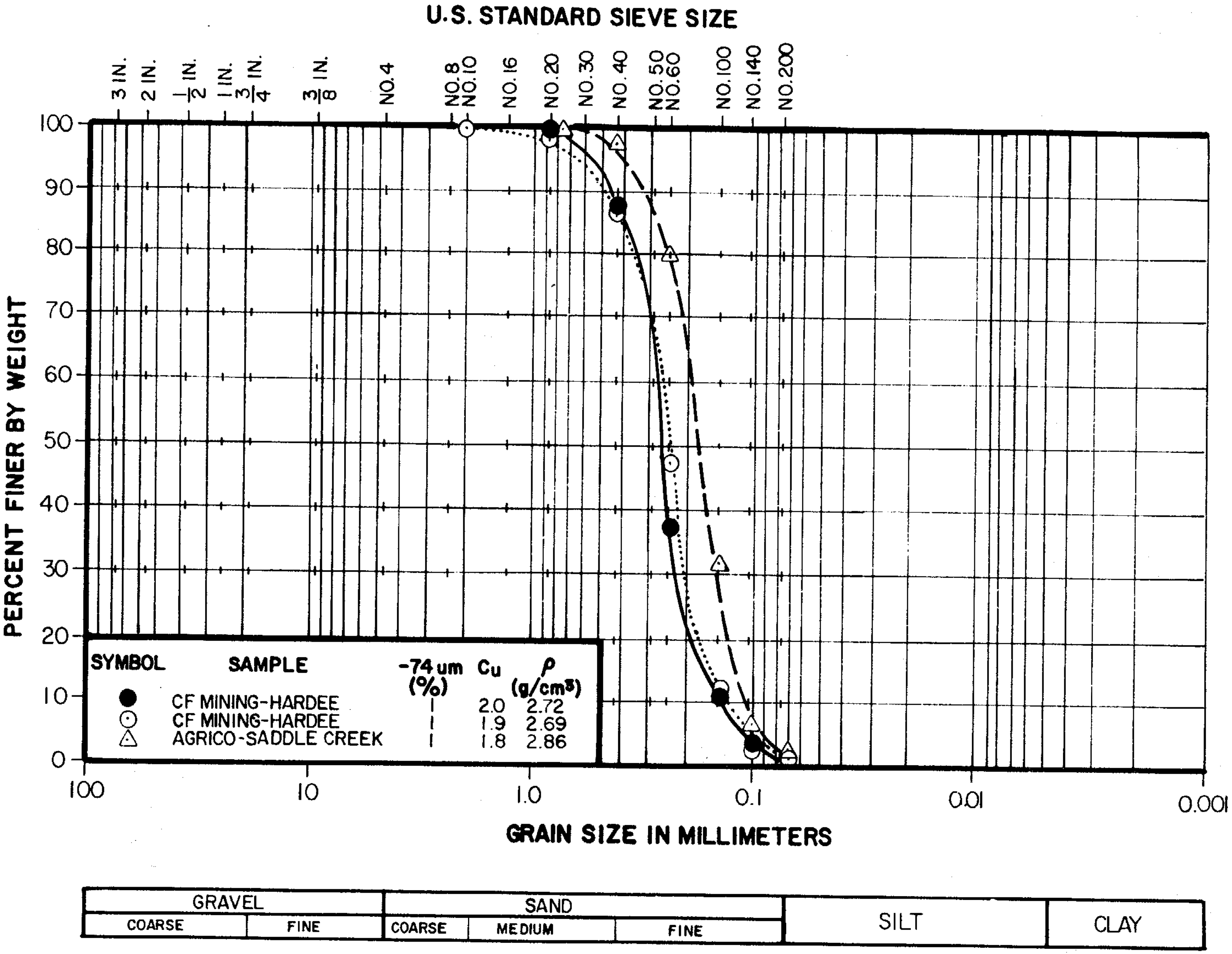

SELECTED SAND TAILINGS PARTICLE SIZE DISTRIBUTIONS

Section 6

CORRELATIONS BETWEEN ENGINEERING. PROPERTIES AND MINERALOGIC COMPOSITION

6.1 **Introduction**

Only a limited number of correlations exists between engineering properties and mineralogic composition. These are referred to by Lamont et al. (1975), Bromwell and Oxford (1977), Bromwell and Raden (1979) and Carrier, et al. (1981). The existing correlations were largely developed from settling tests and mineralogic analyses performed by Lamont et al. (1975) on 15 phosphatic clays. The results from these tests clearly indicated a strong correlation between final settled solids content and palygorskite content (Section 1.2). Other behavior, including viscosity and settling rate, were also found to correlate well with palygorskite content. The mineralogic analyses performed by Lamont et al. (1975), however, did not include quantitative analyses; hence only the relative and not the absolute weight fraction of palygorskite within the samples was known. Therefore, while correlations indicated that the higher the palygorskite content the lower the final settled solids content, the actual amount of palygorskite within a sample producing a given solids content was unknown.

The purpose of developing correlations between engineering properties and mineralogic composition from the results obtained during this study were to: (i) attempt to provide empirical methods to predict engineering properties from the known mineralogy of a clay; (ii) allow a fundamental understanding of the behavior of phosphatic clays; and (iii) establish a basis for comparison of the engineering properties of phosphatic clays from numerous sources. The correlations found from results obtained during the study are presented below. These correlations are based on mineralogic analyses presented in Section 4, settling test results reported in Volume 3, and index properties presented in Volume 1.

6.2 **Methodology**

Correlations between engineering properties and mineralogic composition were evaluated statistically to yield predictive relationships and indicate the degree of correlation between variables. Statistical analyses were performed with the General Electric Information Service Statistical Analysis System II Program STATII*** routines CURV and XREG. Regression analyses of bivariate data were performed with the curve-fitting routine CURV, which fit six curve types to the data: straight line; exponential; power function; hyperbola; reciprocal of straight line; and reciprocal of hyperbola. Regression analyses of multivariate data were performed with the multiple regression curve-fitting routine XREG, which fits a linear model to a series of observations.

6.3 **Correlations with Index Properties**

The index properties commonly determined for phosphatic clays include the Atterberg limits, activity and specific gravity. Comparisons of these index properties with mineralogic composition determined for the twelve selected phosphatic clays are presented below.

6.3.1 Atterberg Limits

The plasticity characteristics of the twelve selected phosphatic clays are shown in Figure 6-l. The plasticity characteristics of individual clay minerals reported in the literature and detected in phosphatic clays are also presented in Figure 6-l. The plasticity of clay minerals within phosphatic clays, namely kaolinite, illite, palygorskite and montmorillonite*, vary considerably from specie to specie as well as for the same clay specie for a given adsorbed cation. Depending on the relative percentage of each clay mineral with a phosphatic clay, therefore, the plasticity of phosphatic clays will also vary considerably. As shown, the smectite group clay minerals generally yield the highest plasticity, whereas kaolinite clay minerals yield the lowest plasticity.

Depending on physio-chemical interactions between clay minerals, a correlation between mineralogy and plasticity may be possible. For example, Seed, Woodward and Lundgren (1964) have shown that the liquid limit of a kaolinite-sodium montmorillonite mixture agrees with theoretically calculated values with each mineral contributing in proportion to the amount present. For this type of linear behavior, a correlation between liquid limit and mineralogy could possibly be developed. Other mixtures of clay species, however, do not display such linear behavior. An illite-sodium montmorillonite mixture, for example, has been shown to produce non-linear behavior between liquid limit and mineralogy, with liquid limits considerably below the theoretically calculated value assuming each mineral contributes in proportion to the amount present (Seed, Woodward and Lundgren, 1964)**.

An attempt to correlate liquid limit with weight fraction of clay minerals in each of the 12 selected phosphatic clays was performed using a multiple linear

---

*Montmorillonite is one clay mineral type within the smectite group of clay minerals where the Atterberg limits are well documented in the literature. The particular type of smectite within the phosphatic clays, however, was not determined.

**This behavior was attributed by Seed, et al. (1964) to excess salt in the illite that, when mixed with sodium montmorillonite, prevented full expansion of the montmorillonite in the presence of water.

regression curve-fitting model with the parameters: weight fraction of non-clay minerals; and weight fraction of smectite, palygorskite and illite (Table 4-14). The results from this analyses indicated a poor correlation between liquid limit and mineralogic composition, with only 35.8% of the variability in liquid limit explained by the selected parameters*. The analysis further indicated that the clay minerals palygorskite and illite displayed the greatest correlation to liquid limit of the four variables, with 34.7% of the variation in liquid limit explained by these two parameters.

The absence of a linear correlation between liquid limit and mineralogic composition indicates that: physio-chemical interactions may occur between clay species producing liquid limits not linearly related to the weight percent of clay minerals; and/or the exchangable cation within a given clay specie varies between phosphatic clays.

6.3.2 Activity

The engineering properties of clays are influenced by both the type of clay mineral as well as the amount of clay present. The relative influence of these two factors on the engineering behavior of a clay can be qualitatively evaluated by the activity of a clay, which is defined as the ratio of the plasticity index to the clay size fraction (Skempton, 1953). As shown in Figure 6-2, the relation between plasticity index and clay fraction for a given clay mineral is typically a straight line passing through the origin.

The activities of clay species reported in the literature and found in phosphatic clays are shown in Figure 6-2. Smectite minerals have activities ranging from 1 to 7 (Mitchell, 1976) with the most active smectite (sodium montmorillonite) having activities of 3 to 7.2. Calcium montmorillonite typically has an activity of 1.3. Illite, palygorskite and kaolinite typically have activities of 0.9, 1.2 and 0.50, respectively. These activities correspond to plasticity indices of 100 to 720% for smectite, and 90, 120 and 50% for illite, palygorskite and kaolinite, respectively.**

The activities of the phosphatic clays ranged from 1.6 to 3.9. These values are higher than typically occur for either illite, palygorskite or kaolinite clay minerals, and reflect the influence of higher activity smectite minerals on the overall activity of phosphatic clays.

An attempt to correlate activity with weight fraction of clay minerals in each of the 12 selected phosphatic clays was performed using multiple linear regression curve-fitting techniques. No meaningful correlations, however, were found to exist indicating that the activity of a phosphatic clay cannot be used to predict

---

*Using plasticity index, PI, instead of liquid limit as the dependent variable produced similar statistical results.

**Refer to Figure 6-1 for comparison of these plasticity indices with those reported for the clay minerals.

correlation is not totally surprising, since Seed et al. (1964) have shown that a kaolinite-sodium montmorillonite mixture in ratios of 1.5:l to 4:l has activities of 3.25 to 1.95, while a sodium montmorillonite-illite mixture in ratios of 4:l to 1.5:1 has similar activities of 3.33 to 1.78*. Hence, phosphatic clays with the same activity may exhibit large differences in mineralogy, precluding the development of a unique correlation between activity and mineralogic composition.

6.3.3 Specific Gravity

A comparison of calculated specific gravities and measured specific gravities** for five of twelve phosphatic clays is shown in Table 6-l. The specific gravity was calculated using reference mineral specific gravities from Tables 3-l and 3-3 only for samples where the total mineral summation, $\sum X_i$, was approximately 100% (Table 4-14). Where mineralogic data were available, both the +105 µm and -44 µm size fraction mineralogic composition were considered. Where the +105 µm size fraction mineralogic composition was not determined, the -44 µm size fraction composition was used for the entire sample.

For the five samples analyzed, the calculated specific gravities agree well with measured values. The ratio of the measured to calculated values averages 101.0%, with a range of 96.7 to 105.1%. Although a correlation cannot be developed between specific gravity and mineralogic composition, since numerous combinations of minerals produce the same specific gravity, the comparison does indicate that the reference minerals are appropriate for calculating the specific gravity of a sample from a known mineralogic composition.

6.4 **Correlations with Sedimentation Behavior**

Correlations between mineralogy and sedimentation behavior have been documented in the literature by Lamont et al. (1975), Bromwell and Oxford (1977), Bromwell and Raden (1979) and Carrier et al. (1981). The most significant finding reported to-date between mineralogy and sedimentation behavior has been the correlation between palygorskite content and final settled solids content. A correlation has also been reported between palygorskite content and laboratory settling velocity. The mineralogy and sedimentation test results obtained during this investigation have been analyzed considering these previously developed correlations. The results are presented below.

6.4.1 Final Settled Solids Content

Correlations between final settled solids content, S_F, and palygorskite weight fraction X_p, are presented in Figures 6-3, 6-4 and 6-5 for initial solids contents, S_i, of 1.0, 3.0 and 8.0%, respectively . The phosphatic clays where mineralogic

---

*These activities were obtained on mixtures composed of sodium montmorillonite (bentonite), illite and kaolinite with clay mineral activities of 5.40, 0.93 and 0.36, respectively.

**Measured in accordance with ASTM Standard D-854.

analyses yield a mineral summation close to 100% (i.e., 88.9 to 105.8%) are distinguished from clays where the mineral summation is less satisfactory, since the mineralogic results are probably more accurate for clays where the mineral summation is close to 100%. For each initial solids content, the best-fit correlation between final settled solids content and palygorskite weight fraction was determined via regression analyses. For each set of data, an exponential regression of the form $X_p = ae\beta(S_F)$ was found to yield the best-fit correlation**.

The sedimentation behavior of the AMAX and Brewster phosphatic clays apparently is not consistent with the established correlation between final settled solids content and palygorskite weight fraction. As shown on Figures 6-3, 6-4 and 6-5, these clays clearly display behavior in disagreement with the remaining ten phosphatic clays. Accordingly, the results for these clays have been omitted from the regression analyses. As discussed in Sections 4.4.4.1 and 4.6.2.4, the Brewster sample may contain 5 to 10% palygorskite. If the Brewster phosphatic clay contains 10% palygorskite, the sedimentation behavior would yield good agreement with other phosphatic clays. The AMAX phosphatic clay, however, is a consistent outlier with a relatively high final settled solids content and a relatively high palygorskite weight fraction.

The correlations shown in Figures 6-3, 6-4 and 6-5 indicate a strong correlation between final settled solids content and palygorskite weight fraction. The trend of increasing final solids content with decreasing palygorskite weight fraction yields correlation coefficients, r, of -0.915, -0.965 and -0.950 for initial solids contents of 1.0, 3.0 and 8.0%, respectively. Although most of the tested phosphatic clays have palygorskite contents of 10 to 20%, the correlation indicates that palygorskite contents of: less than 5% are necessary for "good" settling characteristics ($S_F > 15\%$); and greater than 25% produce "poor" settling characteristics ($S_F<7\%$)***. Unfortunately, the results obtained for the AMAX phosphatic clay suggest that the correlation is not universally applicable to all clays, and that other as yet unknown factors may also control sedimentation behavior (e.g., shape of palygorskite particles, other clay minerals and clay mineral interstratification, etc.).

Attempts to correlate sedimentation behavior with the weight fraction of other clay minerals, total clay content, or total non-clay mineral content were unsuccessful. For example, as shown in Figure 6-6, no correlation exists between final settled solids content and smectite weight fraction, yet smectite was the dominant clay mineral in eight of twelve samples. As shown in Figure 6-6, phosphatic clays with smectite weight fractions of 6 to 51% exhibited simmilar final settled solids contents of 9 to 12%.

**Where a and β are the regression coefficients.

***The classification of "good" and "poor" settling characteristics is arbitrary. The values of S_F are based on $S_i = 3.0\%$ (Figure 6-4).

6.4.2 Laboratory Settling Rate

A weak correlation between the maximum laboratory settling rate, Q_1, and palygorskite weight fraction, X_p, was found as shown in Figure 6-7. The correlation suggests that the maximum laboratory settling rate increases as the palygorskite content decreases. This correlation is expected, however, since settling tests have generally shown correlations indicating that the higher the settled solids content, the greater the laboratory settling rate.

6.5 Correlations with Consolidation and Shear Strength Characteristics

Attempts to correlate mineralogic composition to consolidation and shear strength properties were not successful.

6.6 Summary and Practical Implications

The present attempt to correlate engineering properties with mineralogic composition has generally been unsuccessful, except with respect to the sedimentation behavior of phosphatic clays. Quantitative prediction of clay behavior in terms of mineralogic composition, however, has generally always been a difficult objective. The accurate and complete quantitative determination of composition; unknown physical and chemical interactions between mineral phases; the determination and quantitative expression of the fabric or structure of a soil; and the absence of physio-chemical theories relating composition to engineering properties all present difficulties in predicting engineering properties from mineralogic composition (Mitchell, 1976).

No correlations were found between the Atterberg limits or activity of phosphatic clays and mineralogic composition for the twelve phosphatic clays investigated. The only meaningful correlation found was between palygorskite content and final settled solids content, which is useful in assessing the sedimentation behavior. Even this correlation, however, was not found to be applicable to all twelve of the tested phosphatic clays.

Table 6-1

COMPARISON OF CALCULATED AND MEASURED SPECIFIC GRAVITIES

	+105 μm Size Fraction*		-44 μm Size Fraction*			Bulk Sample		
Sample	+105 μm (%)	ρc_1 (g/cm^3)	-44 μm (%)	$\sum X_i$ (%)	ρc_2 (g/cm^3)	ρm (g/cm^3)	ρc** (g/cm^3)	$\rho m/\rho c$ (%)
Agrico	6.0	2.879	94.0	101.0	2.716	2.788	2.726	102.3
Beker	0.0	n	100.0	101.9	2.808	2.766	2.808	98.5
IMC	8.0	n	92.0	100.8	2.756	2.818	2.756	102.2
Oxy	6.0	2.931	94.0	98.7	2.624	2.778	2.642	105.1
USSAC	0.0	-	100.0	105.8	2.906	2.812	2.906	96.8

Where: ρ_c = Calculated specific gravity; ρ_m = Measured specific gravity; $\sum X_i$ = Mineral summation based on mineralogic analyses (i.e., percent minerals accounted for in calculation of -44 μm size fraction).

*+105 μm and -44 μm size fraction assumed to correspond to measured +74 μm and -74 μm size fractions, respectively.

**Bulk sample $\rho_c = (\rho_{c_1}(\%+105\ \mu m) + \rho_{c_2}(\% -44\ \mu m))/100$.

n = Insufficient material for mineralogic analysis after sample preparation.

FIGURE 6-1

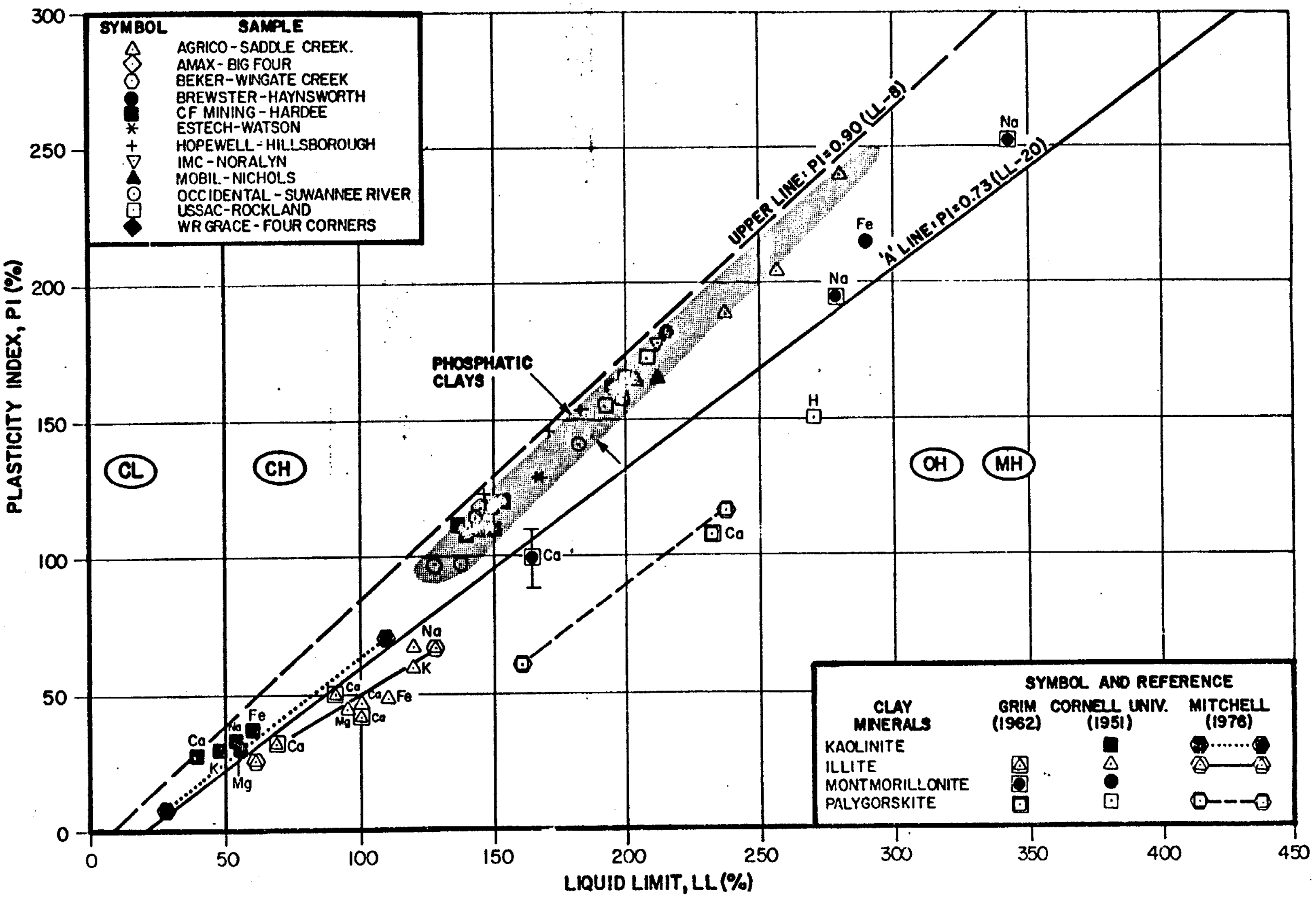

PLASTICITY OF PHOSPHATIC CLAYS AND CLAY MINERALS

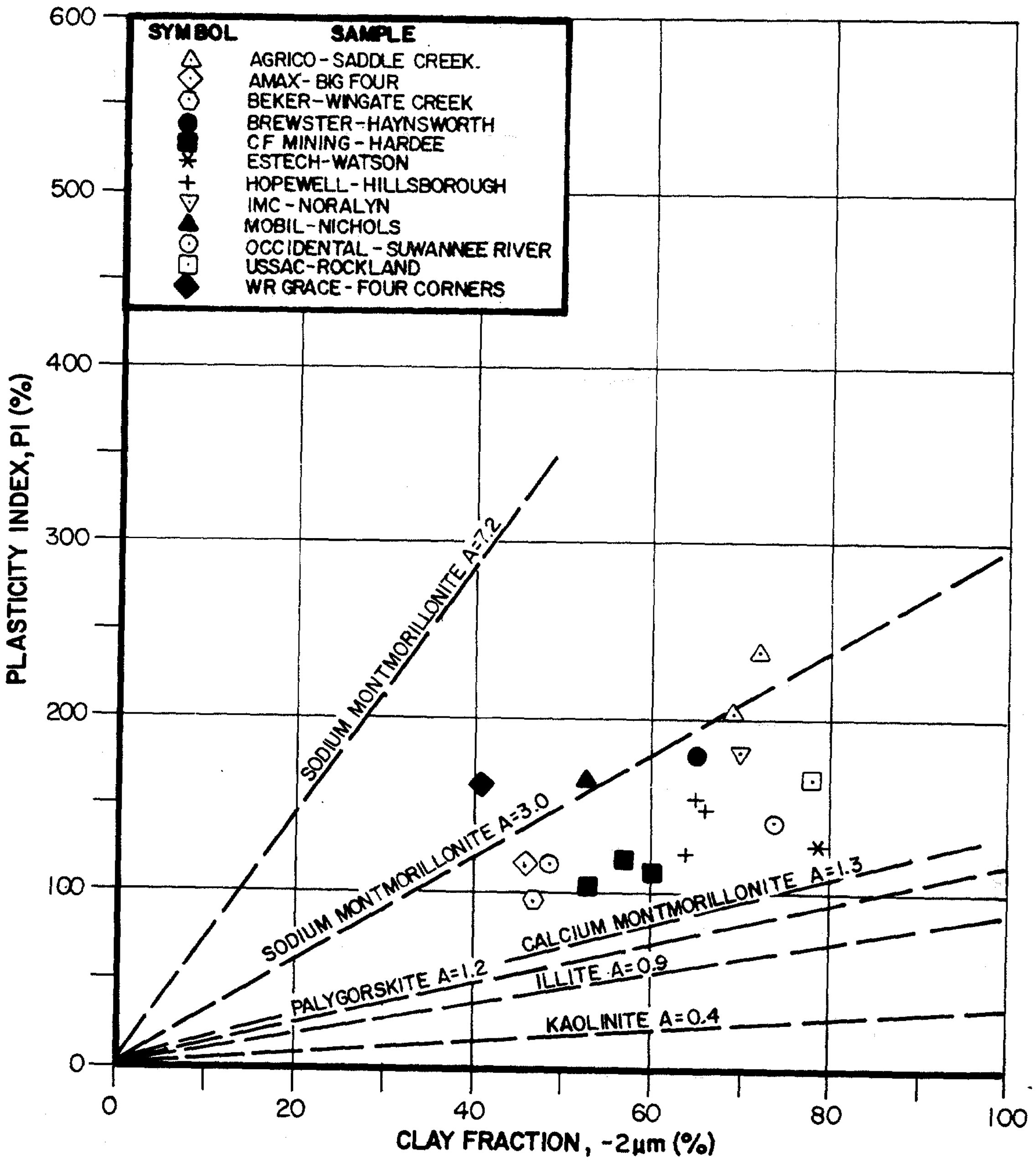

SOURCE: ACTIVITY OF: KAOLINITE, ILLITE AND SODIUM MONTMORILLONITE FROM SKEMPTON (1953); PALYGORSKITE FROM MITCHELL (1976); AND CALCIUM MONTMORILLONITE FROM GRIM (1962)

ACTIVITY OF PHOSPHATIC CLAYS AND CLAY MINERALS

FIGURE 6-2

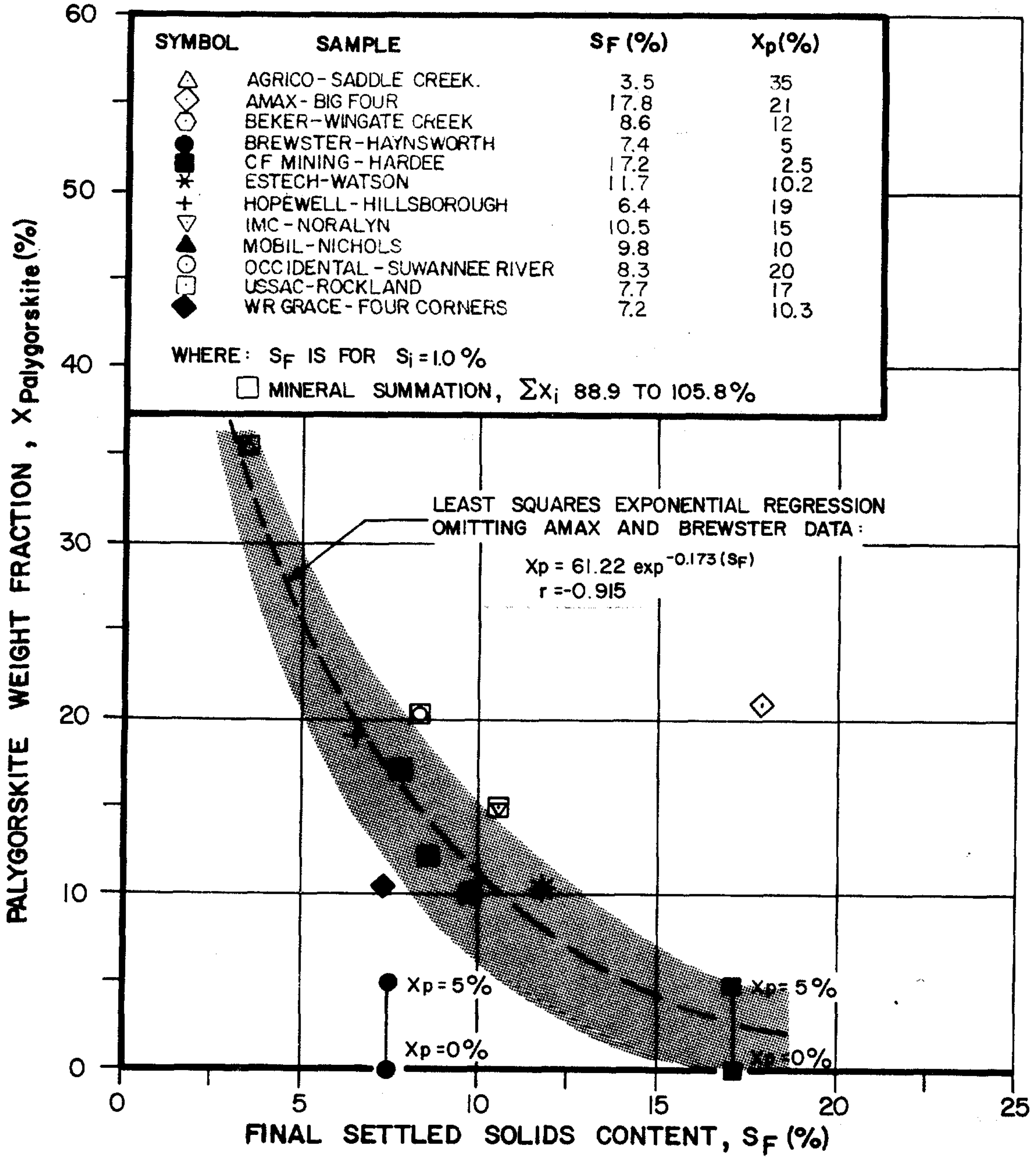

FINAL SETTLED SOLIDS CONTENT VS.
PALYGORSKITE WEIGHT CONTENT
FOR S_i=1.0%

FIGURE 6-3

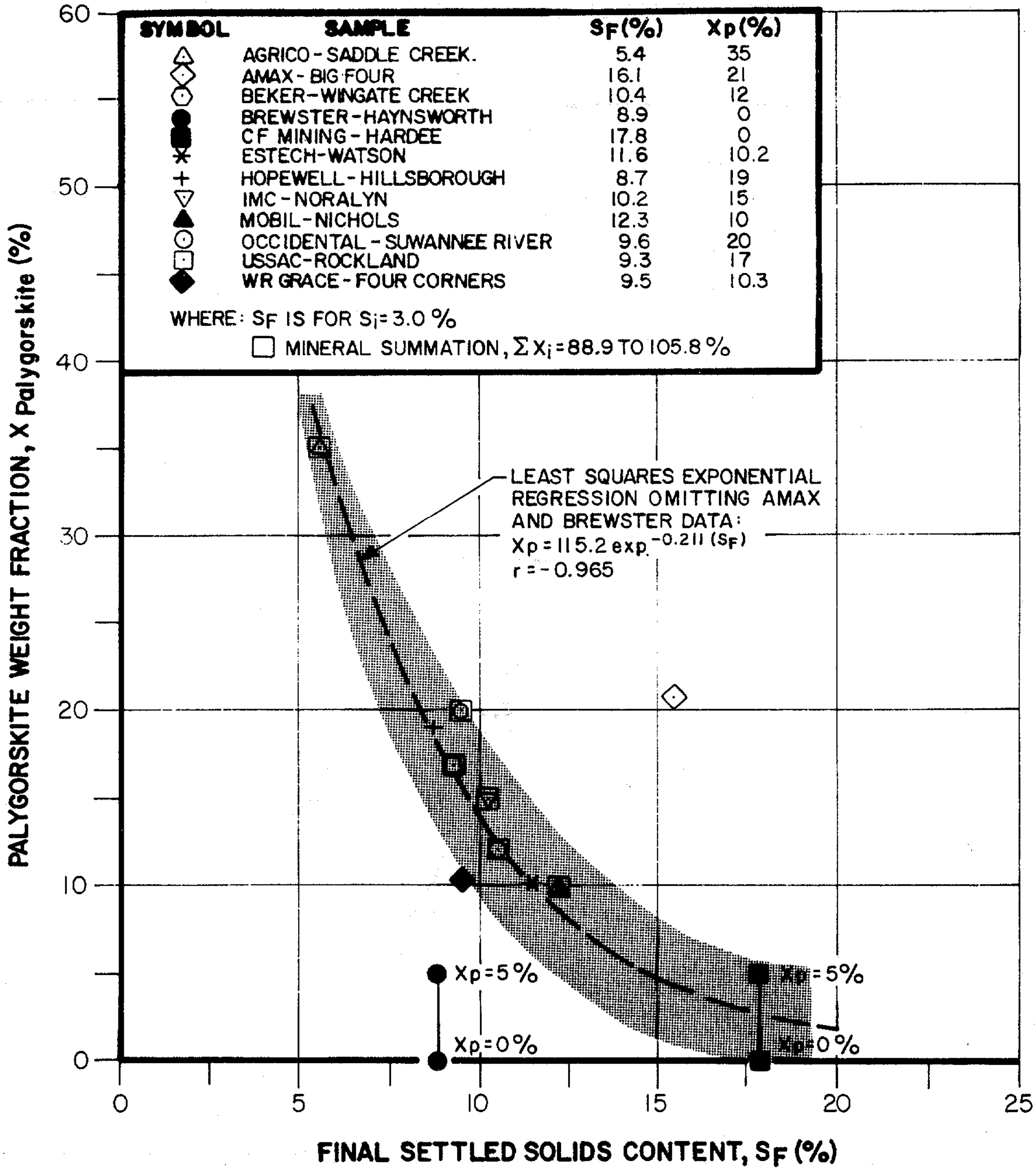

FINAL SETTLED SOLIDS CONTENT VS.
PALYGORSKITE WEIGHT FRACTION FOR Si=3.0%

FIGURE 6-4

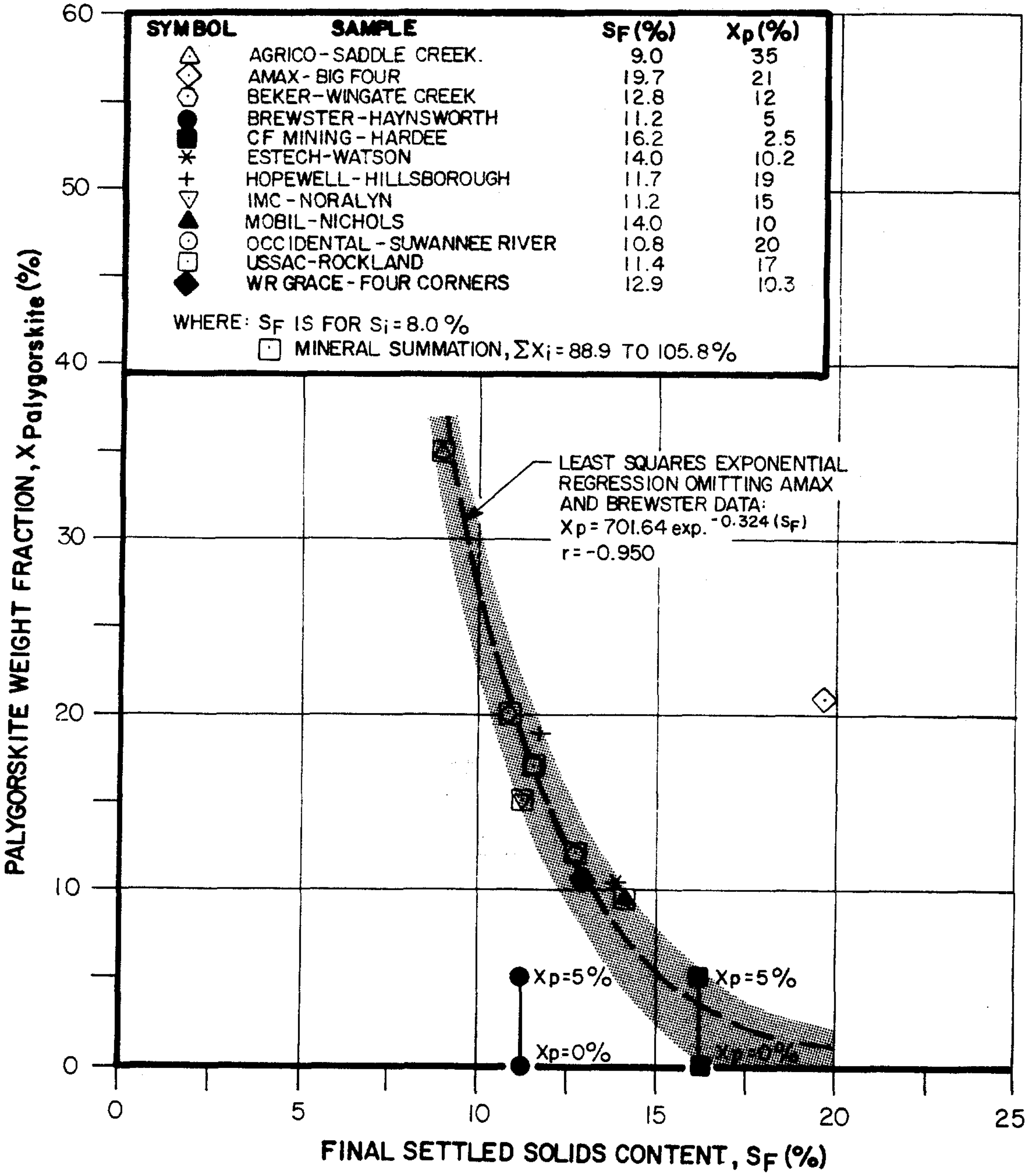

FINAL SETTLED SOLIDS CONTENT VS. PALYGORSKITE WEIGHT FRACTION FOR S_i=8.0%

FIGURE 6-5

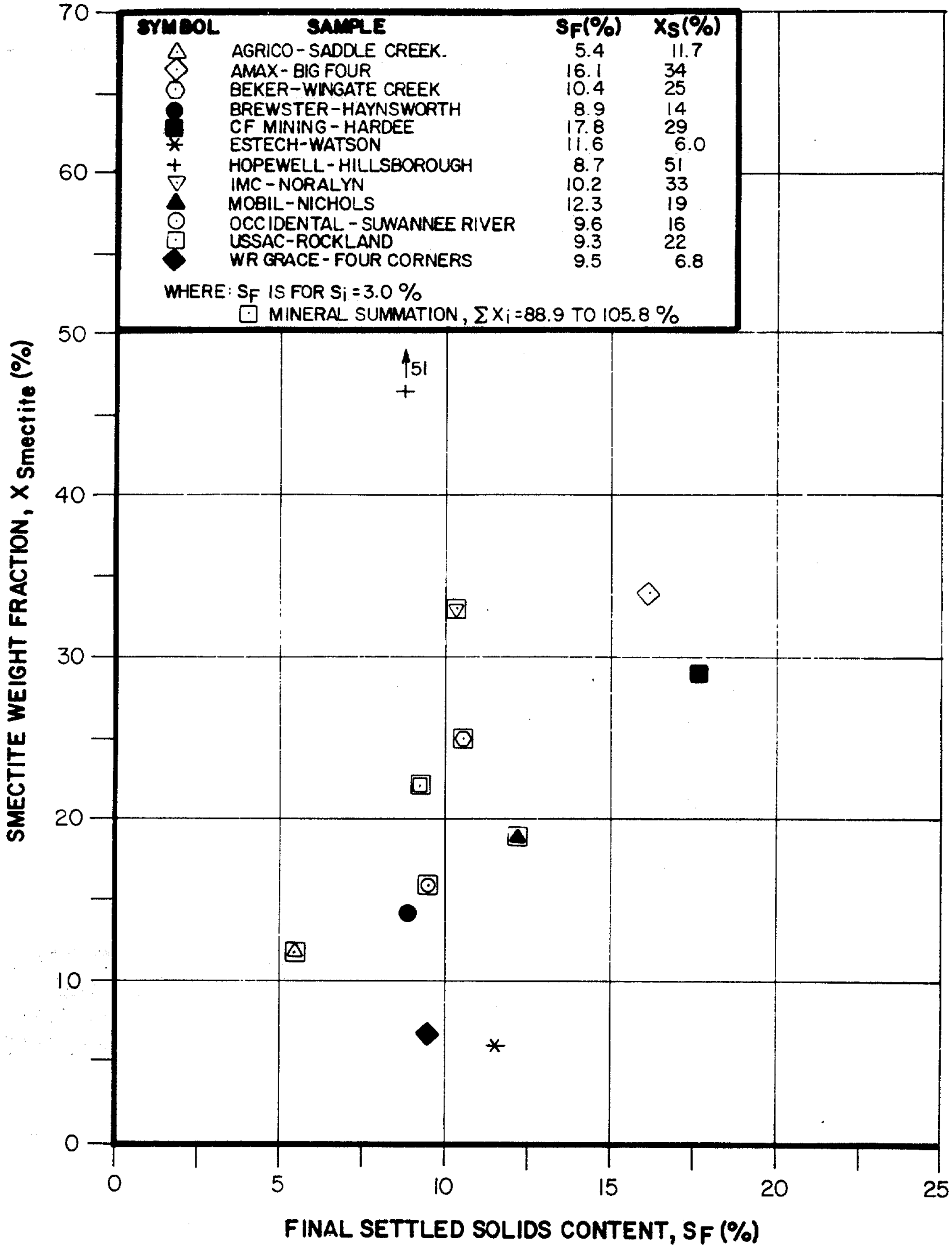

FINAL SETTLED SOLIDS CONTENT VS. SMECTITE WEIGHT FRACTION

FIGURE 6-6

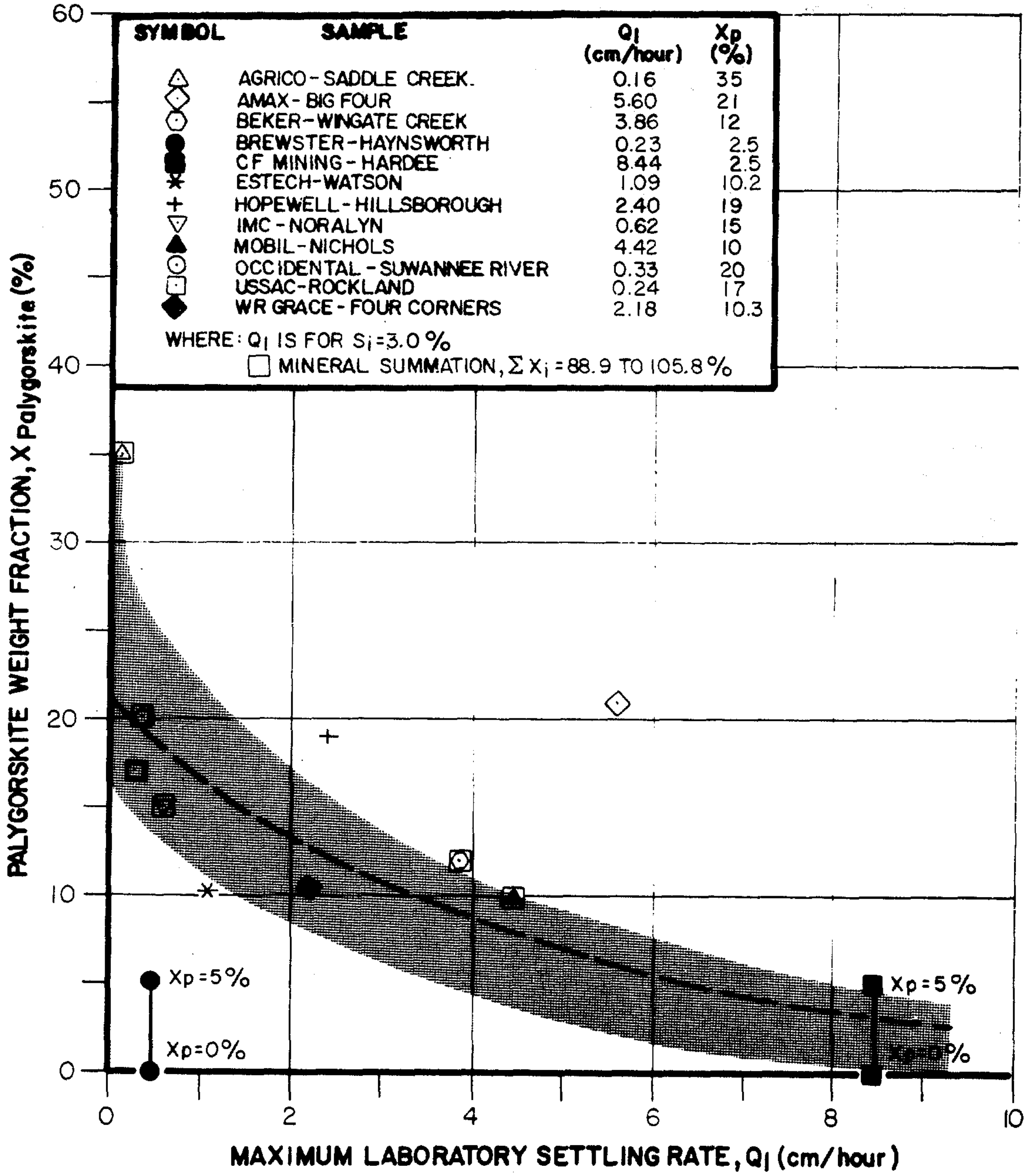

MAXIMUM LABORATORY SETTLING RATE VS. PALYGORSKITE WEIGHT FRACTION

FIGURE 6-7

Section 7

REFERENCES

Blanchard, F. N. (1972). “American Mineralogist”, V. 57.

Bromwell, L. G. (1981). “Evaluation of Alternative Processes for Disposal of Fine-Grained Waste Materials.” Seminar on Consolidation Behavior of Fine-Grained Waste Materials, Lakeland, Florida.

Bromwell, L. G. and Oxford, T. P. (1977). “Waste Clay Dewatering and Disposal,” Geotechnical Practice for Disposal of Solid Waste Materials, ASCE Specialty Conference, Ann Arbor, Michigan.

Bromwell, L. G. and Raden, D. J. (1979). “Disposal of Phosphate Mining Wastes,” Current Geotechnical Practice in Mine Waste Disposal, ASCE, New York.

Bromwell, L. G. (1974). “Progress Report.” Florida Phosphatic Clay Research Project, January-March 1974.

Carrier, W. D., Bromwell, L. G. and Somogyi, F. (1981). “Slurried Mineral Wastes: Physical Properties Pertinent to Disposal.” Seminar on Consolidation Behavior of Fine-Grained Waste Materials, Lakeland, Florida.

Carrier, W. D. and Keshian, B. (1979). “Measurement and Prediction of Consolidation of Dredged Material,” Twelfth Annual Dredging Seminar, Sponsored by Texas A&M University, Houston, Texas.

Cornell University, (1951). “Final Report on Soil Solidification Research.", Ithaca, New York.

Grim, R. E. (1962). Applied Clay Mineralogy. McGraw-Hill Book Company, New York.

International Tables for X-Ray Crystallography. (1974), Volume 4.

Lamont, W. E., McLendon, J. T., Clements, L. W. and Field, I. L. (1975). “Characterization Studies of Florida Phosphate Slimes,” Report of Investigations 8089, U. S. Dept. of Interior, Bureau of Mines, Washington, D.C.

Mitchell, J. K. (1976). Fundamentals of Soil Behavior. John Wiley & Sons, Inc., New York.

Novich, B. E. and Martin, R. T., (1981). “Quantitative Evaluation of Clay Solvation Methods”, Presented at the 18th Annual Meeting of the Clay Minerals Society, University of Illinois at Urbana-Champaign.

REFERENCES (Continued)

Peech, M., Dean, L. A. and Reed, J. (1947). "United States Department of Agriculture Circular 757."

Seed, H. B., Woodward, R. J., and Lundgren, R. (1964). "Clay Mineralogical Aspects of the Atterberg Limits," Journal of the Soil Mechanics and Foundation Division, ASCE, Vol. 90, No. SM-4.

Skempton, A. W. (1954). "The Colloidal Activity of Clay," Proceedings of the Third International Conference on Soil Mechanics and Foundation Engineering, Vol. I.

Weaver, C. E. and Pollard, L. D. (1973). The Chemistry of Clay Minerals. Developments in Sedimentology 15, Elsevier, Amsterdam.